All-Optical Soliton Communications: Devices and Limitations

by

John Demeritt Moores

Submitted to the Department of Electrical Engineering and
Computer Science
in partial fulfillment of the requirements for the degree of

Doctor of Philosophy in Electrical Engineering and Computer
Science

at the

MASSACHUSETTS INSTITUTE OF TECHNOLOGY

February 1994

Author . . . .
Department of Electrical Engineering and Computer Science
February 3, 1994

Certified by . . . .
Hermann A. Haus
Institute Professor
Thesis Supervisor

Accepted by . . . .
Frederic R. Morgenthaler
Chairman, Departmental Committee on Graduate Students

All-Optical Soliton Communications: Devices and Limitations

by

John Demeritt Moores

Abstract

This thesis addresses some of the issues, primarily devices and fundamental physics, relevant to the design of future all-optical soliton communications networks. All-optical switching is discussed in some detail, including an experiment demonstrating cross-phase modulation switching of soliton-like pulses. The known physical limitations on soliton transmission are discussed. A perturbative analysis is presented which suggests how some important high bit-rate limitations on both soliton transmission and storage may be overcome. A catalog of potentially useful devices is presented, including novel proposed devices.

Thesis Supervisor: Hermann A. Haus
Title: Institute Professor

Dedicated with love
to my wonderful parents,
Mr. Barry P. and Mrs. Loretta M. Moores.

Acknowledgments

It has been a pleasure working with Professor Hermann A. Haus, a creative scholar and gentleman for whom I have great respect. I am grateful for the insight (not just technical), guidance, and opportunities he has provided me. His standards of excellence in research and teaching are inspiring. Although I have interacted less with Professor Erich P. Ippen, I have very much enjoyed doing so: he has quite a gift for asking questions and a great sense of humor. Thanks to Professor Haus (who attended my thesis defense despite pneumonia!), Professor Ippen, and to Professor Jeffrey H. Shapiro for graciously serving on my thesis committee.

A very special thanks goes to my mentor and friend, Dr. Kenneth A. Connor, professor at Rensselaer Polytechnic Institute, where I studied as an undergraduate. Dr. Connor drew me into electrical engineering and nurtured in me a deep love for wave phenomena. It was he who introduced me to solitons. I thank him also for the large quantities of time he shared with me to answer my endless questions and to challenge me to pursue interesting ideas.

MIT faculty who did not serve on my thesis committee, but with whom I have had the pleasure of interacting, include Dr. Ron Parker, Director of the MIT Plasma Fusion Center and my graduate counselor; Dr. Peter L. Hagelstein (anyone whose initials are the linear momentum, angular momentum, and Hamiltonian operators ought to be outstanding with quantum mechanics); Dr. Daniel Z. Freedman, who brought to my attention the deep link between solitons and infinite-dimensional Lie algebras; Dr. Victor Kač, who developed much of the latter theory, and who helped me to better appreciate it; Dr. Abraham Bers, who is an excellent teacher, and who taught my very favorite course, 6.633, "Electrodynamics of Waves, Media, and Interactions;" and Dr. David H. Staelin, my first MIT advisor, who, perhaps indirectly through his own success, convinced me to focus on those areas of research which are likely to have significant practical benefits to humankind.

I don't ever expect to encounter a better administrator/secretary than Cindy Kopf – skilled, efficient, and motivated. But beyond the professionalism, I've really enjoyed interacting with her, and have appreciated all of the help she has provided. And her summer lake party is one of the highlights of the year!

David W. Foss, director of the Research Laboratory of Electronics computer facilities, is a fantastic person, and I thank him for assistance beyond the call of duty.

Farzana I. Khatri helped a great deal with the figures and editing of this thesis, and helped in the preparation for my thesis defense. In addition, I have enjoyed supervising her UROP, and programming, modeling lasers, and setting up a switching experiment with her. She is also a treasured friend. Sumanth Kaushik has been a great friend as well. Furthermore, it has been great fun sharing and discussing ideas, doing late night problem sets, and eating his delicious South Indian cooking. It was genuine fun performing the switching experiment, going to conferences, and biking, hiking, and biking some more with Keren Bergman ($\nabla \times$KB). William S. Wong wrote one of the sections of Chapter 5. It has been a pleasure working with this keen-minded friend.

Many thanks to other current and former students, postdocs, and visitors in the

Contents

List of Figures

List of Tables

Chapter 1

Introduction

1.1 Soliton Communications

The idea that solitons might propagate in optical fibers was presented by Hasegawa in 1973 [1]. This paper appeared shortly after the famous paper of Zakharov and Shabat in which an inverse scattering transform was used to solve the nonlinear Schrödinger equation (NSE) [2], in the context of spatial solitons. Mollenauer et al. at Bell Laboratories developed lasers with which they performed experiments demonstrating soliton behavior in fibers [3, 4, 5, 6, 7].

The potential for using optical solitons for communications was recognized [8], and furthermore that solitons might be used over long distances without electronic regeneration. CW Raman pumping along the transmission fiber could provide the gain required to compensate the loss of the fiber [9, 10]. Eventually, as erbium-doped fiber amplifiers (EDFAs) were developed, it was recognized that they could be used for long distance transmission much more conveniently than CW Raman pumping [11]. EDFAs are diode-pumped, relatively polarization-insensitive, have a long upper-state lifetime ensuring relatively data-independent gain, compact, and exhibit gain in a 25-30nm band centered around a wavelength of roughly $1.51\mu m$, which is very close to the minimum loss wavelength for silica fiber.

A brief paragraph on the transmission format of soliton data may be in order. To date, all such systems are on-off keyed (OOK), which is the simplest version of amplitude shift keying (ASK). The presence or absence of a pulse in a (locally synchronous) bit interval represents a binary ONE or ZERO, respectively. The data streams can be time-division multiplexed (TDM) in which case the data are interleaved, and all of the pulses have the same carrier frequency. The data can be wavelength-(frequency-) division multiplexed (WDM), in which case there are several data streams at different carrier frequencies, with sufficiently large frequency separation to avoid crosstalk. Each wavelength channel is partitioned into its own (equally spaced) bit intervals, which overlap those of the other channels. There is a complication in wavelength-multiplexing solitons, however. Their frequency-pulling tendency requires that they be well-separated when multiplexed, to avoid permanent frequency shifts [12, 13]. Polarization-division multiplexing (PZDM) of solitons has been quite successful [14, 15, 16]. There are other more exotic proposed transmission formats as
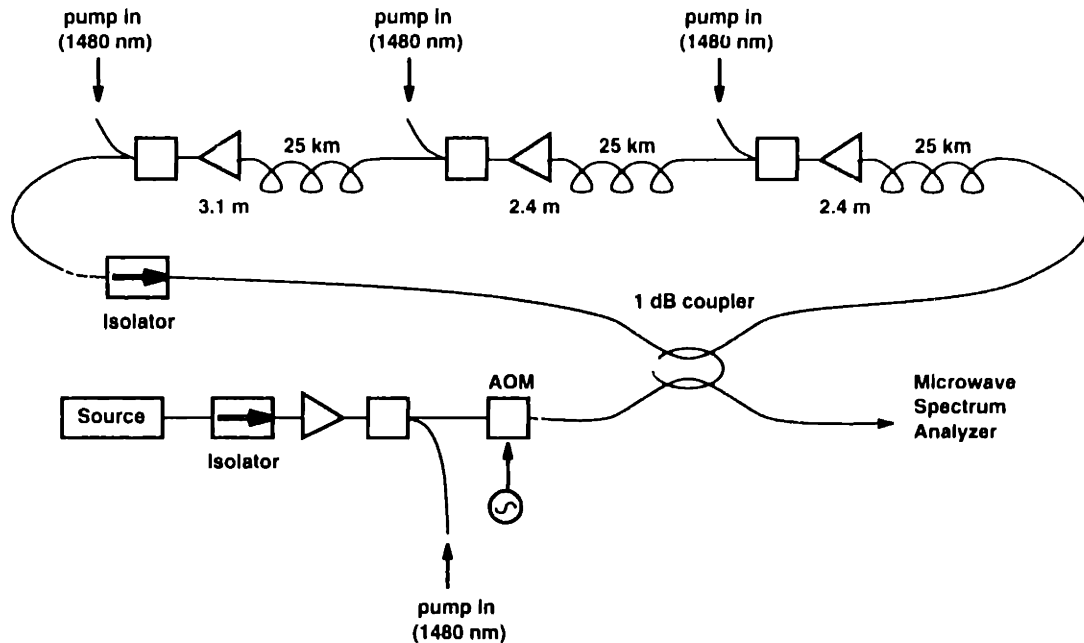
Figure 1-1: A recirculating loop for simulating long-distance soliton transmission.

well, e.g., Refs. [17, 18].

Currently, even better performance can be achieved by introducing filters into the transmission fibers [19, 20, 21, 22, 15]. Bandpass filters provide a restoring force which pulls solitons towards the center wavelength(s) of the filters, reducing noise-induced timing jitter due to the Gordon-Haus effect [23] and other similar effects [24] (see Chapter 5). The filters also improve the signal-to-noise ratio by suppressing the (linear) noise while not destroying the (nonlinear and "self-correcting") solitons.

Most recent experiments have used recirculating loops of fiber containing several EDFAs. Solitons propagate around a loop many times to simulate ultra-long distance transmission. A typical recirculating loop experiment looks something like Fig. 1-1, which is based upon the work of Mollenauer et al. [25, 16], and is similar to the set-up used by Nakazawa et al. [26].

Modulators have also been successfully incorporated into transmission experiments to reduce timing jitter [26, 27] in conjunction with filters [21]. Of course, timing recovery would be required at every modulator to maintain synchronism with the data. Although this approach has been successful, modulators may not be used in actual long-distance transmission links because of complexity, cost and reliability. In fact, there are those who question the use of passive filters for these very same reasons [28] - how much moreso for modulators!

Lately, (expensive) straight-line experiments have been performed as well, with similar results. However, it has been found that polarization selectivity in the components can lead to time-dependent fading of the data, as the components (including the

14

fiber) stretch, bend, heat up, and cool down [29]. Solitons have also been successfully wavelength-multiplexed and polarization multiplexed over long distances [16, 30].

Other techniques, such as tailoring the dispersion along the spans between amplifiers in order to keep the pulses as soliton-like as possible [31, 32, 33] are likely to further improve the performance of soliton systems. Distributed amplification would be wonderful because it would reduce the spatial inhomogeneity due to the gain, which causes the solitons to lose energy as dispersive waves, and is a serious factor limiting the achievable bit rates. CW Raman pumping can approximate distributed gain. Distributed doped erbium fibers (long fibers with low doping concentrations) have been fabricated and successfully utilized by BT, but the cost is likely prohibitive, and the pumping scheme could prove cumbersome.

Simultaneously, as soliton transmission has advanced, so has nonsoliton non-return-to-zero (NRZ) transmission. By alternating sections of positive and negative dispersion fiber, a very low average dispersion can be achieved. This keeps the data from spreading outside the allotted bit intervals, and also serves to discourage self-phase modulation and the resulting spectral broadening. NRZ data can also, like solitons, be transmitted along links which contain amplifiers rather than repeaters. In fact, the 1995 trans-Atlantic cable will use EDFAs and NRZ format. However, it will be difficult to wavelength multiplex many channels, because the engineered cancellation of dispersion is perfect for only one wavelength. Furthermore, these pulses will not restore themselves in the presence of filtering as solitons do, so filtering likely cannot be used.

1.2 All-Optical Switching

Switching is an essential operation for any information handling system, be it a communication system, computer, etc. Broadly, we use the term "switching" to refer to a process by which one channel (the "signal" channel) of information is modified by information in another channel (the "control" channel). It is clear from our working definition of switching that it is an inherently nonlinear process. We shall also allow for the degenerate case in which the control channel and signal channel are the same: here we refer to self-switching or self-routing processes.

The nondegenerate case is more functional, and for the most part we shall concentrate on this case. However, self-switching devices certainly do have applications, and they shall not be overlooked.

1.2.1 All-Optical vs. Electrooptical vs. Electronic Switching

Before discussing the technical issues, we present several applications of switching. Subsequent subsections will be more technical.

The first question is why should switching be done all-optically. The term "all-optical" means different things to different people. Purists would say that the signal and control streams must be and remain optical throughout, and furthermore that any

control operations which might be required to accompany the switching operation, such as clock extraction and delay for synchronous switching must be performed optically. There are those who would relax the latter constraints and only require that the signal and control streams be and remain optical. The relaxed definition of "all-optical" is definitely desirable, especially for the short-term, because of the reasonably well-developed technology of integrated electrooptical devices.

First, consider purely electronic switching. This has the advantage of extremely well-developed and sophisticated devices which are readily commercially available. However, there are serious concerns regarding bandwidth and complexity. Electronic processing for optical pulses at bit rates exceeding electronics speeds might require parallelism and could make difficult the subsequent conversion from electrical signals to properly timed short optical pulses. If optical switches can be built with functionality comparable to electronic switches, all-optical switching could prove simpler. While electronics speeds may appear to grow without bound, it is widely believed that there are bounds, and that optics should be considerably less constrained.

Although the issues are not precisely the same, a related issue of electronic vs. optical implementation is amplification in long-distance undersea cable transmission. There are several motivating factors for replacing electronic regenerators with EDFAs including cost, bulk, complexity, and flexibility (e.g., retrofitting, or applicability despite changes in bit rate, data format, etc.). The 1995 AT&T trans-Atlantic cable will have EDFAs instead of electronic regenerators.

While there are clear reasons to avoid purely electronic switching in an optical network, it is less clear, at least in the near-term, if there is any advantage to performing control operations purely optically, rather than electro-optically. Electrooptics is advantageous because data streams can remain optical throughout the switching fabric, without the need for conversions to and from electronics. But electrooptics is still restricted by the ultimate speed of the electronics. At the time of writing, several transmission experiments have involved the use of electro-optic modulators at rates of 2-10 GHz (for example [34, 35, 16, 36]). Laboratory rates have reached 40 GHz. It is not clear how much higher these rates can be pushed.

All-optical switches, however, should be capable of switching at THz rates. However, most of the designs to date are pipelined and suffer from large latencies. That is, although the switching is performed on THz-rate data, the delay from the time a pulse enters the switch to the time it exits, based upon published switch experiments, is in the range of 30 ns to 10 μs! At 200 GHz, a bit interval is 5 ps, which is more than three orders of magnitude less than the switching delay.

The problem is the medium in which the switching is performed: optical fiber. The nonlinearity is just too weak. Yet, at present, there is no substitute material which is unquestionably superior to silica fiber. Fibers with higher nonlinearity have been fabricated, but invariably the loss is much higher than in ordinary silica [37, 38, 39].

Semiconductors, when operated with large nonlinear indices of refraction, suffer from multiphoton absorption, which can ruin pulse shapes. Semiconductors also tend to have large linear loss (but they can be made active), as well as much greater insertion loss than fibers. Balancing the extra loss likely implies increased ASE noise in the system. Active devices may suffer from data-dependent gain because of the

rapid gain dynamics. Nevertheless, there are some very promising semiconductor switches [40, 41].

Polymer waveguides suffer from similar problems, but much worse, they tend to have very slow nonlinearities, plus many of them degrade too rapidly to be used in a real-world system [39].

It is hoped that a material will be discovered, or a heterostructure engineered, which will exhibit refractive nonlinearity that is much stronger (orders of magnitude) and as fast or faster than that of silica fiber, will have low two photon absorption, and have low net linear loss. Coupling losses should also be minimal, ideally by making completely integrated optical circuits for cascaded switching operations. If solitons are desired, this will further require that the material be highly (linearly) dispersive. If the material is not intrinsically so dispersive, it may be possible to design distributed feedback-type structures to increase the dispersion [42].

1.2.2   Optical Switching Applications

With regard to a communication system, switching has several applications.

It may be desirable at certain points within a network to replace the pulses constituting a channel with new pulses. There are several reasons why one might wish to do this. First, if the transmission is over extremely long distances, the pulses will eventually degrade, and it may be desirable to replace them to maintain an adequate eye diagram and signal-to-noise ratio. Furthermore, if the bit rate is sufficiently high and the distance sufficiently great (not necessarily very far, at high bit rates) then (if unchecked) Raman self-frequency shifts will accrue. Switches which replace the old pulses with new upshifted pulses could be fabricated.

Second, nodal routing might be achieved via frequency-selection. The intended destination of a data stream would determine the carrier frequency, and this could change at each node. Tunable switches could be used to perform the frequency conversion.

Third, the author and others independently have proposed that a tunable switch in conjunction with a section of dispersive fiber and the inverse switch (to return the pulses to the original carrier) could serve as a variable delay line. This is an important node function useful for multiplexing, contention-handling, and other control operations.

Another application of switches is that they can perform Boolean logic operations. These could be useful for a variety of signal processing applications. Nodal control operations and routing are useful within the network, and end-users may wish to process incoming information.

Switches are useful as time-division demultiplexers [43, 44, 45, 46, 47, 41, 48, 49, 50].

1.3 Brief Soliton Review

Loosely, a solitary wave is a localized disturbance or wavepacket whose derivatives with respect to the propagation coordinate vanish at $\pm\infty$, and which propagates without changing shape unless it encounters another wave. Solitons are very special solitary waves which are natural modes of certain nonlinear and dispersive media. Solitons have the remarkable property that after fully colliding with each other, they emerge unchanged, except for possible phase and position shifts. Fundamental solitons are single humps or kinks which propagate without change. Higher-order humped solitons, or "breathers," are periodic.

In an optical fiber in which there is group velocity dispersion (GVD) and Kerr nonlinearity (the index of refraction of the medium changes proportionally with the intensity of the light present, and essentially instantaneously), the nonlinear Schrödinger equation (NSE) describes the propagation of light. The self phase modulation of the fiber through the Kerr effect counteracts the dispersion. The nonlinear Schroedinger equation (NSE) can be written:

$$-j\frac{\partial u}{\partial z} = \frac{k''}{2}\frac{\partial^2 u}{\partial t^2} - \kappa|u|^2 u \tag{1.1}$$

where $u(t,z)$ is the slowly varying pulse envelope (the carrier frequency and wavenumber have been scaled out), z is the propagation distance, t is the time in the moving frame of the pulse, k'' is second-order dispersion, and κ is the Kerr coefficient. This equation is in a retarded coordinate frame. The coordinate frame moves with the group velocity of the pulse.

Perhaps the most useful solution to this equation is the fundamental (also N=1, or first-order soliton) soliton:

$$u(t,z) = A\,\text{sech}\left(\frac{t}{\tau}\right)\exp\left\{j\frac{k''}{2\tau^2}z\right\} \tag{1.2}$$

The soliton area is fixed by the ratio of the dispersion to the Kerr nonlinearity:

$$A\tau = \sqrt{\frac{-k''}{\kappa}} \tag{1.3}$$

where the sign of k'' must be negative if $\kappa > 0$, as is the case for an ordinary optical fiber. At a given carrier frequency, there are (theoretically) infinitely many possible fundamental solitons, of different amplitude and width, but all with the same area.

The distance in which a soliton acquires a 2π (nonlinear) phase is:

$$8\left(\frac{\pi^2\tau^2 c}{\lambda^2 D}\right) \equiv 8z_0 \tag{1.4}$$

where the pulse Full-Width at Half Maximum intensity

$$\tau_{\text{FWHM}} = 2\tau\cosh^{-1}\sqrt{2} \approx 1.762747\tau\,, \tag{1.5}$$

18

λ is the carrier wavelength in vacuum, c is the vacuum speed of light, and D is the time-of-flight group velocity dispersion (units of time per square length, which physically represents the amount of time shift per wavelength shift per distance). Dispersion is sometimes given as k'' (or β''), meaning the second derivative of wavenumber with respect to frequency. The relationship between k'' and D is

$$k'' = -\frac{\lambda^2 D}{2\pi c} .$$
(1.6)

The term "soliton period" usually refers to the quantity z_0 as defined above. Thus a simpler expression for the soliton period is

$$z_0 = -\frac{\pi \tau^2}{2k''} .$$
(1.7)

The peak power of a single fundamental soliton is

$$P_{N=1} = \frac{\lambda A_{\text{eff}}}{4n_2 z_0}$$
(1.8)

where A_{eff} is the effective area [51] of the fiber (the cross-sectional area within which is most of soliton power) and n_2 is the nonlinear index of refraction in m^2/Watt. For an ordinary silica optical fiber,

$$n_2 = 3.18 \times 10^{-20} \text{m}^2/\text{W} .$$

Higher-than-first-order solitons are essentially oscillating bound states of fundamental solitons. The number of solitons comprising the bound state is the (integer) order of the higher-order soliton (e.g., an N=3 soliton is a bound state of three N=1 solitons). Higher-order solitons are unlikely to be used for communications. Perturbations are much more likely to disturb these somewhat delicate (weak binding energy) bound states than they are to disturb fundamental solitons.

1.4 Basic Fiber Propagation Equations

In this section, we shall examine the simplest coupled nonlinear Schrödinger equations (CNSEs) for pulse propagation in optical fibers. This thesis would not really be enhanced by the inclusion of a derivation of these equations. The reader is referred to Menyuk for the painstaking details [52]. Let the reader beware: these equations become less adequate as pulse widths grow shorter and/or propagation distances grow longer, and when operating near zero dispersion. Many higher-order effects manifest themselves in these regimes. Typical pulse widths used in soliton transmission experiments to date are of the order of 30 to 60 ps. Pulses of such great duration are essentially unaffected by higher-order nonlinearities (some of these effects are discussed in the chapter on High Bit-Rate Limitations, Chapter 4) such as Raman scattering, self-steepening, frequency-dependence of Kerr, etc. (however, electrostriction

does lead to timing shifts). Such pulses will most definitely be affected by third-order linear dispersion, if propagated too close to the zero dispersion wavelength of the fiber Otherwise, current communications solitons are well-described by the standard CNSEs.

In the second subsection, we consider some of the implications of these equations. In particular, we take a brief look at polarization rotation and instability.

1.4.1 The Equations

The unnormalized equations can be written:

$$
\begin{aligned}
U_z = {} & -jk_oU - k'U_t + j\frac{k''}{2}U_{tt} \\
& - \frac{j}{2k_o}\left\{(2a + b\cos^2\theta)|U|^2U + 2(a + b\sin^2\theta)|V|^2U\right. \\
& + b\cos^2\theta\,V^2U^* \\
& + \left.b\cos\theta\,\sin\theta\left[U^2V^* + (2|U|^2 + |V|^2)V\right]\right\}
\end{aligned}
\tag{1.9}
$$

$$
\begin{aligned}
V_z = {} & -jl_oV - l'V_t + j\frac{l''}{2}V_{tt} \\
& - \frac{j}{2l_o}\left\{(2a + b\cos^2\theta)|V|^2V + 2(a + b\sin^2\theta)|U|^2V\right. \\
& + b\cos^2\theta\,U^2V^* \\
& + \left.b\cos\theta\,\sin\theta\left[V^2U^* + (2|V|^2 + |U|^2)U\right]\right\}
\end{aligned}
\tag{1.10}
$$

where the subscripts z and t indicate partial derivatives with respect to propagation distance and time, respectively; the field quantities U and V are defined such that the positive frequency component (denoted by superscript $+$) of the electric field in one polarization (denoted by subscript 1) is

$$
E_1^+(z,t) = U(z,t)\exp[j(\omega_o t - k_o z)]
\tag{1.11}
$$

and the positive frequency portion of the electric field in the orthogonal polarization is

$$
E_2^+(z,t) = V(z,t)\exp[j(\omega_o t - l_o z)]\,;
\tag{1.12}
$$

the dispersion relation for polarization 1 for wavenumber k as a function of frequency ω is

$$
k = k_o + k'|_{\omega=\omega_o}(\omega - \omega_o) + \frac{1}{2}k''|_{\omega=\omega_o}(\omega - \omega_o)^2 + H.O.T.,
\tag{1.13}
$$

H.O.T. are higher-order terms which are ignored; the dispersion relation for polarization 2, denoting wavenumber for this polarization as l, is

$$
l = l_o + l'|_{\omega=\omega_o}(\omega - \omega_o) + \frac{1}{2}l''|_{\omega=\omega_o}(\omega - \omega_o)^2 + H.O.T.\,;
\tag{1.14}
$$

$a = \tilde{\chi}(\omega_o, -\omega_o; \omega_o)$, $b = \tilde{\chi}(\omega_o, \omega_o; -\omega_o)$, where $\tilde{\chi}$ is the (temporal) Fourier transform (denoted by the tilde) of the third-order susceptibility assuming isotropic nonlinearity (thus it is a scalar function rather than a tensor) so that

$$\underline{P}(z,t) = \int_{-\infty}^{t} dt_1 \int_{-\infty}^{t} dt_2 \int_{-\infty}^{t} dt_3\, \chi(t - t_1, t - t_2; t - t_3)\left(\underline{E}(z,t_1) \cdot \underline{E}(z,t_2)\right)\underline{E}(z,t_3)\,;$$

(1.15)

$a = b$ in fiber, in which the nonlinear response is essentially instantaneous compared with the rate of change of the pulse envelope [52, 53]; and the polarization basis is specified by the angle θ which is the azimuthal angle on the Poincaré sphere (the polar angle is the phase difference between the fields U and V and does not appear explicitly in the CNSEs) so that $\theta = 0$ for linear polarization and $\theta = \pm\pi/2$ for circular polarization.

Let us consider the physics of each of the terms in Eq. (1.9). The equation says that the evolution of the field U with distance is governed by the effects on the right-hand side (RHS). The first term is the carrier wavenumber phase term. The second term is simply an inverse velocity term which suggests that a natural inverse velocity for U is k'. The third term represents linear group velocity dispersion (GVD). The $|U|^2 U$ term is the self-phase modulation (SPM) term which, in isolation, would result in a change of phase profile proportional to the intensity profile. The $|V|^2 U$ term is the cross-phase modulation (XPM) term whereby (with no other effects) a pulse accumulates phase at a rate proportional to the intensity profile of V, the orthogonally polarized pulse. The remaining RHS terms are referred to as coherence terms, varying sinusoidally with z if the birefringence is fixed and nonzero.

It is common to redefine the field envelope variables U and V so that they include their spatial phase with respective wavenumbers k_o and l_o. This is what is done for the scalar NSE, and for the CNSEs it makes the coherence terms instantly identifiable as those with complex exponential multipliers:

$$
\begin{aligned}
U_z =\ & -k'U_t + j\frac{k''}{2}U_{tt} \\
& - \frac{j}{2k_o}\Big\{(2a + b\cos^2\theta)|U|^2 U + 2(a + b\sin^2\theta)|V|^2 U \\
& + b\cos^2\theta\, V^2 U^* e^{2j(k_o - l_o)z} \\
& + b\cos\theta\,\sin\theta\left[U^2 V^* e^{-j(k_o - l_o)z} + (2|U|^2 + |V|^2)V e^{j(k_o - l_o)z}\right]\Big\}
\end{aligned}
$$
(1.16)

$$
\begin{aligned}
V_z =\ & -l'V_t + j\frac{l''}{2}V_{tt} \\
& - \frac{j}{2l_o}\Big\{(2a + b\cos^2\theta)|V|^2 V + 2(a + b\sin^2\theta)|U|^2 V \\
& + b\cos^2\theta\, U^2 V^* e^{-2j(k_o - l_o)z} \\
& + b\cos\theta\,\sin\theta\left[V^2 U^* e^{j(k_o - l_o)z} + (2|V|^2 + |U|^2)U e^{-j(k_o - l_o)z}\right]\Big\}\,.
\end{aligned}
$$
(1.17)

One typically defines self- and cross-phase modulation coefficients to simplify no-

	linear $\theta = 0$	Menyuk $\theta = 35.3$ deg.	circular $\theta = 90$ deg.
$\delta k_o / a$	3/2	4/3	1
$\delta_2 k_o / a$	1	4/3	2

Table 1.1: Self- and cross-phase modulation coefficients for three polarization bases.

tation,

$$\delta = \left(\frac{2a + b\cos^2\theta}{2k_o} \right) , \qquad (1.18)$$

$$\delta_2 = \left(\frac{a + b\sin^2\theta}{k_o} \right) . \qquad (1.19)$$

Self-phase modulation is strongest for linear polarization and weakest for circular, while cross-phase modulation is weakest for linear polarization and strongest for circular. Table 1.1 summarizes some important values, with $a = b$.

1.4.2 Polarization Instability and Rotation

One of the dangers to be avoided in all-optical device design and in pulse transmission is polarization instability, which has been treated by numerous authors [54, 55, 56, 57, 58, 59, 60]. This instability can arise with high-powered CW, or with pulses, and it occurs in birefringent (and in other more unpleasantly anisotropic) media. Exact analytic results can be obtained for dispersionless birefringent media, as in many of the references. There are several ways to think about polarization instability. The author prefers the following view, which is simply phase-matching of the two polarization axes mediated by the Kerr effect: suppose light polarized along one of the birefringent axes has an effective wavenumber k_1. Suppose furthermore that if the same light were polarized along the orthogonal axis, it would have wavenumber k_2. The Kerr effect changes the effective index of refraction, and we can think of this as an extra wavenumber which can provide coupling between the waves with wavenumbers k_1 and k_2. If the potentially unstable light happens to be a soliton, then instability will be automatically phase-matched if the soliton phase period is less than or equal to the birefringence beat length $L_b = 2\pi/|k_1 - k_2|$, and the soliton is polarized along the fast axis of the birefringent medium. Experimentally and numerically it has been found that a soliton tends to remain rather soliton-like despite the instability - it rotates, certainly shedding some radiation, but seeming to maintain its character.

Nonlinear polarization rotation, as the term is usually used, refers to a different behavior. It is simply the difference between the rates of accumulation of nonlinear phase between two orthogonally polarized components. It is simplest to think about this in the circular polarization basis because there are only two nonlinear phase terms in each equation: the SPM and XPM terms. The phase accumulation difference occurs because the power is different in the two polarizations and also because the

SPM and XPM coefficients are different. The phase difference is zero for circularly polarized light, since the only nonlinear phase is the SPM of the one component. The difference is also zero for any linear polarization, since the circular components have equal power. Any elliptic polarization will rotate. Because XPM is twice as strong as SPM in the circular basis, the rate of differential nonlinear phase accumulation is proportional to the difference in power between the two circular components. So although we said that there is no rotation for circular polarization because there is only one component, in fact the maximum rate of differential phase shift occurs with circular polarization. However, there is no power in the second polarization with which to measure this phase "difference." Note that despite the name rotation, there is no exchange of power between the circularly polarized components.

Polarization rotation is useful for self-switching (or as the essential ingredient in a transmissive fast saturable absorber) [61]. One can cause a pulse to undergo nonlinear rotation, possibly convert it to another polarization, and pass it through a polarizer to achieve the switching or fast saturable absorber (FSA) action [61, 62, 63, 64].

1.5   Overview of This Thesis

In Chapter 2, I discuss optical switching in greater detail. This includes a discussion of experimental work I have done with others at MIT, as well as a few of my proposals for new devices.

In Chapter 3, I present my work on an important problem which must be solved if many wavelength channels of solitons are to be multiplexed. The problem is how to ensure equal gain for all of the WDM channels. The gain spectrum of a typical EDFA is far from flat. The loss spectrum for fiber is much flatter. Passive filtering alone may be suitable, but there will likely be crosstalk between the WDM channels. I have proposed the use of inhomogeneously broadened fiber amplifiers, to reduce the crosstalk. Such amplifiers do exist, and in an example, I use measured data to model such an amplifier. I describe in detail one possible gain equalization scheme, employing passive filters for crude equalization, and an inhomogeneously broadened fiber amplifier to provide fine-tuning of the equalization via a servo-loop. The implementation is likely more complex than is required to achieve adequate equalization with EDFAs, but might be necessary with other inhomogeneously broadened amplifiers with much shorter upper state lifetimes.

In Chapter 4, I briefly summarize the known limitations to high bit rate soliton transmission. This chapter further serves to motivate Chapter 5.

Chapter 5 is predominantly my own work, and it includes a perturbative analysis of some important high bit rate soliton transmission limitations. The work is also relevant to optical soliton storage ring memories, and these are discussed as well.

Chapter 6 is an overview of all-optical devices that are necessary or desirable for the implementation of all-optical pulsed fiber telecommunications networks. Much of the chapter gives the reader a rough idea of the current status of the devices. But much of the chapter is speculative, including many new ideas proposed by the author.

Chapter 2

All-Optical Switching

Switching is an essential operation for any information handling system, be it a communication system, computer, etc. Broadly, we use the term "switching" to refer to a process by which one channel (the "signal" channel) of information is modified by information in another channel (the "control" channel). It is clear from our working definition of switching that it is an inherently nonlinear process. We shall also allow for the degenerate case in which the control channel and signal channel are the same: here we refer to self-switching or self-routing processes.

The nondegenerate case is more functional, and for the most part we shall concentrate on this case. However, degenerate, or self-switching devices have applications as well, and we shall briefly discuss these.

In the descriptions of all-optical devices in this chapter and in others in this thesis, I have provided design parameters (real numbers) for implementation in currently available materials, and especially in readily available grades of silica optical fiber. It is expected that better materials will be developed in the near future. "Better" can mean higher Kerr coefficient, less two-photon absorption, less linear loss, greater stability, etc. In particular, optical fiber would be far more desirable for devices if the Kerr nonlinearity were much stronger (orders of magnitude). Commensurate with increased Kerr, one would need increased dispersion in order to exploit solitons, and there are ways of engineering dispersion into a device [42].

Candidate materials include chalcogenide fibers, for use in the infrared over a wider range than the usual 1.3-1.55μm wavelength regime. It is believed that a two-order-of-magnitude improvement in linear loss may be achievable with these fibers, especially at longer wavelengths where Rayleigh scattering is weak. Such fibers have been used in switching experiments with only one meter of fiber [37]. In the experiment, an As_2S_3-based fiber was used, which was quite lossy (1 dB/m), but had a high nonlinear index ($n_2 = 2 \times 10^{-18}$ m^2/W).

There is also hope that new engineered structures may offer improved performance. The device concepts presented here can be fairly easily modified to take advantage of materials advances.
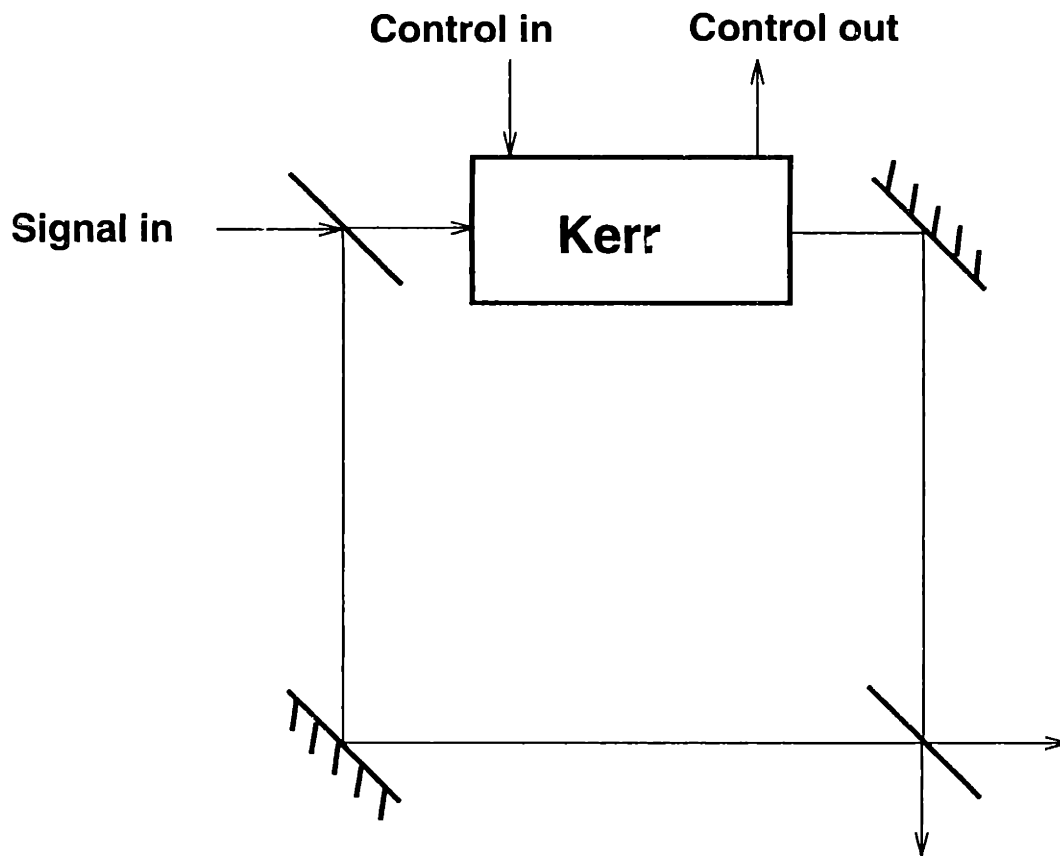
Figure 2-1: Conceptual interferometric switch with Kerr medium in one arm of interferometer.

2.1 Overview of All-Optical Switching

This section presents some basic all-optical switching ideas. Self-switching and three-terminal switching are discussed. This section serves as a transition to the more detailed discussions of subsequent sections.

2.1.1 Illustrative Example

An impractical but illustrative example of non-degenerate optical switching in the broad sense involves two streams of pulses, which we label the signal and control streams. Let us assume, as usual, that the streams are partitioned into equally-spaced bit intervals. Suppose further that information is modulated onto the streams in on-off keyed (OOK) fashion. That is, the presence of a pulse within a bit slot represents a binary ONE while the absence of a pulse in a bit slot represents a binary ZERO.

We can perform a Gedanken experiment with the components in Fig. 2-1. This is a
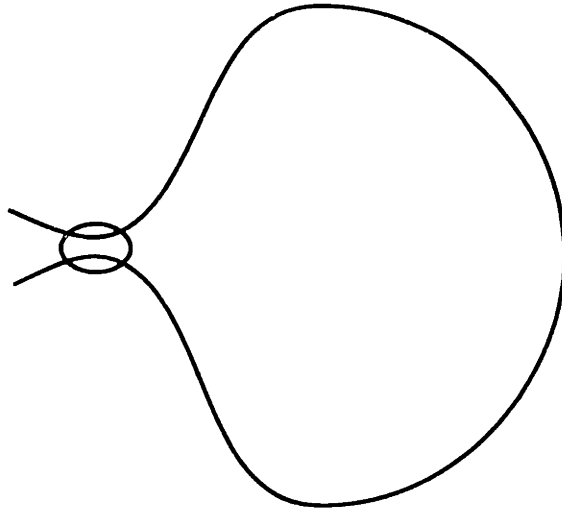
Figure 2-2: A fiber Sagnac interferometer.

Mach-Zehnder (M-Z) interferometer with a Kerr medium in one arm. The signal data
enters the interferometer and is split equally into the two arms of the interferometer.
One arm contains a Kerr medium. A dichroic coupler allows us to couple in our
control data into the Kerr medium, where it can impart phase and/or timing shifts to
the half-signal. The two channels interact until the second dichroic coupler is reached,
at which point, the control data is physically separated from the signal. If the control
imparts a π phase shift to a signal pulse, then the signal pulse will exit from the
opposite output port than it would exit if there were no control pulse present.

Geometries and the means by which the phase shift is imparted distinguish the
various interferometric switches. While on paper a standard M-Z would appear to
be a reasonable geometry, in reality, the M-Z would be difficult to stabilize against
thermal and acoustic fluctuations. Perhaps the most popular geometry at the time of
writing is the Sagnac loop, usually implemented with optical fiber. (see Fig. 2-2). The
Sagnac is popularly referred to as a M-Z "folded back on itself." Rather than travel
through two physically distinct arms of an M-Z, the pulses counterpropagate around
the same loop of fiber. Instead of distinct beamsplitters or couplers at the input and
output of the M-Z, the Sagnac has a single coupler which closes the loop and provides
input/output ports (note the orientation of the coupler - the alternative orientation
makes for an interesting signal processing device [65], or with other components inside
the loop can be a storage ring [66, 67, 68, 69, 70]).

A Sagnac with a 50:50 coupler (light entering one port of the coupler is equally
divided between the ports on the other side of the coupler), zero birefringence, and
zero loss acts as a perfect reflector [71]. This is easy to see once one recognizes that

the coupler is a lossless, time-reversal symmetric (and therefore reciprocal) four-port device, which implies a $\pi/2$ phase shift between the output ports for a single input [51]. Alternatively, there are ways to make the loop act as a perfect transmitter, with a nonreciprocal element or by using waveplates (achievable, e.g., with fiber polarization controllers) in the nonlinear regime of operation [72]. Fiber is of course a Kerr medium, and although the Sagnac appears to be symmetric unlike the interferometer of Fig. 2-1, there are ways to asymmetrize the loop. Some of these methods are discussed below.

2.1.2 Self-Switching

A simple way to achieve (intensity-dependent) self-switching is to use an imbalanced fiber Sagnac interferometer [73, 74, 75, 76, 77]. By making the coupler other than 50:50, and using a loop of sufficient length, the counterpropagating pulses will accumulate nonlinear (Kerr) phase at different rates. The difference will be proportional to intensity (assuming zero dispersion). In fact, with zero dispersion, each pulse inside the loop will acquire phase porportional to its intensity profile. This nonlinear differential phase will distribute the pulse to the output ports as a function of intensity. Using an imbalanced coupler, however, some light will always leak to the output port through which the pulse did not enter the loop.

Another way to imbalance a fiber loop is to asymmetrically place gain or loss within the loop [78, 79, 80, 81, 82, 83, 84, 41, 85]. This way, a 50:50 coupler can close the Sagnac so that there is no leakage. The asymmetric location of the gain/loss results in differential Kerr phase for the counterpropagating pulses. In this way, one can combine amplification with artificial fast saturable absorption (FSA) action to clean up some of the low intensity garbage between pulses in a TDM system (noise from previous amplifiers, or other dispersive waves). For there to be no leakage, the gain must be the same for the counterpropagating pulses (with a 50:50 coupler), which requires that the gain either must have a response time much longer than the loop roundtrip time, or must be well-saturated so that the response is small. The gain could be stabilized by saturating it with another source (e.g., in another polarization or at another frequency, so it can easily be separated from the data), or perhaps with feedback control of the pump if the control can respond as quickly as the gain. No matter how well the gain is stabilized, however, the amplified spontaneous emission (ASE) noise acquired by the counterpropagating pulses will be different. The loop will not serve to reduce noise-imparted effects of the internal amplifier. Such effects are important limitations on transmission, and are discussed in other chapters.

Self-switching can also be achieved with waveplates, polarization rotation, and a polarizer [61].

Self-switches are designed with a specific peak intensity in mind. If soliton data is being used in a network, and different bit rates are being used, this could be a problem (solitons of different widths have different intensities).

27

2.1.3 Three-Terminal Switching

Self-switching has obvious limitations for applications. Much more flexible are devices in which pulses switch pulses. Such a device has two inputs and one output, as does a primitive Boolean logic gate.

There is an enormous body of literature relating to nonlinear directional couplers as switches [86, 87, 39, 88]. Nonlinear couplers will not be discussed here. They are generally implemented in semiconductors which suffer from high insertion loss, multi-photon absorption, and if active, can provide data-dependent gain. Even in an ideal medium, it is not clear that these devices could accurately preserve the data in the switching process. But such devices would certainly have the advantage of compactness.

There are a host of resistive switches as well. Again most of these devices require semiconductors, which have many problems including large insertion loss, two-photon absorption which modifies pulse shapes, relatively fast saturation time constants which can make the response data-dependent, and the usual electronics limitations (e.g. capacitances and transport times) if the devices are hybrid. The general question of reactive versus resistive switches is interesting, because it might appear that resistive devices would be more wasteful, but often reactive devices require high switching powers and if the switching pulse energy is not recovered, the reactive switch could actually use more energy. However, in the case of a reactive switch, this energy can be transported away from the switch, whereas in a resistive switch, the energy is deposited within the switch. In any event, resistive devices such as reflection modulators, self electro-optic devices (SEEDs), etc. will not be discussed here.

There are numerous ways to make switches utilizing the cross-phase modulation of one pulse upon another. Many of these utilize interferometers. Others use small frequency shifts followed by dispersive delay lines, for pulse position shifts. Polarization rocking devices may be used. Four-wave mixing is another possibility. These and other ideas are discussed in the remainder of this chapter.

2.2 XPM Collision Switches

At MIT, Keren Bergman and I, with the guidance and facilities of Professors H.A.Haus and E.P.Ippen, have demonstrated that switching can be achieved using collisions of orthogonally polarized solitary waves, in a Sagnac interferometer. The concept is influenced by the nature of solitons. Namely, that the net result of a soliton collision is that each soliton is displaced and phase-shifted. Otherwise, the solitons remain unchanged. This is a remarkable property, and it would be ideal for designing all-optical switches, if nature were so kind. But of course, optical fibers do not lend themselves to easy-to-build soliton switches.

First of all, consider using copolarized solitons of different frequencies. Although the pulses can undergo a near-perfect soliton collision, they cannot in one collision achieve the full π-radian phase-shift required for interferometric implementation. To impart such a large phase shift to a fundamental soliton would require a fifth-order soliton. Such pulses are rather unstable to perturbations. Achieving multiple colli-

sions would not be easy. One might think of splicing together fibers of opposite dispersion, but the pulses would not be solitons in the positive GVD fibers, and would therefore tend to dispeise unless some averaged-soliton game could be played. That is, the spreading in the positive GVD fibers would be compensated by compression in negative GVD fibers. It would be essential to avoid resonance with the averaged soliton period, or to use large values of dispersion, to eschew sideband generation. Furthermore, it is not clear that the averaged pulses would still act as averaged solitons in the presence of the collisions, although it seems plausible. In any event, there is still the problem of the two different frequencies. It is less convenient to design a system if we must keep track of different frequencies which are used in the same channel. Many two-color switches have been built and proposed [89, 90, 91, 92, 93, 94, 95, 96, 83]. These switches may be less convenient than other switches. If a two-color pulse-replacement switch is used, the output pulse will be at a different frequency than the input. It could be rather cumbersome to have frequencies flipping back and forth from stage to stage.

As an alternative, we might use orthogonally polarized "solitons" of the same frequency, in birefringent fiber. Although it is possible to launch solitons in a fiber, these solitons act as solitons only with light of the same polarization. Propagation in a fiber can be described with two coupled nonlinear Schrödinger equations, as in Chapter 1. If one of the polarizations is completely unexcited, then light in the other polarization behaves according to the dynamics of the one-dimensional nonlinear Schrödinger equation, which is an integrable equation, meaning that it has soliton solutions. A soliton, after colliding with another, remains completely intact, merely acquiring a uniform phase shift and a timing shift. In contrast, the system of coupled equations is not integrable. This means that the coupled equations do not exhibit true soliton behavior. Specifically, orthogonally polarized "solitons" are distorted by a collision, and shed dispersive waves. More distortion and shedding occur for slower collisions. Neither distortion nor continuum is desirable for switching.

There is an integrable pair of coupled nonlinear Schrödinger equations, the Manakov system [97, 98], but fibers support Manakov-like behavior only for a specific elliptic polarization [52] (and this case is not strictly integrable, because of coherence terms - the coherence terms are often neglected because they vary rapidly, averaging to zero). Achieving and maintaining such polarization states might not be an easy task, and thus far there have been no experimental papers demonstrating such switching.

One might imagine that rapidly scrambling the polarizations of the pulses might give rise to averaging over the Poincaré sphere, yielding averaged Manakov solitons, but it is not clear whether or not this concept would be applicable to switching. In fact, it seems unlikely that polarization scrambling can be achieved on a desirably short distance scale for switching.

Again, a single collision will not achieve a π phase shift, and because the collisions must be "fast," even less phase might be achieved in one collision than in an integrable system. However, it is now easier to achieve multiple collisions. We simply splice together birefringent fibers with the birefringence axes rotated by $\pi/2$, so that a pulse which was on the fast axis of the first fiber enters the second on the slow
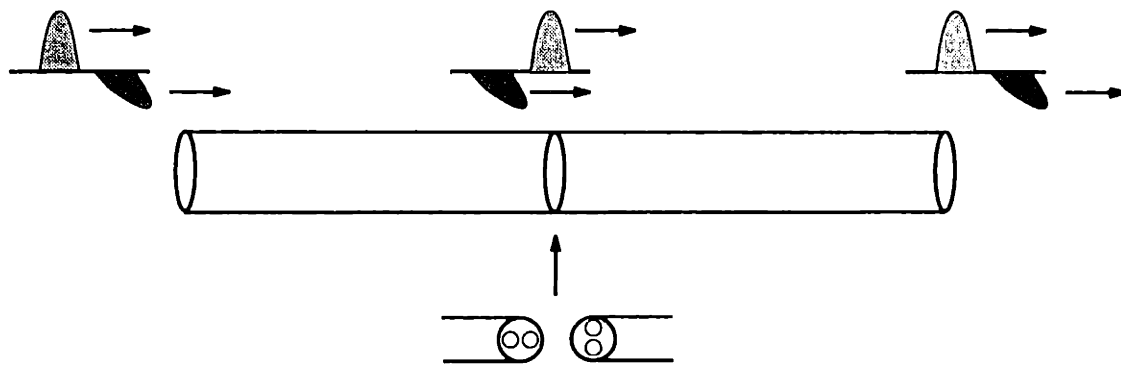
Figure 2-3: Orthogonally polarized pulses collide once in each of two sections of cross-spliced high-birefringence fiber.

axis. This is illustrated in Fig. 2-3. This was the approach used at MIT for a proof-of-principle experiment with a fiber Sagnac loop [99], and discussed in greater detail, with discussion of applications and generalizations [100]. A single-collision polarization switch was demonstrated back in 1987 [101]. Use of the special integrable (if one ignores coherence terms) elliptic polarization was discussed in Ref. [102]. The MIT work was followed up by more sophisticated experiments at AT&T [103, 43, 104, 105]. Some of those follow-up experiments did not use solitons, and although it was not stated in those papers, it is likely (based upon the physics, and for one of the papers, based upon simulations by F.I.Khatri) that the output of those devices was chirped. This very likely means that the devices would not be cascadable. In Ref. [104], the AT&T group used the near-soliton operation of the MIT switch to build a successful circulating shift register with inverter.

There are many advantages to the MIT type of switch. First, the pulses remain nearly fundamental solitons, and this is highly advantageous because the output of a switch need not be post-processed in order to be compatible with whatever follows the switch, e.g. subsequent switches or transmission lines. Most other all-optical switch designs to date require some type of post-processing. What most authors avoid saying is that their output pulses are highly chirped. Such chirping implies that the devices do not lend themselves well to cascading. Some sort of chirp cancellation is required. Two-frequency switches utilizing a single collision cannot possibly use fundamental solitons to achieve a π phase shift. Time domain chirp switches [106] or soliton dragging switches [107, 108] would require some sort of gating or cross-correlation at the output, and no one to date has published a demonstration of such a post-processor.

Another advantage is timing jitter insensitivity. If an incoming bit stream which has accumulated some timing jitter is input to the switch, the other input stream has no jitter, and the switch is designed to replace the jittery stream with the other stream, then the switch can effectively perform timing correction. This can be achieved
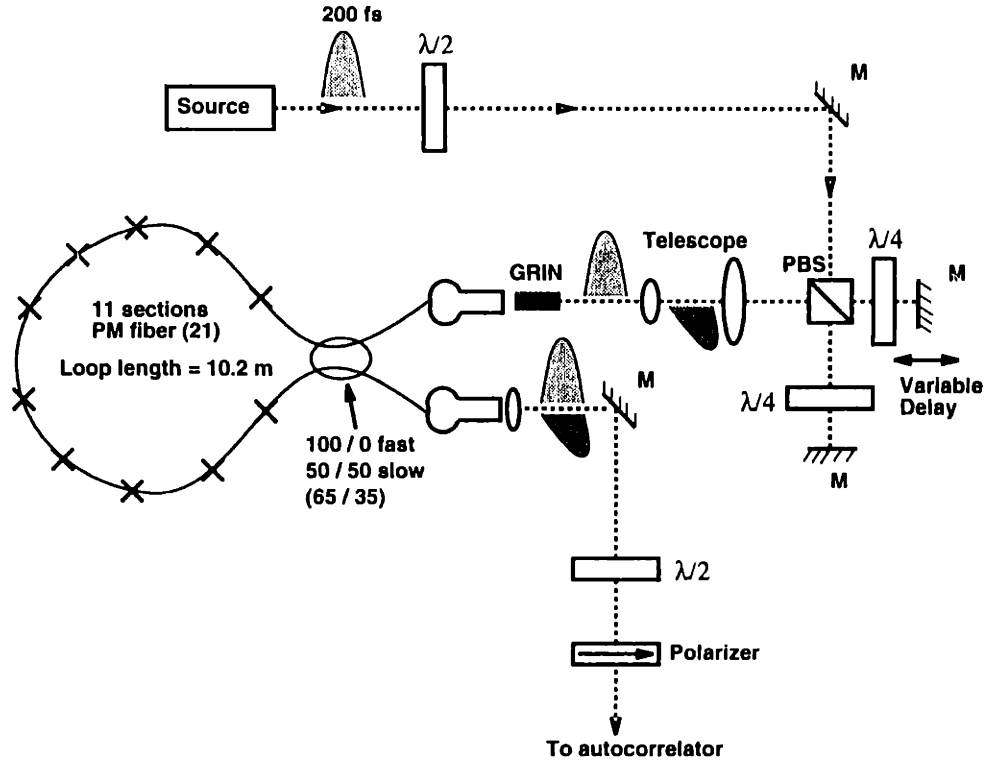
Figure 2-4: Set-up of MIT switch proof-of-principle experiment. M = mirror, PBS = polarizing beam splitter, $\lambda/2$ = half-wave plate, $\lambda/4$ = quarter-wave plate, dashed curve = free space light path, solid curve = fiber, × = PM fiber cross-splice.

because the switch consists of several segments, each of which supports one collision. If the segment length exceeds that required for a collision, and one of the pulses is slightly mistimed, then the collision can still be confined within that one segment.

The details of our experiment may be found in Ref. [99], but will be briefly summarized here. The experimental set-up is shown in Fig. 2-4. The switch consisted of eleven segments of Alcoa Fujikura PM fiber, and the total loop length was 10.2 m. Kevin Champagne of C.S.Draper Laboratories performed the splicing. With our parameter values, a complete switch would have required twenty-seven segments. The refractive index difference between the ordinary and extraordinary axes was $\Delta n = 5.4 \times 10^{-4}$, the polarization extinction ratio was at least 30 dB, the dispersion at free space wavelength 1.52 μm was 8.8 ps/(nm-km) anomalous, and the fiber core diameter was 7.5 μm. The Sagnac was joined by a specialty coupler which was specified to be 50:50 for one linear polarization and 100:0 for the orthogonal polarization. In this way, the signal would be split into two counterpropagating pulses, while the control would traverse the loop in one direction only. The control and half of the signal would undergo repeated collisions, so as to achieve a phase shift. Interference of the phase-shifted half of the signal with the reference half of the signal would result in some transmission from the normally reflective Sagnac.

As a source, we used an additive pulse mode-locked Tl:KCl color center laser which was synchronously pumped at 100 MHz by an actively (acousto-optically) mode-locked Nd:YAG laser. The APM laser provided 230 fs pulses, each of which was split into orthogonally polarized control and signal pulses of equal energy for the switch. Each pulse had twice the fundamental soliton energy, and the switching energy was 195 pJ. A delay stage was used to adjust the timing difference between signal and control.

Because the differences between the colliding signal and control pulses, and because of the pulse widths and distance, I designed the switch such that every other section of fiber was of the same length, while neighboring fibers differed in length by a small amount. This was so that the more intense pulses would spend more time along the slow axes of the fibers than the lower intensity pulses, to compensate the differential Raman self-frequency shift. This alternation of lengths would of course be unnecessary if all of the pulses in the loop were the same.

In the lab, we found that the specialty coupler did not behave as advertised, nor were we able to improve its performance. While the coupler leaked very little of the polarization which was supposed to be unaffected by the coupler, the polarization which should have undergone a 50:50 splitting underwent a 61.5:38.5 splitting (at best). This was a serious problem because the split pulses were supposed to be solitons, and since the device length was four soliton periods, each imperfect pulse underwent significant shape modification and radiated considerable dispersive wave radiation. This degraded the constructive interference and led to pedestals. The results are shown in Fig. 2-5. A polarizer was used at the output to select only the signal polarization. The lower trace shows the leakage through the device when only signal pulses were present. The upper trace shows the enhanced transmission with control pulses present. We found that, as expected by design, the enhanced transmission persisted as we adjusted the delay between signal and control by several pulse widths. The autocorrelation contrast ratio was 2.82:1.

2.3 MIT Switch Design

The switch design is quite straightforward. In fact, the basic approach to design is applicable to a variety of switches based upon collisional phase-shift accumulation. First, the amount of phase shift per collision depends upon the relative speed of the pulses, their energies and polarizations. The collision must be sufficiently rapid that the pulses not undergo significant shape changes during a collision (what is "significant" depends on the purpose of the switch). The number of sections in the switch is simply the number required to achieve a π-radian phase shift. Section lengths are determined by the amount of timing jitter to be tolerated. Another constraint, which is perhaps surprising but could be very relevant at high bit rates and high powers, is that the average power passing through the switch should not exceed a Watt or so, or the fiber core could melt. If narrow, high-intensity pulses are used, Raman can become a problem. If the pulses within the loop are unequal, they will downshift by different amounts in the loop, and the section lengths will have to be
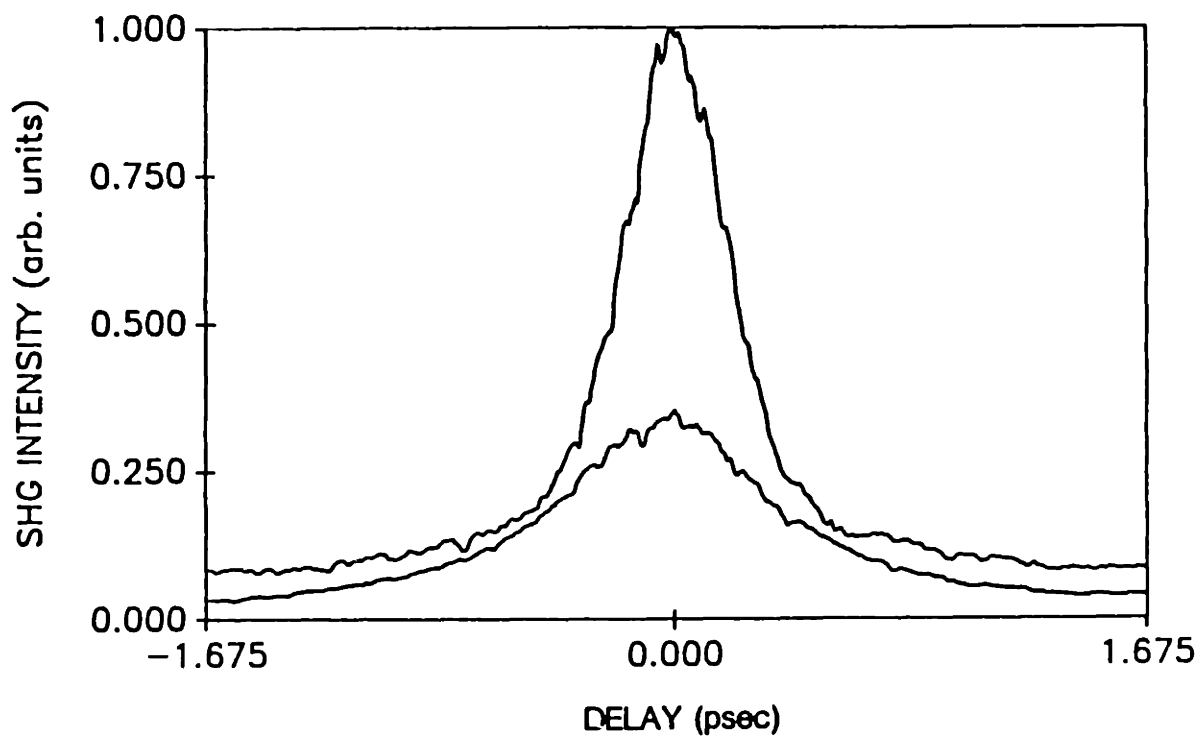
Figure 2-5: Signal pulse at output. Lower trace: no control pulse. Upper trace: enhanced transmission via collisions with control pulse. SHG, second-harmonic generation.

adjusted to compensate.

We can estimate the phase shift in one collision using soliton perturbation theory [109, 110, 21] (see also Chapter 5). In the rapid-collision limit for equal-frequency pulses, we ignore the coherence terms. The nonlinear Schrödinger equation is linearized about soliton #1, the cross-phase modulation term from the coupled nonlinear Schrödinger equations is treated as the perturbation, and a projection is performed onto that linear bound-state eigenfunction which is interpreted to represent the change in soliton phase. The reader should refer back to the description of the CNSE's in Chapter 1. The equation of motion for the soliton phase is

$$\frac{d\,\Delta\theta}{dz} = \mathrm{Re}\int_{-\infty}^{\infty} dt\, \underline{f}_{\theta}^* \left(-j\delta_2|v|^2 u^{(o)}\right) \tag{2.1}$$

where

$$u^{(o)} = A_1 \mathrm{sech}\left(\frac{t}{\tau_1}\right) \tag{2.2}$$

is a solution of the CNSE's if $v = 0$ and is used as the zeroth-order solution for the perturbation theory,

$$A_1^2 = \frac{|k''|}{\delta\tau_1^2}\,, \tag{2.3}$$

$$\delta = \left(\frac{2a + b\cos^2\theta}{2k_o}\right)\,, \tag{2.4}$$

$$\delta_2 = \left(\frac{a + b\sin^2\theta}{k_o}\right)\,, \tag{2.5}$$

and the product of the phase projection function with $u^{(o)}$ is

$$\underline{f}_{\theta}^* u^{(o)} = -\frac{2j}{n_o} A_1^2 \mathrm{sech}^2\left(\frac{t}{\tau_1}\right) \left[1 - \frac{t}{\tau_1}\tanh\left(\frac{t}{\tau_1}\right)\right]\,. \tag{2.6}$$

I have used the subscript "1" just as a reminder that the v-pulse may have a different amplitude and width than the u-pulse. We are interested in the total phase shift from the collision, so we should integrate over z. The only z-dependence in the integrand on the right-hand side (RHS) is that of $|v|^2$. Suppose that the intensity profile of v remains essentially unchanged as it collides with u, so that $|v|^2$ is a function of the single argument $(t - v_g^{-1}z)$. Then,

$$\int_{-\infty}^{\infty} dz|v|^2 = \frac{1}{|v_g^{-1}|}\int_{-\infty}^{\infty} dt|v|^2 \equiv E_v/|v_g^{-1}| \tag{2.7}$$

where we have denoted the field energy of v as E_v. So, if we reverse the order of integration in the equation for $\Delta\theta$, performing the integral over z first, then the integral over t is simply the integral over δ_2 times the projection function. The latter integral evaluates to δ_2, and the result is that the increase in phase resulting from one collision is

$$\boxed{|\Delta\theta| = \delta_2 E_v/|v_g^{-1}|.} \tag{2.8}$$

The phase shift equals the product of the cross-phase modulation coefficient with the energy of the v pulse, divided by the magnitude of the relative inverse group velocity.

If one channel has index of refraction n and the second channel has index $n + \Delta n$, then

$$v_g^{-1} = \left(\frac{n + \Delta n}{c} - \frac{n}{c} \right) = \frac{\Delta n}{c}, \tag{2.9}$$

which is not the reciprocal of the group velocity. This is simply because the equation of motion describes the change of the time profile with distance. The relevant measure of "speed" is the timeshift over a fixed distance, rather than the usual notion of velocity as a shift in position over a fixed time interval.

Now we have an expression for the collisional phase shift, but the expression is approximate, and, conservatively, we would like to achieve collisions which leave the pulses undistorted. A rough (and conservative) rule for equal pulses, based upon comparison of simulations and theory [111] is to keep the normalized slip parameter

$$\text{slip} = \frac{(k' - l')\tau}{|k''|} \approx \frac{\tau \, \Delta n}{|k''|c} \tag{2.10}$$

greater than 3 or so. The meaning of this is that the pulses should travel at least 3τ (roughly five FWHMs) relative to each other over a distance of one characteristic length. The value selected for the normalized slip depends upon the total number of collisions, length of the device, and tolerance for distortion. If slip is measured in terms of the switched pulse (thus, $\tau = \tau_1$), then the required minimum slip will increase as the switching pulse power increases. Not only is this a limitation in the above approach, but also it is unlikely that a large improvement can be attained using (say, N=1) pulses of different widths.

Timing jitter insensitivity is a very desirable feature of the MIT switches. The amount of insensitivity depends upon the length of each section of birefringent fiber. The length of a section can be written

$$L_{\text{section}} = \frac{N_\tau \tau c}{\Delta n} \tag{2.11}$$

where N_τ is the number of pulsewidths of timing shift between the pulses in the fast and slow axes in propagating through the section, τ is the pulsewidth, c is the vacuum speed of light, and Δn is the difference in the effective index of refraction of the fast and slow axes. One might expect that $N_\tau = 2$ would be a minimum value, and that this would be a good value only where the timing jitter is negligible. With timing jitter, $N_\tau \geq 4$ is perhaps a good rule of thumb. Reasonable numbers might be $N_\tau = 4, \tau = 500\text{fs}$, and $\Delta n = 3 \times 10^{-4}$, which gives $L_{\text{section}} = 2\text{m}$.

It seems unlikely that the spatial periodicity of an MIT switch will lead to significant coupling of energy out of the pulses and into dispersive waves. This is especially true if the splices are not very lossy (so that there is little pulse amplitude variation) and the birefringence is high (suppressing nonlinear polarization rotation). However, it is wise in general when designing devices to bear in mind the potential for instabilities.
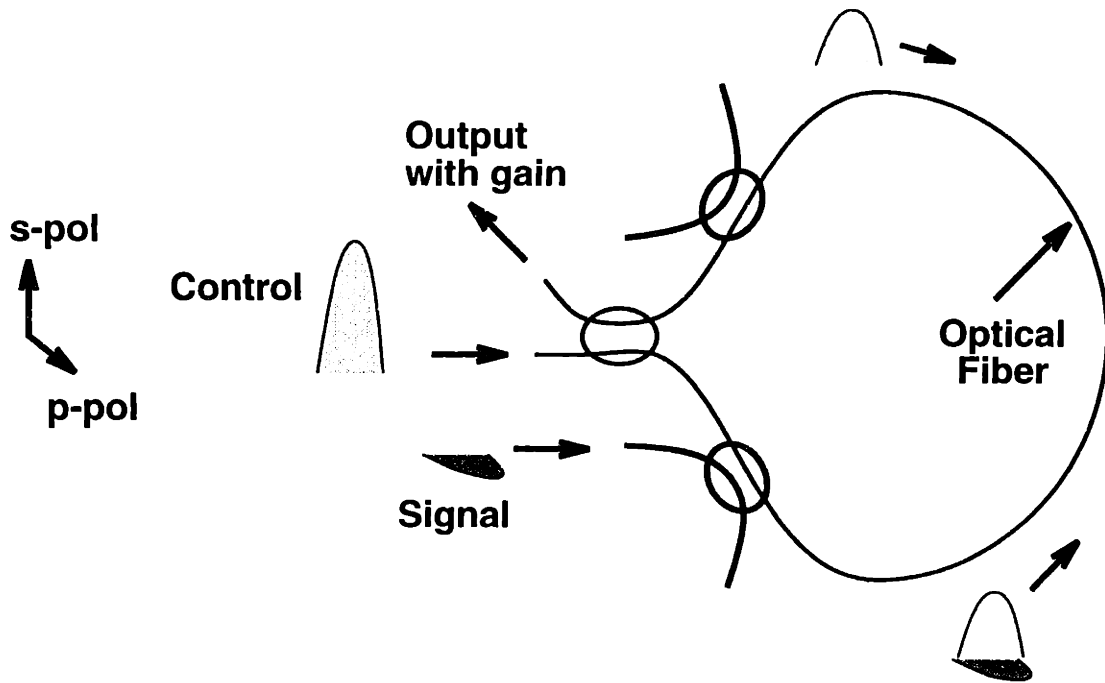
Figure 2-6: A two-input AND gate. Cross-splices in loop not shown. The coupler closing the Sagnac is 50:50. The couplers inside the loop are BAR for the control polarization and CROSS for the signal polarization.

It is desirable to minimize the propagation delay in an all-optical switch. Contrary to this goal is the desire to minimize the amount of energy required for switching. Likewise, avoiding short pulses avoids Raman downshifting. Optimizing the switches depends on the types of operations being performed, and conversely, the details of the architecture are optimized depending upon the characteristics of the switches.

It is quite straightforward to design switches which perform any Boolean operation. For example, an AND gate which uses only the two input pulses is shown in Fig. 2-6. One input, which I shall call A (the control in Fig. 2-6) is split by the Sagnac and the other input, B (the signal in Fig. 2-6), is coupled inside the loop in the orthogonal polarization. If the loop is normally reflecting for A, then this device acts as an AND gate, with Boolean output AB. Of course gain or loss is required for one input if the device is to be perfectly balanced and use solitons in the loop. If the device does not need to have symmetric inputs, and there is no loss or gain at the inputs, then the control A will have greater energy than B, so relative to B, the device has gain. If the loop is normally transmitting, this device will output $A\overline{B}$. This is not a standard logic gate, but it is nevertheless useful at times to be able to distinguish two inputs (e.g., for pattern recognition).

Other gates can be designed which have two data inputs and a clock input. The clock could in principle be used in a manner similar to its usual use in digital electronics so that a switched output only appears if the data inputs are properly timed.
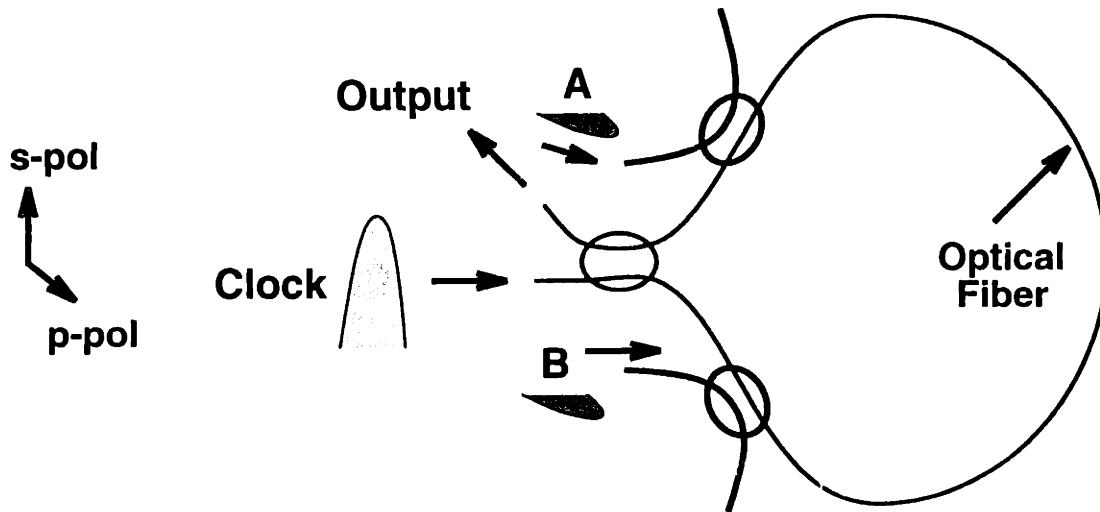
Figure 2-7: An XOR or $\overline{\text{XOR}}$ gate. Cross-splices not shown. The coupler closing the Sagnac is 50:50. The couplers inside the loop are BAR for the control polarization and CROSS for the signal polarization.

However, in this case, the motivation is simply to design gates which can output ONEs when there is no data input. An example is shown in Fig. 2-7. This device is completely symmetric in A and B, and when there is an output, it is the clock pulse. In this device, the inputs travel in one direction around the loop, opposite to each other, adding nonlinear phase to the corresponding half of the clock pulse. If the device is normally reflecting for the clock, then a single input provides the π phase shift needed for transmission of the clock. If both inputs are high, both halves of the clock are phase shifted so that there is no relative phase and the clock reflects. Thus, this is an XOR gate. If the device is normally transmitting, then we have an $\overline{\text{XOR}}$ gate. Note that an $\overline{\text{XOR}}$ gate with a single input is an inverter. With inverters and AND gates we can construct any Boolean logic gate. For example NAND and NOR are Boolean complete. To build a NAND gate one can follow an AND gate with an inverter, as illustrated in Fig. 2-8. To build a NOR gate, one can invert the two inputs to an AND ($\overline{\text{A} + \text{B}} = \overline{\text{A}}\,\overline{\text{B}}$).

It is the nature of the switches discussed above that one loop serves to compare only two inputs. To do multi-input comparisons generally requires cascaded loops, which implies greater latency. So long as latency is a problem, parallelism (a tree structure) with two-input gates will likely be preferable to single multi-input gates (unless of course the "multi-input gate" is the appropriate tree structure).

There are uses for nonstandard gates such as the $\text{A}\overline{\text{B}}$ gate discussed above. An-
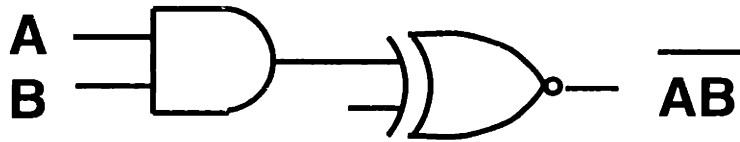
Figure 2-8: NAND gate as cascade of AND and $\overline{\text{XOR}}$ inverter.

other type of alternative gate compares bits in different clock cycles. This is again useful for pattern recognition. An example is shown in Fig. 2-9, which is essentially the same as Fig. 10 in Ref. [100]. Special polarization-sensitive coupler is shown in the figure, but as in Figs. 2-6 and 2-7, more ordinary polarization-selective couplers can be used internal to the loop, and a simple 50:50 coupler can close the Sagnac. The device has two inputs A and B which are offset in time. The C input is polarized orthogonal to A and B. It can be timed to be between the A and B pulses, as shown. The device is designed so that C and B collide repeatedly in the first loop, and C and A collide in the second loop. So if both loops act as AND gates, the device outputs a ONE only when A and B (and C) are high. If the first loop is an AND and the second is a $\overline{\text{CA}}$, then the output of the device is high only when B is high and A is low. Continuing in this manner, any sequence of two bits can be identified. In fact, we can cascade as many loops as we wish, and match patterns of any length. However, we incur latency which grows linearly with the number of bits in the pattern. For large patterns, it may be more efficient to replicate the pattern and perform parallel pairwise comparisons. To design a reconfigurable pattern-matcher, one could have both an AND and a $\overline{\text{DE}}$ at each stage, with a routing switch to select one of the gates. The routing switch could be activated with a control stream of pulses.

2.4   Other Switching Concepts

2.4.1   XPM Collision Switches Using Pulses Other Than Fundamental Solitons

Instead of collisions of fundamental (N=1) solitons, one might try to achieve a large phase-shift quickly by using an N≫1 pulse to perform the switching on an N=1 soliton. If phase-shift is proportional to switching pulse energy, and if 25 collisions would be required if v were an N=1, then v would have to be an N=5 for switching in a single collision. One problem is that such pulses spread very rapidly in the time domain, and would likely do so irreversibly because the high power of these pulses makes them more sensitive to non-NSE fiber properties. Such pulses would have to be

38
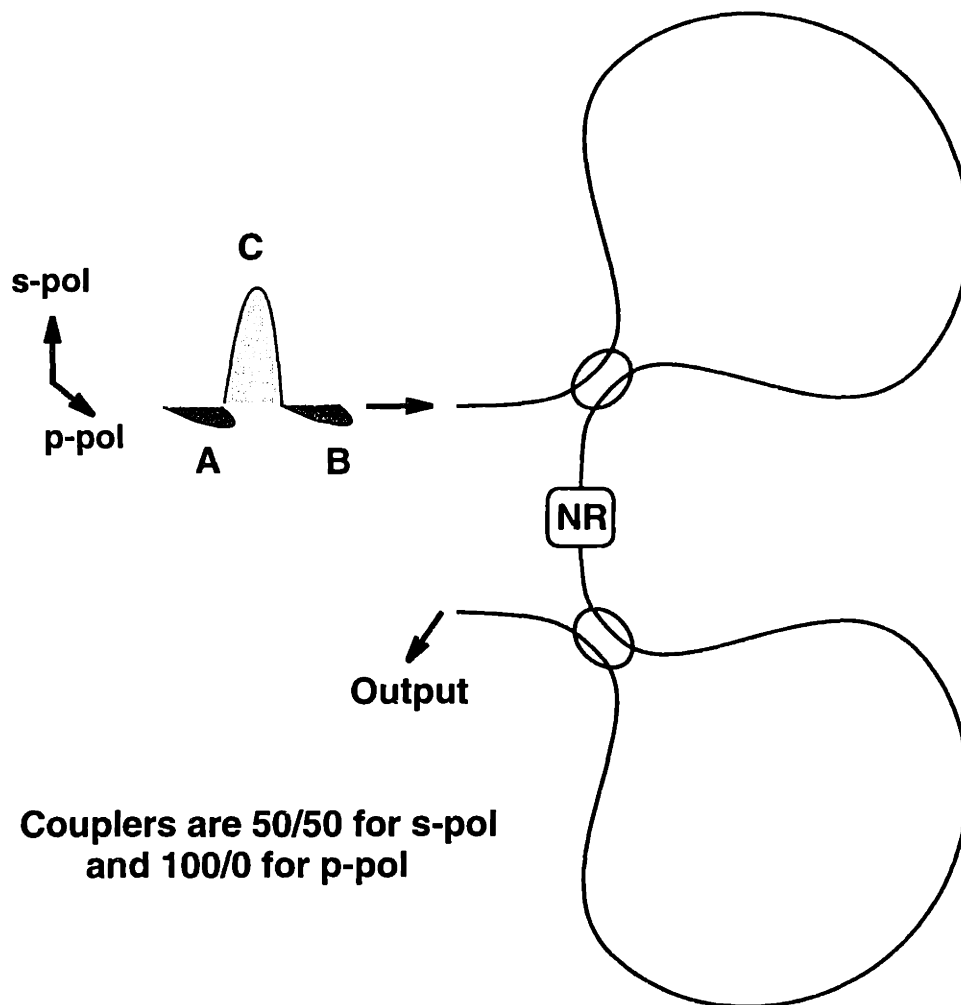
Figure 2-9: Two-bit pattern recognition gate: if both loops act as ANDs, output is high iff both inputs A and B are high. NR = nonreciprocal element. Cross-splices not shown.

removed from the switch before the wings spread outside the bit interval. This would likely require that all collisions would have to occur in much less than one soliton period. Furthermore, such high-power collisions would likely result in large timing shifts per collision, so it would probably be necessary to choose an even number of collisions.

One could go even further by using both switched and switching pulses which are supersolitonic and for which the dispersion length greatly exceeds the length of the switch. As usual, collisions could be achieved using pulses in different polarizations or of different frequencies. By using one or more complete collisions, the cross-phase modulation-induced phase shift should be uniform. However, each pulse acquires significant chirp from self-phase modulation. This goes completely counter to the philosophy of the soliton switches, in which solitons are used because they maintain constant temporal shape AND spectral shape. Using solitons ensures cascadability and WDM-compatibility. Nevertheless, if active devices are used to replace pulses before they degrade, solitons may be unnecessary.

2.4.2 XPM Copropagation Switches

Farzana Khatri and I have begun an experiment, described in the paragraph following this one, to test a cross-phase modulation switching concept which sacrifices timing-jitter insensitivity for gain and reduced switching energy, and perhaps reduced latency. It is likely that timing restoration need only be performed on data which have traveled some distance greater than the distance between ports of a node. Thus incoming data would pass through a single timing restoration device, and then subsequent logic within the node would be performed with devices which are timing-jitter sensitive.

The device concept we are testing uses a Sagnac loop which splits pulses in one polarization (label it "signal") and can be biased so that the loop is normally reflecting or transmitting for these pulses. The same layout as shown in Fig. 2-6 is used, except that ordinary fiber can be used - no cross-splices are required. The pulses in the orthogonal polarization ("control") traverse the loop in one direction only. Rather than using collisions, we launch the pulses into the loop of nonbirefringent fiber so that they copropagate, phase shifting each other continuously through the loop, achieving XPM phase very efficiently. However, if the loop length is great enough that the dispersion plays a role in pulse shaping, it will be necessary to make both a half-signal and the half-signal-plus-control nearly solitons within the loop. The control pulses are very much sub-solitonic in the loop. When a control pulse is launched simultaneously with a half-signal pulse, the two form a near-soliton which is in a different polarization than the half-switching pulses alone. If the loop is normally transmitting for the signal pulses, and there is a polarizer at the output which selects the signal pulses and rejects the controls, and the controls are the incoming data, then the device operates as an inverter with "gain" (the small data pulse has been replaced with a big signal pulse). If the device is too long, or the data pulses too energetic, the nonlinear polarization rotation of the copropagating pulses must be accounted for. Our experiment is very much like this example.

It might appear that it would be best to use very intense pulses to make the

switch short and to avoid the distortion from the interplay of nonlinear phase and dispersion, but in order to do so, the data pulses would have to have constant intensity across the switching pulses to achieve flat nonlinear phase and complete switching. There are lots of ways to produce pulses which would be sufficiently square for this application - examples being cascaded nonsoliton loop mirrors, cascaded polarization rotation intensity discrimination devices, and perhaps other overdriven Ginzburg-Landau [112] devices. High power may in fact prove to be the best approach, but silica fiber will probably not be the right medium because of the small product of nonlinearity and melting energy [113].

2.4.3 Time-Domain Switches

Switches which do not utilize interferometers include time domain switches, such as soliton trapping gates [108], soliton dragging switches [107, 114], and time-domain chirp switches [106, 115, 116], all of which have been fabricated and tested by M.Islam et al. at AT&T and analyzed by both the AT&T group and by C.R.Menyuk et al. at the University of Maryland. As with most gates, the presence/absence of a pulse in an input port (or polarization, etc.) indicates a ONE or ZERO in that port. The basic principle of a time-domain switch is that the time delay for a pulse traveling from the input to the output of a device can be used for logic. However, this requires very fast gating (i.e., another ultra-fast all-optical logic gate...) or cross-correlation (inefficient) at the output of each switch.

As an example, consider a device which has inputs A and B, and which passes only the (possibly modified) A pulse as its output. Suppose furthermore that the time delay for A traveling from input to output is different (by at least two pulse widths) depending on whether B is a ONE or a ZERO. If the cross-correlator operates as a gate to pass pulses arriving within a time window which includes the output A pulse only when the B input was present, then the device operates as an AND gate.

Soliton trapping switches utilize the frequency shifts of pulses which are orthogonally polarized and overlapping in birefringent fiber, and which form a bound state. Trapping switches require that the incoming pulses be nearly synchronized so that each will be trapped in the potential well of the other pulse, in a birefringent fiber. The concept is illustrated in Fig. 2-10. For a given birefringence, there is a minimum power requirement in order for the bound state to be formed, obviously with more power required at higher birefringence. In order to form a bound state, the pulses must shift their center frequencies (initiated by cross-phase modulation) so as to have equal group velocities. Of course, pulses which are orthogonally polarized and are detuned so as to cancel the birefringence walk-off will more readily form a bound state, but this would not be useful for the device described here. The bound state of the equal-frequency pulses is generally a nonequilibrium state, and will radiate dispersive wave energy. If the bound state is to be close to an N=1 soliton-like pulse [117, 118, 119], without radiating too much continuum, then the input pulses must be sub-solitonic, and the interaction must occur soon after the pulses enter the fiber, or else they will disperse and not trap.

The bound state travels at a group velocity which is between the group velocities

41
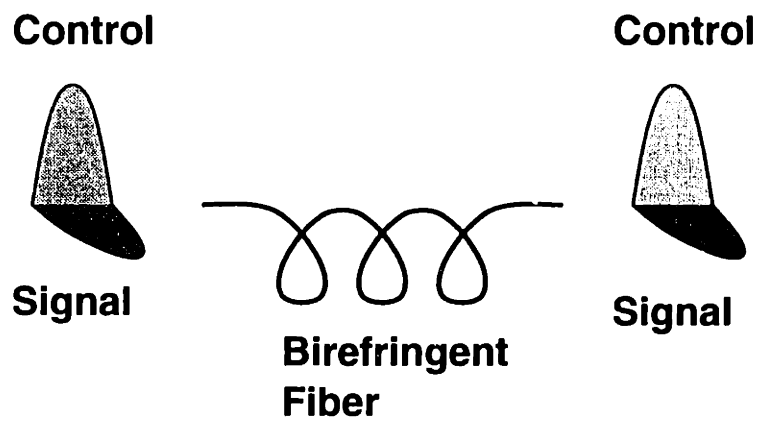
Figure 2-10: Soliton trapping. Coincident, equal-carrier-frequency, orthogonally polarized solitons are launched into a moderately birefringe , fiber. Through cross-phase modulation, they shift each other's carrier frequencies so as to remain a bound state. One of the output pulses is upshifted and one downshifted from the launched carrier frequency.

Signal

Control → | Nonlinear Chirper | → | Soliton Dispersive Delay Line | → **Control**

(a)

Control

Signal

Moderately Birefringent Fiber

Polarization- Maintaining Soliton Fiber

Polarizer   **Control**

(b)
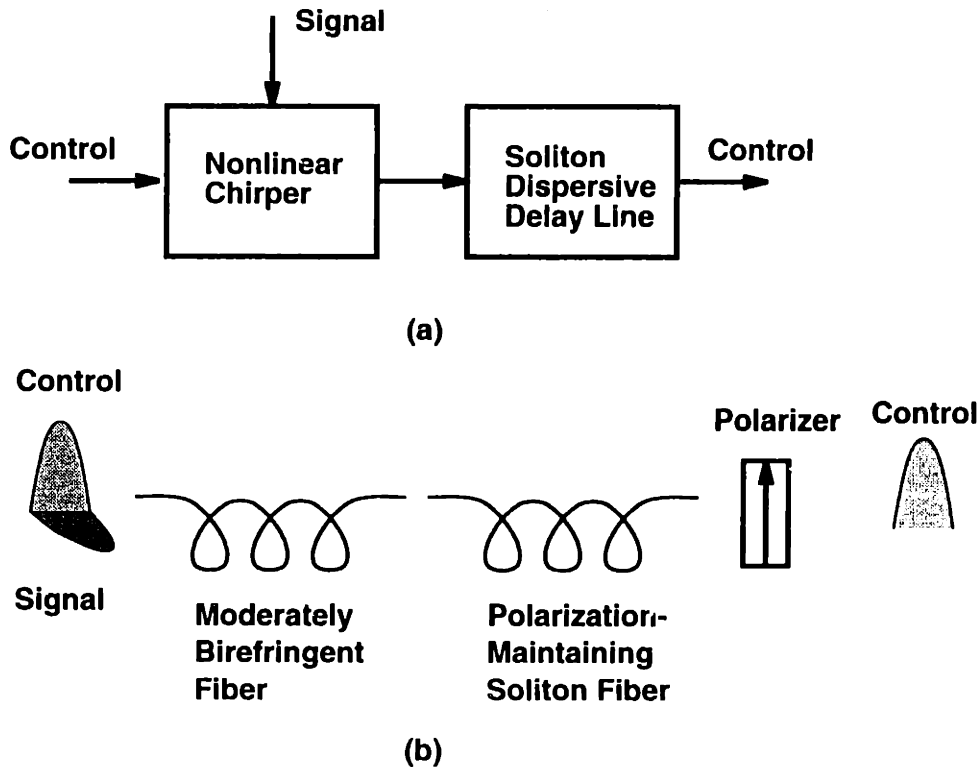
Figure 2-11: Time-domain chirp switch. (a) block diagram. (b) one implementation.

that each pulse would have in the absence of the other pulse. Thus, with ultra-fast gating (likely another type of all-optical switch) or with some sort of cross-correlation scheme, the timing shifts can be used for logic operations. If the trapping results in sufficiently large frequency shifts, filtering could be used to remove one of the pulses. Trapping devices are very sensitive to timing errors in the inputs, they do not produce clean solitons, and they generate dispersive waves.

An improvement is the soliton dragging approach. Rather than forming a bound state of two orthogonally polarized pulses, we cause the two pulses to collide in an asymmetric fashion. This can be done by launching the pulses into the birefringent fiber so that they overlap, and the collision is incomplete. A device using this approach is illustrated in Fig. 2-11 (the figure is based upon a figure of Islam et al. [106]). Or the collision can be asymmetrized by prechirping one of the pulses so that it compresses during the collision. Or an amplifying or lossy birefringent fiber could be used, etc. Early switches used collisions with large frequency shifts, leading to shifted carrier frequencies, so that filtering could be used to separate the pulses. Such strong interactions lead to distorted pulses and continuum, in addition to the problem of frequency-shifted output. More recent switches have used small frequency shifts, followed by long sections of fiber in which the small chirp leads via GVD to a timing shift. These time-domain chirp switches offer improved, but still far from perfect timing insensitivity. And the problem of cross-correlation remains.

43

2.4.4 Nondegenerate Four-Wave Mixing

An alternative might be to use nondegenerate four-wave mixing (4WM) in semiconductor traveling wave amplifiers [40]. The data and a frequency-shifted pump (e.g. a train of pulses or a block of strong CW of length equal to that of a packet) would mix in the TWA and generate new pulses at a new frequency which could then be filtered out. One likely problem is that the new pulses are not transform-limited -- two photon absorption and self- and cross-phase modulation degrading the pulses. Second, the device in this simple form can perform only an AND function, which is not Boolean complete.

If this approach were used for switching out of a soliton storage ring, the residual pulses would be a problem. As a possibility, successful tapping could trigger the suppression of a packet's worth of clock pulses in a regenerative buffer (see Chapter 6, Network Devices, the section on Buffers/Memories). Or, in a laser-style buffer, the 4WM pump could be fed into the loop to saturate the gain to kill the residual data. The pump could be filtered out of the loop after one roundtrip. This approach might render the ring inoperable for an unacceptably long time, however.

2.4.5 Polarization Rocking Switches

Another concept which can be applied to switching is the polarization rocking concept, which was originally employed in the design of passband filters [120]. The device consists of sections of birefringent fiber of equal length spliced together in series. Every other section of fiber has the same birefringence axis orientation. Neighboring sections have axes which differ by some small angle (twist angle θ_t), e.g. by one degree. Two adjacent sections of fiber constitute one twist period. For some frequency, each section of fiber is exactly one-half of a beat length (beat length $= \lambda/\Delta n$, where λ is the wavelength and Δn is the difference in index of refraction between the fast and slow axes). This means that the light components along the slow and fast axes acquire an extra π-radian phase shift between them, in traversing one section. So if light enters the device linearly polarized along the fast axis of the first section of fiber, it remains so polarized throughout the first section. Upon entering the second section, the light is linearly polarized at an angle θ_t to the fast axis of this second section of fiber. When it reaches the end of the second section, it is linearly polarized at an angle of $-\theta_t$ to the fast axis. Upon entering the third section, the light is linearly polarized at an angle of $2\theta_t$ to the fast axis of the third section. This continues with the light advancing by an angle of $2\theta_t$ in each twist period.

At other frequencies, power will not be so efficiently coupled. Thus, with a polarizer, the device acts as a passband filter. Stolen et al. demonstrated filters with the following typical numbers: passbands of the order of 5-10nm at a wavelength λ of around 600nm, twist period of 1.5cm, $\Delta n = 4 \times 10^{-5}$, and total fiber length of 200cm. Even scaling to 1.55μm, the device would be only around one half meter long.

So far, the analysis has been entirely linear. As discussed in the introductory chapter, through the Kerr effect, the index of refraction of the medium changes by an amount proportional to the intensity of the light propagating within the medium.

44

Thus, in a birefringent medium, light can change the birefringence, and therefore the beat length. For example, suppose the usual pulses entering the device are effectively linear and that high-power control light is launched into the device orthogonal to the signal. The full analysis could get rather complicated, but it is clear that in the presence of the control light, the birefringence will be different than when the control light is absent. Thus, it should be possible to design a device which rotates the signal light by angles differing by 90 degrees depending upon the presence or absence of the control. This has actually been achieved experimentally [50]. The author suggests that with CW pump light over a packet interval, this device could serve as a compact (less than one meter!) packet switch.

2.5 Summary

In this chapter, I have provided an overview of current all-optical switching ideas, with emphasis on (nearly) lossless switches. A significant portion of the chapter was devoted to the cross-phase modulation switches designed, fabricated and tested at MIT and C.S.Draper Laboratories by the author and coworkers at MIT and C.S.Draper Labs. Some of the author's ideas for switches which have yet to be built were presented, as well.

Chapter 3

Ultra-Long Distance Wavelength-Division-Multiplexed Soliton Transmission Using Inhomogeneously Broadened Fiber Amplifiers

3.1 Introduction

Note to the reader: this chapter is based upon reference [121].

It may be possible to wavelength-division-multiplex (WDM) solitons for multi-megameter distances, while it appears less likely that WDMed conventional linear transmission will be feasible for such distances[11, 122, 123, 124]. Two-channel WDM soliton transmission has been achieved [16] An important problem to be solved before multi-channel soliton WDM becomes a reality, however, is the problem of gain equalization. That is, each of the WDM channels should experience the same average gain over the course of transmission. However, the gain spectrum of an EDFA is generally quite peaked, and the frequency-dependence of the fiber loss only tends to make matters worse. Practical schemes exhibiting dynamic gain equalization for more than two wavelength channels for ultra-long distance soliton transmission have not been demonstrated to date, to the author's knowledge.

Many of the EDFAs discussed in the literature to date exhibit primarily homogeneous broadening. It may be difficult to dynamically equalize the gain for multiple WDM channels using such amplifiers [125]. Some sort of channel scrambling scheme, in which the data hops (via nonlinear mixers) between channels at several locations along the transmission line, might achieve net gain equalization for all channels [126]. However, here I propose that inhomogeneously-broadened gain media may be suitable for soliton WDM. Several authors have reported inhomogeneous broadening with erbium-doped fibers with germanosilicate ($GeO_2{:}SiO_2$) cores [127, 128, 129, 130].

In inhomogeneously broadened media, there is some degree of independence of the

46

gain saturation for channels at different wavelengths. If nearest-neighbor channels are separated by a homogeneous linewidth, one can saturate so that each channel sees the same gain. Cross-saturation limits the minimum channel-spacing. Continuously-operating low-power lasers (control lasers) tuned in between the channels could be adjusted through feedforward/feedback to maintain the desired saturated gain profile with time-varying data. A related compensation scheme has been demonstrated with homogeneously broadened fiber amplifiers [131]. Narrowband notch filters, such as the proposed channel-dropping filters [132, 133], could be used to filter the control laser output.

3.2 Amplifier Model

For the purposes of this discussion, it will suffice to consider a simplified model of an erbium-doped fiber amplifier. I shall assume a superposition of simple two-level systems, and I shall use a truly lumped model, assuming that the effects of propagation within the amplifier can be incorporated into an overall gain profile. For more thorough modeling, see Giles and Desurvire [134] and references therein.

The lineshape of the gain for a two-level system can be written (this is a simple generalization to several narrowband saturating signals, and simplification to a two-level system, of an expression given by Yariv [135])

$$\gamma(\nu) = \frac{\Delta N^0 c^2}{8\pi n^2 \tau_{sp} \nu^2} \int_{-\infty}^{\infty} \frac{g_h(\nu, f) g_i(f) df}{\left(1 + \frac{c^2}{8\pi n^2 h} \sum_{j=1}^{M} \frac{g_h(\nu_j, f) I_{\nu_j}}{\nu_j^3}\right)} \tag{3.1}$$

where $I(\nu, z) = I(\nu, 0) \exp\{\gamma(\nu)z\}$, z is distance of propagation through the gain medium, the notation $I(\nu)$ or I_ν henceforth implies $z = 0$, ν is frequency, I is spectral intensity, ΔN^0 is the steady-state population inversion with no optical signal present, c is the speed of light in vacuo, τ_{sp} is the spontaneous emission lifetime for transitions from the upper state to the lower state, $g_i(f)$ is the probability distribution of homogeneous packets (used in determining the inhomogeneous lineshape) satisfying

$$\int_{-\infty}^{\infty} g_i(f) df = 1, \tag{3.2}$$

f is frequency, $g_h(\nu, f)$ is the homogeneous lineshape centered about $\nu = f$ satisfying

$$\int_{-\infty}^{\infty} g_h(\nu, f) d\nu = 1, \tag{3.3}$$

ν is frequency, M is the number of WDM channels plus the number of control lasers, ν_j denotes the center frequency of a narrowband signal (WDM channel or control laser), I_{ν_j} denotes the corresponding intensity temporally-averaged over several bit periods, n is index of refraction, and $h = 6.6262 \times 10^{-34}$ J·s is Planck's constant. Note that the integral is symmetric in ν, but the lineshape is not quite symmetric, because of the ν^2 in the denominator. Wanting values for ΔN^0 and z, I shall conservatively

assume a peak unsaturated gain of 31 dB, which is 3 dB below the value measured by Laming et al. [127].

For WDM transmission, $I(\nu)$ is the spectral intensity of several on-off keyed (OOK), return-to-zero (RZ) pseudorandom trains of pulses (most probably solitons). I choose to simplify things by assuming that the gain recovery time is long compared to the bit-spacings in any channel, so that the amplifier sees the signal spectral density averaged over several bit-spacings. Fluorescence lifetimes of erbium-doped fibers are typically a few milliseconds [136]. bit being a ONE,

Soliton peak power is a function of wavelength,

$$I_{\text{sol}} = P_{\text{sol}}/A_{\text{eff}} = \frac{\lambda}{4n_2 z_0}, \tag{3.4}$$

I is intensity, P is power, A_{eff} is the effective mode area (which also varies with wavelength, but I shall ignore this), n_2 is the Kerr coefficient which for pure silica is 3.18×10^{-20} m^2/W, and

$$z_0 = \frac{\pi^2 c t_s^2}{4(\cosh^{-1}\sqrt{2})^2 \lambda^2 D} \tag{3.5}$$

is a soliton scale length, where t_s is pulse width, c is the vacuum speed of light, and D is the magnitude of the anomalous group velocity dispersion.

The signal spectrum will be taken to be a series of Dirac delta functions at the channel carrier wavelengths and control laser wavelengths. This is justifiable because the pulse bandwidth, which is the width of the envelope of the (noise-free) data spectrum, is much less than the homogeneous linewidths and the channel-spacings. In the example below, the pulse bandwidth is more than two orders of magnitude less than the smallest homogeneous linewidth. The average intensity at the input to an amplifier for the jth WDM channel is

$$
\begin{aligned}
I_j &= (I_{\text{sol}_j})(\text{weight for sech train})(\text{fiber loss factor}) \\
&= (I_{\text{sol}_j})\left(\frac{t_s R}{2\cosh^{-1}\sqrt{2}}\right)\left(\frac{\alpha_j L_{\text{span}}}{(\exp\{\alpha_j L_{\text{span}}\} - 1)}\right)
\end{aligned} \tag{3.6}
$$

where R is the bit rate, α_j is the (positive) power loss coefficient (m^{-1}) for the jth channel for propagation between amplifiers, and L_{span} is the length of transmission fiber between successive amplifiers.

The objective is to saturate each channel to approximately the same level of gain. The target gain for each channel will not be identical in general, since the loss between amplifiers (and therefore the requisite gain) may be different for the different channels. Equalization in this context is used to mean that the signal power in one channel is preserved when path-averaged, or equivalently, that the level diagram does not manifest growth or decay on a length scale greater than the amplifier spacing. I remind the reader that any wavelength-dependent variations in gain within the amplifier are absorbed into the lumped gain profile in our simplified model.

Zyskind et al. [129, 130] have measured linewidths for transitions near 1.5-1.6 μm in erbium-doped fibers with germanosilicate cores. They have found that the mea-

sured lineshape can be modeled reasonably well between 1.53 μm and 1.55 μm with a Voigt profile with the following: transitions at 1.552 μm (193.2 THz) and 1.543 μm (194.3 THz) with homogeneous linewidths of 3 nm (0.38 THz), and inhomogeneous linewidths of 11 nm (1.4 THz), and a transition at 1.535 μm (195.3 THz) with a homogeneous linewidth of 4 nm (0.51 THz), and an inhomogeneous linewidth of 8 nm (1.0 THz). The relative oscillator strengths of these transitions are 0.53, 0.13, and 1 respectively. Linewidths are taken to be half-power linewidths. In the example below, the gain profile is a superposition of terms of the form (3.1) with the above parameters.

I take the homogeneous lineshapes to be Lorentzian

$$g_h(\nu, f) = \frac{\delta_h}{2\pi\{(\nu - f)^2 + (\delta_h/2)^2\}}, \tag{3.7}$$

with δ_h being the width of the distribution at half of its peak magnitude, and f the center frequency. I shall assume that $g_i(f)$ is gaussian

$$g_i(f) = \frac{2}{\delta_i}\sqrt{\frac{\ln 2}{\pi}} \exp\left\{\frac{-(4\ln 2)(f - f_{ctr})^2}{\delta_i^2}\right\}, \tag{3.8}$$

where δ_i is the full-width at half-maximum, and f_{ctr} is the frequency of the center of the distribution.

In this chapter I will consider an example with soliton transmission in seven WDM channels at 2 Gb/s each. I shall suppose that within a channel, the solitons are separated by 5 times the pulsewidth [122]. Thus the solitons have a 100 ps width, corresponding to a transform-limited power spectral density half-width of $0.314/(100\text{ps}) = 3$ GHz. Thus another simplification is possible, as mentioned above, because the pulse bandwidth is much smaller than the homogeneous linewidth and the channel-spacing. I shall assume non-bursty traffic, and equal numbers of ONEs and ZEROs averaged over the gain recovery time. I shall also assume that the loss between amplifiers is the same for each of the seven WDM channels, and therefore that the desired gain is indeed equal for each channel. When specific results are presented, the following parameters are assumed: anomalous group velocity dispersion $D = 1$ ps/nm/km, loss between amplifiers = 0.21 dB/km, distance between nearest-neighbor amplifiers $L_{\text{span}} = 20$ km, and total transmission distance $L_{\text{system}} = 10^7$ m.

3.3 Gain Equalization

The unsaturated lineshape is far from flat (see top curve of Fig. 3-1). There are several ways to achieve equalization. I shall consider an approach which is likely more complex than would be required in practice. The idea is to use passive notch filters to approximately flatten the gain spectrum. The data in each channel further saturates the gain. Finally, fine-tuning is achieved with CW power which is fed into the amplifier (and filtered out afterwards if desired) at strategic frequencies which are detuned from the signal channels. The pulse widths and bit rates, although
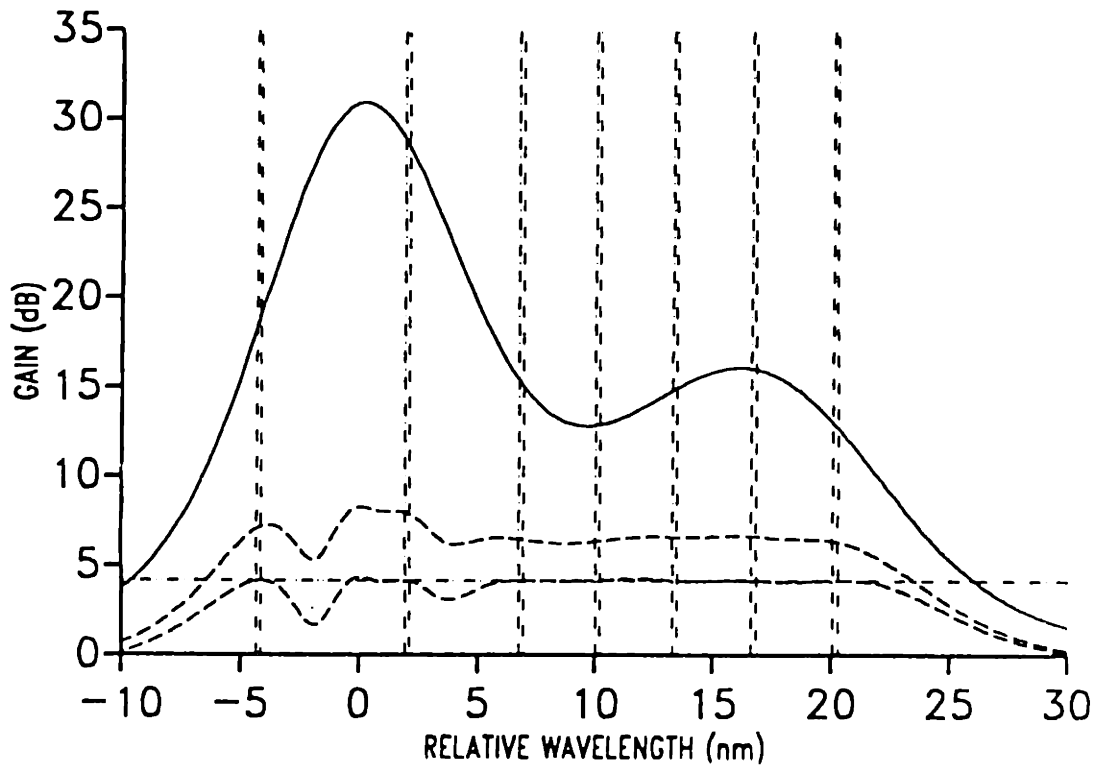
Figure 3-1: Inhomogeneously broadened gain lineshape (log scale). Vertical lines – WDM channels. Horizontal line – target gain. Top (solid) curve – unsaturated. Middle curve – with linear filters for coarse equalization. Bottom curve – with linear filters, 2-Gb/s data in each channel, and control lasers.

potentially useful degrees of freedom, will be assumed to be the same in each channel. A set of passive, linear, Lorentzian notch filters of different stopband bandwidths will be included at each amplifier, to achieve coarse equalization.

More importantly, a control system is needed for dynamic gain equalization. For example, a set of semiconductor lasers, operating continuously at wavelengths in between adjacent channels, could be placed before each amplifier. These control lasers would affect the saturation of the gain without disturbing the bit streams. Through a feedforward/feedback system (see Ref. [131]) the output powers of the individual lasers could be dynamically adjusted in response to data power fluctuations.

Narrowband notch filters could be cascaded following the amplifiers, to remove this power from the transmission fiber, if desired. The consequences of such filtering on interacting pulses, whose spectra are broadened during interaction, need to be investigated. It should be possible to design channel-dropping filters with stopband bandwidths of less than 1 GHz and passbands of over 50 nm [126].

The control systems could perhaps be spaced by several amplifier-spacings. This would impose stricter requirements on the dynamic range of the control systems. The control laser power should be low, so that its propagation between amplifiers is effectively linear.

3.3.1 Linear Filters

Next, consider an example. A set of linear filters and WDM channels was selected to achieve very rough equalization (top curve of Fig. 3-2 and middle curve of Fig. 3-1). The gain profile is a sum of terms of the form (3.1), one for each gain transition. The gain is multiplied by the (power) transfer functions of the intensity-independent passive filters. The I_{ν_j} correspond to the WDM channels, and the control laser wavelengths. The control lasers are conservatively tuned 50 GHz away from the WDM channel center frequencies (50 GHz above each of the three highest frequency channels and 50 GHz below each of the four lowest frequency channels).

The model passive lossy filters have the following (power) transfer characteristic:

$$H_k(\nu) = 1 - h_k \frac{(\delta\nu_k/2)^2}{(\nu - \nu_k)^2 + (\delta\nu_k/2)^2}, \qquad (3.9)$$

where $k = 1, \ldots 5$ labels the filter, h_k is the depth of the notch $(0 < h_k < 1)$, $\delta\nu_k$ is the half-width of the notch, and ν_k is the center frequency. Table 3.3.1 contains the parameters used in the example discussed here.

3.3.2 Channel Separation

In addition to the homogeneous linewidths, another important consideration in determining channel-spacing is the problem of collisions between solitons in the presence of amplifiers. Amplification asymmetrizes the frequency-pulling effect of one pulse on the other, resulting in undesired net frequency-shifts, with subsequent timing jitter [122].

51
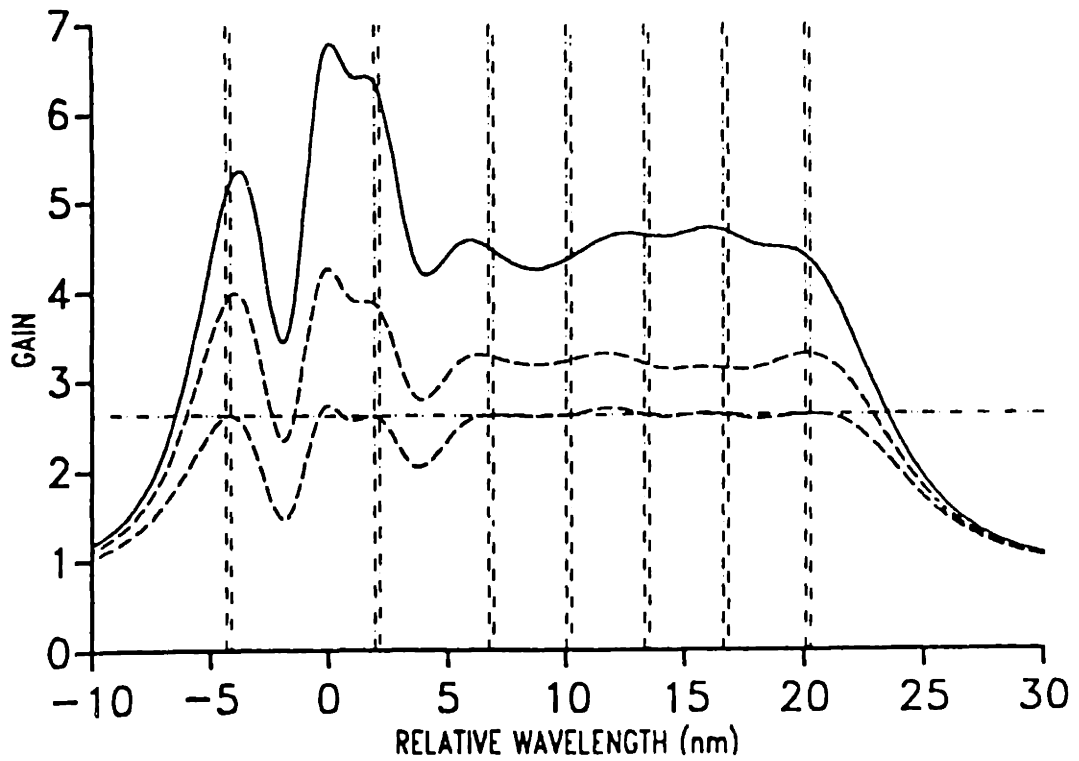
Figure 3-2: Inhomogeneously broadened gain lineshape (linear scale). Vertical lines –
WDM channels. Horizontal line – target gain. Top (solid) curve – with linear filters
for coarse equalization. Middle curve – with filters and 2-Gb/s data in each channel.
Bottom curve – with filters, data, and control lasers.

$\lambda_k^{filter} - \lambda_0$ (nm)	width $\delta\lambda$ (nm)	depth h
-1.80	11.0	0.9597
0.90	12.0	0.9360
3.60	8.0	0.8197
14.60	11.0	0.6448
18.05	11.0	0.6920

Table 3.1: Lorentzian notch filter parameters: center wavelength λ_k^{filter} (nm), $k = 1, \ldots 5$ relative to $\lambda_0 = 1.535\mu$m; width of notch (nm); and depth of notch (fraction of unity). See text.

The maximum such frequency-shift, for one collision of a soliton pair passing through a single amplifier, occurs when the pulses maximally overlap at the location of the amplifier. That is, the collision is centered about the amplifier. Preceding the amplifier, the interacting solitons are weak, having suffered fiber losses, and they interact weakly. There is a weak unidirectional frequency-pulling effect on each soliton due to the nonlinearity. The effect is opposite for the two pulses - i.e. one is redshifted while the other is blueshifted. Beyond the amplifier, the pulses are more intense, and the interaction is stronger, giving rise to a stronger frequency-pulling effect. This frequency-pulling is in the opposite direction (i.e., a pulse which was blueshifted preceding the amplifier is redshifted following the amplifier). In the absence of the amplifier, these effects cancel.

Next I consider how this collisional frequency-shift changes as the wavelength difference $\Delta\lambda$ between the two solitons is varied. Through group velocity dispersion, $\Delta\lambda$ determines the relative speed of the collision. $L_{coll} = 2t_s/(D\Delta\lambda)$ is the collision length which is defined as the distance in which a pulse in one channel travels two pulsewidths with respect to a pulse in the other channel. Solitons colliding at high relative speeds (large $\Delta\lambda$, small collision length L_{coll}) interact weakly. In fact, in the limit $L_{coll}/L_{span} \rightarrow 0$, the net frequency-shift is zero, regardless of the amplifier. As L_{coll}/L_{span} is increased, the interaction becomes stronger, resulting in increasing frequency-shifts. However, when $L_{coll} \approx L_{span}$, the effect of neighboring amplifiers cannot be neglected. The result is that the net frequency-shift is reduced. For example, the amplifier preceding the center amplifier gives rise to frequency-pulling which partially counteracts the frequency-pulling due to the center amplifier. In fact, as L_{coll}/L_{span} is further increased, the net frequency-shift again approaches zero. In summary, the net frequency-shift goes to zero for $L_{coll}/L_{span} \rightarrow 0$ or ∞ and reaches

a maximum in the neighborhood of $L_{coll}/L_{span} = 1$.

In Ref. [122], the authors suggest choosing narrow channel-spacings so that soliton collisions are spread over at least two inter-amplifier spacings, in order to average-out the frequency-shifts. The authors explain that this is a safe upper bound on the separation between the lowest- and highest-wavelength channels for a given amplifier spacing; smaller amplifier-spacing allowing larger wavelength separation. In our equalization example, channels separated by less than 5 nm satisfy the criterion that the ratio L_{coll}/L_{span} be greater than 2. Most of our channel-spacings violate this criterion, but the net timing-shifts are tolerable, as shown below.

The expression for the magnitude of the frequency-shift experienced by a pulse in a collision is

$$\Delta f_{coll} = \frac{8\alpha L_{span}^2 x^4}{\pi^2 t_0 z_0} \sum_{j=1}^{\infty} \frac{j^4 \operatorname{csch}^2(jx)}{\alpha^2 L_{span}^2 + (2\pi j)^2}, \tag{3.10}$$

where $\alpha = 48$ Mm^{-1} is the (power) loss coefficient, $x = 2.80 L_{coll}/L_{span}$, $t_0 = t_s/1.763$, and the soliton period is

$$z_0 = \frac{\pi^2 c t_0^2}{\lambda^2 D}.$$

This result can be derived as in the appendix of Ref. [122].

The frequency-shifts incurred by pulses separated by greater than 5 nm are not unreasonably large. Amongst the channel-spacings in our example, the spacing 17.6 nm (between the third and seventh channels counting from the shortest wavelength channel), results in the largest frequency-shift per pulse per collision, 2.3 MHz. This is near the maximum of the Δf_{coll} vs. L_{coll}/L_{span} curve. After undergoing a single 2.3 MHz shift, a pulse would walk off by a pulse width after traveling 5.5 Gm $\gg L_{system} = 10$ Mm.

Next, we find a conservative upper bound on the timing-shift at the receiver which results from the frequency-shifts for two channels, labeled l and m. Suppose a pulse underwent only worst-case collisions (same frequency-shift as a collision centered at an amplifier) over the entire 10 Mm distance. The total timing-shift resulting from frequency-shifts would be

$$\delta t_{lm} = \sum_{j=1}^{J} j(\Delta \lambda_{coll}^{lm}) D L_{bb}^{lm} \tag{3.11}$$

where $\Delta \lambda_{coll}^{lm}$ is the collisional wavelength shift between channels l and m (which can be calculated from the appendix of reference [122] although several harmonics must be included in the Fourier expansion), D is dispersion, L_{bb}^{lm} is the distance in which an unshifted pulse in one channel moves one bit-spacing relative to the second channel, $J = (L_{system}/L_{bb}^{lm})$ approximates the number of collisions, $L_{system} = 10^7$ m is the total transmission distance, and

$$L_{bb}^{lm} = \frac{1}{RD\Delta\lambda_{lm}} = \frac{L_{coll}^{lm}}{2Rt_s} \tag{3.12}$$

54

$\lambda_j^{WDM} - \lambda_0$ (nm)	$< P_{data} >$	$< P_{CL} >$	$< P_{total} >$
-4.178	6.018	17.160	23.178
1.997	6.091	3.215	9.306
6.812	6.149	5.260	11.409
10.144	6.189	7.170	13.359
13.415	6.228	2.470	8.698
16.701	6.268	0.410	6.678
20.150	6.310	9.960	16.270
Totals:	43.253	45.645	88.898

Table 3.2: Time-averaged power (μW) at amplifier input for channels centered at λ_j^{WDM}, $j = 1,...7$. $\lambda_0 = 1.535\mu$m. $< P_{data} > =$ unmodulated 2 Gb/s soliton streams; $< P_{CL} > =$ control lasers tuned 50 GHz away from λ_j; $< P_{total} > =$ sum.

where R is the bit rate, L_{coll}^{lm} is the collision length which is defined as the distance in which a pulse in channel l travels two pulsewidths with respect to a pulse in channel m, t_s is the pulse full-width at half-maximum, ar l $\Delta\lambda_{lm}$ is the wavelength separation between channels l and m. Thus,

$$\delta t \approx \frac{(\Delta\lambda_{coll}^{lm})DL_{system}^2}{2L_{bb}^{lm}} \tag{3.13}$$

for each pair of channels l, m.

Consider collisions between a pulse in the longest wavelength channel with streams of ONEs in the remaining six channels. Summing Eq. (3.13) over these six channel pairs we find a displacement upper bound of 112 ps, or 1.12 pulse widths. For a pulse in the shortest wavelength channel, colliding with streams of ONEs in the other six channels, the upper bound is 153 ps, in the opposite direction.

The reader is reminded that we have only considered frequency-shift-induced timing-shifts above. Soliton collisions result in pure timing-shifts as well, which were addressed by Mollenauer et al. [122].

3.3.3 Numerical Results

It is essential that the control system have sufficient dynamic range to handle power-level extremes. Consider a string of ONEs with no ZEROs being transmitted in each channel. Numerically, the output powers of the control lasers have been adjusted to achieve static equalization. Table 3.3.3 lists the center wavelengths of the WDM channels in the first column. For each channel is listed the soliton power at the input of an amplifier, the (nearest) control laser power required for equalization, and the sum of soliton and control laser power. The total average power at the output of an amplifier is 233.83 μW.

Fig. 3-1 shows the gain lineshape (dB) in the absence of optical signals (top curve); in the presence of the passive, linear, lossy, Lorentzian notch filters (middle curve); and with the filters, seven WDM channels at 2 Gb/s each, and control laser equalization (lower curve). The flat horizontal line indicates the desired gain. The vertical lines indicate the locations of the WDM channels. The ordinate in Fig. 3-2 is gain on a linear scale. The horizontal and vertical lines are as in Fig. 3-1 The top curve is the gain in the presence of the linear filters. The middle curve shows the gain with the filters and with the WDM channels. The lower curve includes filters, WDM channels, and control lasers adjusted for equalization.

3.4   Discussion

Flatter gain could be achieved with better linear filtering. Better linear filtering would also reduce the power required for several of the control lasers. Alternatively, if filtering is problematic, or if amplifier flexibility for retrofitting is desired, more control laser power could be used for equalization.

There is an advantage to tuning the control lasers as close as possible to the WDM channels. In doing so, equalization can be nearly achieved simply by keeping the total power associated with each channel (sum of data and nearest control laser power, as in column 4 of Table 2) fixed. In the example above, equalization for the continuous streams of ONEs was better than 10^{-3} dB. In the other extreme of no signals (all ZEROs), simply choosing control laser powers from column 4 numerically resulted in equalization to within 0.08 dB. Better consistency could be achieved by placing the control lasers closer to the WDM channels (recall that our spacing was 50 GHz, while the pulse spectral full-width at half-maximum was only 3 GHz). Of course, it might be possible to increase the WDM channel density, so that the channels are spaced more closely than a homogeneous linewidth. The filter specifications, stability of filters and lasers, and the soliton frequency-jitter impose lower bounds on the permissible frequency-spacing between channels and control lasers.

In the example considered in this chapter, the control laser power typically exceeds the signal power. In the previous section, we found upper bounds on the timing-shifts of data which resulted from frequency-shifts from asymmetrized interactions with data in other channels. If the control laser power were not filtered immediately following each amplifier, this power would contribute substantially to the the frequency-shifts, and consequently to the timing-shifts.

Alternative schemes have appeared in the literature following Ref. [121]. One scheme replaces the control lasers with a fiber ring which includes the EDFA [137]. The loop is similar to an inhomogeneously-broadened gain laser, within which lasing can occur at each of the longitudinal modes within the bandwidth of net gain, and for each mode the steady state saturated gain equals the loss (which may be frequency-dependent) in the laser. How the data and circulating CW are isolated from each other, I am not certain.

A cascade of inhomogeneously-broadened EDFAs with no servo-control has been tested experimentally [138], with reasonable results, but the author believes much

better results could be achieved with (much more expensive and perhaps unreliable) servo-control.

Another recently proposed approach uses a twin-core EDFA which acts like a coupler [139]. The coupling period is frequency dependent, and inhomogeneous broadening is achieved because each individual channel overlaps with a different set of erbium ions.

In summary, I have proposed that inhomogeneously broadened lumped fiber amplifiers may be appropriate for wavelength-division-multiplexed optical soliton transmission. WDM channel-spacing may be limited by the homogeneous linewidths and by timing-jitter from interchannel collisions in the presence of amplifiers. I have demonstrated equalization with an example with achievable parameter values. I have proposed a dynamic gain equalization scheme, in which the output powers of control lasers, tuned between the WDM channels, are dynamically adjusted as controlled by a feedback/feedforward control system. Better performance could be achieved using amplifiers with wider inhomogeneous linewidths and narrower homogeneous linewidths than those considered in ([129, 130]).

Chapter 4

High Bit-Rate Limitations

This chapter attempts to summarize all currently understood limitations on both soliton and nonsoliton optical pulse communications, both for long distance propagation (e.g. greater than 100 km) and for shorter distances. The first section summarizes limitations for nonsoliton pulse communications. The second section summarizes limitations for soliton pulse communications.

Some of the limitations which the author has researched are treated in the chapter on Stability and Timing Maintenance of Solitons. The other chapter analyzes limitations due to RSFS, third-order dispersion, and noise.

4.1 Summary of Optical Transmission Limitations

4.1.1 Amplifier Noise

Propagation over multi-kilometer and longer distances requires amplification. Current optical fibers impose a minimum of around 0.2dB/km loss. Quantum mechanically, any loss or gain by necessity (fluctuation-dissipation theorem) introduces noise.

When people speak of amplitude noise, they are imagining that the transmission line is linear with regard to amplifier noise. A receiver at the end of the transmission line has some threshold(s) for distinguishing ONEs and ZEROs. The system is designed to be relatively error-free, with some nominal bit error rate (BER), e.g. 10^{-12}, meaning that on average there should be no more than one incorrectly read bit for every trillion bits transmitted.

Consider a system with optical repeaters (amplifiers) spaced at a distance L. Furthermore, consider one wavelength channel (i.e., *the* channel in a purely TDM system, or one of several WDM channels) with net transmission loss α (meaning $P_{\text{out}}/P_{\text{in}} = \exp\{-\alpha z\}$). The amplifier is treated as discrete, which is reasonable if the soliton period is much greater then the length of the amplifier, the latter being typically in the vicinity of 30m. Therefore the required power gain is $G = \exp\{\alpha L\}$ (meaning $P_{\text{out}}/P_{\text{in}} = G$).

The amplified spontaneous emission (ASE) noise power spectral density from an amplifier of power gain G is

$$\beta(G-1)h\nu \qquad (4.1)$$

per polarization where β is the excess noise factor (noise figure), h is Planck's constant, and ν_0 is the carrier frequency. One should also consider the shot noise of the detector, the beating between the ASE and the data at the detector, and the beating between the ASE and itself, not to mention the intensity fluctuations of the source lasers themselves. There are of course other sources of "noise" as well, such as continuum generation from pulses, various scattering effects in the transmission fiber and other components. Given expressions for the noise sources, and characteristics of the detector, one can calculate the minimum signal power required for a given amplifier spacing for a given bit error rate. With their personal choices, some authors have published such calculations [140, 141, 142].

In most of the work done by our group at MIT, we are interested in the opposite limit, the high power limit. This is the limit considered in the chapter on Stability and Timing Maintenance.

4.1.2   Self-Phase Modulation (SPM)

Self-phase modulation (SPM) is a limitation only for nonsoliton transmission. Solitons maintain their unchanging nature through a balance of group velocity dispersion with SPM. Thus, soliton proponents consider SPM to be beneficial.

In nonsoliton transmission, signal powers are kept as low as possible to avoid SPM. However, there is a minimum power required in order maintain adequate signal-to-noise (S/N) ratio for a desired amplifier spacing, and in practice the Kerr effect cannot be overlooked in long distance propagation. In a fiber, the index of refraction is reasonably well modeled as

$$n = n_o + n_2 I$$

where n_o is the linear index of refraction, n_2 is the Kerr coefficient ($n_2 = 3.18 \times 10^{-20}$ m^2/W in ordinary glass fibers), and I is the instantaneous intensity of the linearly polarized light traveling in the fiber. The nonlinear index is actually a tensor, so that light in different polarizations will see different effective indices of refraction. This is discussed in Chapter 1.

The actual Kerr response is not instantaneous, of course, but is for the most part extremely fast, as near infrared light is far away from any resonances in the fiber. The noninstantaneous portion is primarily the Raman response, which is usually negligible unless sub-picosecond pulses or very long propagation distances are involved. While the "instantaneous" Kerr effect is a photon-photon interaction, the Raman response involves coupling to optical phonon modes which have no electric dipole moments.

If the fiber had no dispersion at all, over the bandwidth of the pulse (which would be a rare situation, requiring a dispersion-flattened fiber which is flattened at the zero-dispersion wavelength, or requiring very narrowband "pulses"), then any amplitude variation in the time profile of the pulse would give rise to chirp, and the pulse bandwidth would grow with distance, but the amplitude profile would remain constant.

In a direct detection TDM system, spectral broadening with truly zero dispersion would not be a problem. It most certainly would be a problem in directly-detected

FDM or WDM systems where neighboring channels began to overlap, and in co-herent communications. In reality, there will be some dispersion of some order in any fiber, and it will lead to distortion of highly chirped pulses (see the Dispersion subsection below). A successful trick used in so-called "linear" transmission (usually non-return-to-zero or NRZ format), is to use alternating sections of positive and neg-ative dispersion fiber, so that the average dispersion is near zero, but the dispersion at any particular point is nonzero, suppressing phase-matching for SPM.

4.1.3 Cross-Phase Modulation (XPM)

In a WDM or FDM system, one must also consider the Kerr effect induced by one pulse on pulses in the other wavelength channels. In a fiber which is dispersion-free over the total bandwidth of the WDM channels (as mentioned in the SPM section above, the pulses in the different WDM channels would all travel at the same speeds. If they were TDMed as well as WDMed, cross-phase modulation (XPM) would not be an issue. If, however, there were more channels than time slots available between intrachannel pulses, there would have to be some overlapping pulses. This would lead to further spectral broadening than from SPM alone.

The reality of current systems is that the dispersion is not zero for any channel, although the second-order dispersion (GVD) might be zero for one channel. This means that each channel has its own group velocity, and interchannel collisions will occur. There is no doubt as to whether or not this would have to be taken into account for nonsoliton transmission.

Quantitatively, the amount of XPM is a function of the polarization states of the interacting pulses. The weakest interaction occurs for pulses which are linearly and orthogonally polarized, and which are traveling relatively rapidly with respect to each other (to make the coherence terms negligible). At the other extreme, pulses which are orthogonally circularly polarized see 2/3 as strong SPM and twice as strong XPM as linearly polarized pulses.

4.1.4 Dispersion

Group velocity dispersion (GVD) is the quadratic dependence of wavenumber on frequency:

$$k = k_o + k'\omega + \frac{k''}{2}\omega^2 + \frac{k'''}{6}\omega^3 + ... \tag{4.2}$$

which if nonzero describes a linear variation of phase velocity and group velocity with frequency. In ordinary optical fiber, there is a zero-dispersion point at a (free-space) wavelength around 1.3μ, with longer wavelengths being in the anomalous GVD regime ($k'' < 0$). The zero-dispersion point can be shifted to longer wavelengths by changing the geometry of the fiber cross-section.

The effect of dispersion, acting alone, is to cause the different frequency com-ponents of a waveform to travel at different speeds. The waveform might initially compress if chirped properly, but if it travels sufficiently far, it must eventually spread.

Dispersion could make extraction of information difficult. In a pulse code mod-

ulation system, the pulses spread and overlap. In a phase-shift keyed (PSK) or frequency-shift keyed (FSK) system, the waveform becomes amplitude modulated, and subsequently phase-shifted by the Kerr effect. A group in Germany has designed a system in which information is transmitted as PSK or FSK but is received as an amplitude modulated signal [143]. If dispersion were the only problematic effect other than noise, then there would be a simpler solution. One could simply equalize prior to detection. That is, we would send the waveform through a medium with the dispersion of the opposite sign of that in the transmission fiber and much stronger than that in the transmission fiber. Dispersion is a linear operator, and perfect equalization would be achievable in principle.

Of course, things are never that easy. In reality, there is self-phase modulation to contend with. The signal power may seem rather low, but the Kerr effect cannot be neglected. If the signals overlap at all, then the distortion will be pattern-dependent, so that fixed equalization will not be optimal.

Operating at the zero dispersion point is not a good solution because self-phase modulation is uninhibited and leads to much spectral broadening. Although it has been neglected in most studies of nonsoliton transmission, if the pulses are too short, third-order dispersion will also distort the pulses in time, and will alter the Kerr spectral broadening. "Too short" means that τ^3/k''' is less than the system length.

Current wisdom suggests that the best solution is to perform near-equalization quasi-continuously in the transmission fiber. The transmission fiber consists of alternating positive and anomalous dispersion sections of fiber spliced together [123, 124]. This gives net zero dispersion. The nonzero dispersion inhibits phase-matching in each section of fiber and reduces the spectral broadening, but broadening will still occur. Note that one might be tempted to model this analytically by saying that to lowest order, dispersion is the only dominant effect, path average over the dispersive spreading and compression to obtain an effective equation for the path-averaged nonlinearity. We would expect that such an approximation would tell us that the nonlinearity seen by the pulse on average is proportional to the intensity averaged over one period of dispersive spreading and compression. It would be interesting to compare the analytic prediction and the simulations of Marcuse [123, 124].

Whether intentional or not, the alternating-dispersion approach for nonsoliton transmission might also reduce the deleterious effects of third-order dispersion. SPM and third-order dispersion together wreak more havoc than SPM and GVD (see e.g. Refs. [144, 145, 146, 147, 148, 149]).

A serious drawback of "current wisdom," (the alternating dispersion approach) is that it would be impossible, if the pulses behaved truly linearly, to wavelength multiplex nonsoliton channels and achieve proper equalization in each channel. This limits the wavelength multiplexing capability. Inability to wavelength multiplex could be the eventual downfall of nonsoliton transmission.

4.1.5 Polarization

The use of non-polarization maintaining (nonPM) fiber can create a number of problems. Cost is a primary reason why nonPM fiber will be used. It is also appar-

ently quite difficult to produce fiber which is uniformly birefringent for long lengths. Nonuniformity of the birefringence axes can lead to polarization scattering.

NonPM fiber is of course not nonbirefringent. Birefringence would not be a problem if it were predictable. However, fibers come with intrinsic and unknown birefringence which varies along the length of the fiber. This birefringence results from the stresses of the drawing and cooling processes. The processes are too rapid for all stresses to equilibrate before the fiber is frozen.

The stresses described above are effectively time-invariant with regard to communications. There are also birefringences resulting from externally applied stresses, such as thermal expansion and contraction, and any bending or torsion. These birefringences are time-varying.

A headache for development teams has been polarization-dependent loss. Received signals fade in and out as the polarization wanders. It has been found that small polarization dependent losses do not significantly affect polarization mode dispersion (PMD) [150]. However, PMD in the general sense, which includes wandering of the states of polarization, leads in a system with polarization-dependent losses to time-dependent fading [29, 151].

Polarization mode dispersion is an important concern for several reasons. The source of this dispersion is the birefringence of the fiber. Consider an unchirped pulse launched into a birefringent fiber in some polarization state other than one of the birefringent axes. The pulse can be thought of as a superposition of its projections onto the birefringence axes. The birefringence will tend to pull these projections apart. At very low powers, the two projections will simply separate at an inverse velocity of $\Delta n/c$. One could define a differential group delay (DGD) to be the difference between the delays for light polarized along the birefringence axes.

Ordinary telecommunications fibers have weak birefringence which varies along the length of the fiber and varies with time. This of course complicates the measurement of PMD. It is generally assumed that the power is sufficiently weak that the nonlinearities can be ignored. When a number for PMD is given, it is a measure of the amount of DGD in the fiber. One such measure is the mean square timing deviation

$$\text{PMD} = \sqrt{<T^2> - <T>^2} \tag{4.3}$$

where T is the deviation of the elapsed time of flight from the mean time of flight along a given fiber, and the averaging is ensemble averaging.

In the linear limit, PMD is completely characterized by a wavelength-dependent three-dimensional polarization dispersion vector [152]. This is equivalent, in turn, to specification of two principal states of polarization (PSPs) and a differential group delay, both as a function of wavelength. Indeed, for light whose coherence time is greater than the DGD, the two PSPs are the fastest and slowest polarization modes, they are orthogonal if the losses are polarization-independent, and they are stable to first order in wavelength [153]. The change in DGD with wavelength can be termed differential group delay dispersion (DGDD) and is equivalent to GVD [154]. The change in PSPs with wavelength can lead to distortion.

With higher powers, cross phase modulation can provide the glue necessary to

keep the projections bound into a single pulse. However, in the process, the pulse will likely spread and shed some linear dispersive waves. Such complications are typically ignored in theoretical discussions, but could be important for soliton transmission and for long-haul nonsoliton transmission. Some authors have attempted to model these effects, with some success in characterization [155, 156, 157].

4.2 Summary of Soliton Transmission Limitations

4.2.1 Amplifier Noise - Linear Limit

Just as in the linear case, amplified spontaneous emission (ASE) degrades the signal-to-noise ratio in the system. There is a minimum signal power required for a target bit error rate. The use of guiding filters [19, 20, 21] or sliding guiding filters [22, 15] can suppress much of the ASE without destroying solitons, and this reduces the minimum power requirement.

4.2.2 Gordon-Haus Effect

Because solitons travel in a dispersive medium, independent noise-induced frequency shifts of the individual pulses will in the course of propagation give rise to timing jitter [23]. This effect is analyzed in detail in another chapter (stability and timing maintenance...), along with several ways to reduce the jitter, such as filtering, modulation (amplitude and/or phase), (saturating) fast saturable absorption or gain, and various dispersion compensation techniques. The latter techniques are discussed in the chapter on network devices, in the section equalization, in the subsection on reactive equalization. These methods of jitter reduction apply to a host of other effects besides the Gordon-Haus effect.

4.2.3 Raman-Induced Timing Jitter

This is similar to the Gordon-Haus effect, in that it is a noise-induced effect which gives rise to frequency shifts which then lead to timing jitter. However, the frequency-shift mechanism is different. Raman self-frequency shift (RSFS) has a strong fourth-power dependence upon photon number of a soliton. Furthermore, RSFS is a rate of change of frequency, which through dispersion is like an acceleration in timing. Thus, noise-induced photon number fluctuations lead to different rates of acceleration for the individual pulses, leading to timing jitter. At bit rates exceeding 30 Gb/s, this effect can dominate the Gordon-Haus effect.

Even the classical RSFS poses potential problems for transmission and storage because the pulses arrive at a different frequency than that at which they were transmitted. In a multipoint network with dynamically allocated data paths, the relationship between the received and transmitted frequencies would be unknown to the receiver.

I have analyzed this problem, especially the noise-induced problem, in some detail as it applies both to high-speed transmission and to storage rings. The analysis

appears in another chapter, which I hope to publish with W.S. Wong and H.A.Haus.

4.2.4 Third-Order Dispersion

Ordinary optical solitons exist in media with second-order dispersion. Third-order dispersion causes solitons to radiate dispersive waves. If the third-order dispersion is strong enough, one wing of the spectrum will perfectly phase-match to dispersive waves at one frequency, and the soliton will dump energy into this mode. Periodic amplification provides a nice set of grating wavenumbers which can phase-match the soliton to even more sidebands.

Similar to the RSFS noise problem, noise-induced photon number (bandwidth) fluctuations change the speed of solitons, giving rise to timing jitter.

Third-order dispersion is discussed in some detail in another chapter.

4.2.5 Pulse Phase Resonances

A soliton has, in addition to its carrier wavenumber, a nonlinear wavenumber. It is truly a single wavenumber, as the phase does not change across the pulse (in a coordinate frame moving with the soliton).

Small amplitude dispersive waves are essentially unaffected by the Kerr effect (if they are well away from any pulses). These linear waves obey the linear dispersion relation in the medium, and they have a continuum of possible wavenumbers.

There is a wavenumber bandgap between a soliton and the dispersive waves. For ideal transmission, we would like to have solitons with no dispersive waves. However, if there are spatial inhomogeneities in the transmission fiber with significant (spatial) spectral components which cross the wavenumber bandgap in a portion of the (temporal) spectrum where the soliton has significant energy, then the soliton will dissipate energy into dispersive wave modes.

That this was a problem was discovered in transmission systems with periodic amplification/loss [10]. It is also a performance limitation for soliton fiber lasers [158, 159, 160, 161]. The effect does not in general disappear if non-soliton pulses are used, of course, but solitons are quite susceptible because of their fixed wavenumbers.

The most practical way to solve the problem is to choose large enough pulse widths with low enough dispersion that the soliton period is much greater than the amplifier spacing. However, when pushing to bit rates over, say, 25 Gb/s, this may become a problem because the amplifier spacing will have to be reduced. The phone companies seem to be quite unwilling to reduce the amplifier spacings to less than roughly 20 km. In non-ultra-long-haul links within a network, all-optical regeneration (see chapters on Switching and Network Devices) may be a good solution.

Distributed erbium fibers have been fabricated and used successfully to reduce the gain/loss transients seen by pulses, but these fibers are very expensive, and would probably require a fairly complicated pumping scheme. Distributed Raman amplification was the first scheme tried, but this approach is too complex.

4.2.6 Electrostriction

In a 1989 paper, K.Smith and L.F.Mollenauer noted a strange interaction amongst solitons traveling very great distances [162]. They found that solitons seemed to attract or repel each other in a phase-independent manner.

This is in contrast to the well-known phase-dependent soliton-soliton interaction which is a consequence of the overlap of the pulse tails. In this effect, solitons which are in phase are attracted to each other, while those which are out of phase repel.

Another strange feature of this effect is that the strength of attraction (positive and negative) is an oscillatory function of the pulse separation.

This effect remained a mystery until 1990, when Dianov et al. [163] found that they could roughly model the behavior by taking into account electrostriction in the fiber. Electrostriction refers to mechanical deformation resulting from an applied electric field. In this case, the electric field is provided by the optical pulses, and the mechanical deformation is constriction of the optical fiber. As a result of the constriction, the index of refraction of the fiber changes. Clearly, for a fixed location in the fiber, this is a transient effect: wherever a pulse is located, the fiber is constricted, perhaps with a delayed response. In its wake, the fiber radius and index of refraction undergo a damped oscillation. If the pulses are sufficiently intense and closely spaced, then a pulse following another pulse will see a different index of refraction than the lead pulse, and the two pulses will travel at different speeds.

What Dianov et al. did not discuss in their paper was the tensor nature of the electrostriction. They treated the problem as if the light caused a radial response regardless of the polarization of the light. It might be interesting to investigate the sensitivity of the effect to changes in the eccentricity of the fiber cross-section.

4.2.7 Raman Bit-Rate Compression

RSFS bit-rate compression is a rather weak effect which I have investigated. With narrow pulses or long distances, self-Raman can also lead to bit rate compression and expansion. Compression can occur in TDM or WDM. Consider TDM for simplicity. Consider a packet being launched onto a fiber. The first bit immediately begins to redshift (spectrally shift to longer wavelengths). This pulse decelerates in time. The second bit does not begin to decelerate until it enters the fiber, one bit interval later. Thus the leading pulse is always traveling slower than the pulses behind it, and the data temporally compresses as it travels through the fiber. Fortunately, this effect is quite weak.

In WDM systems the effect can be exacerbated. The reason is that interchannel collisions modify the rate of self-frequency shift during the collision, and lead to energy transfer from the higher frequency channel to the lower frequency channel. Energy loss (gain) leads to a weakening (strengthening) of the subsequent self-frequency shift for a pulse. As an example, consider a two-channel WDM system. Assume that the fiber is filled with pulses (a sequence of ONEs) in the lower frequency channel, channel 1, and contains no pulses in the higher frequency channel, channel 2. Now a sequence of ONEs in channel 2 enters the fiber and a sequence of ZEROs in channel 1 enters the

fiber. The first channel 2 pulse begins to decelerate before the other pulses as before, etc. This time, however, the first pulse also catches up with a pulse in channel 1, before any other pulse in channel 2 can do so. The lead pulse transfers energy to channel 1 and decelerates even more, etc. Clearly, with real (pseudorandom) data, this effect is also a source of timing jitter. Because this is an amplification/loss process, we might expect a noise contribution as well.

4.2.8   Polarization Dispersion

Polarization is a rather interesting topic in the soliton communications arena because of the length scales involved. Polarization-maintaining (PM) fiber is readily available, but currently considerably more expensive than non-PM fiber. PM fiber "maintains polarization" because of its large linear birefringence. Light coupled along one of the birefringence axes (linearly polarized) will remain on that axis up to very high powers. Only when the nonlinear birefringence (from XPM) exceeds the built-in birefringence does the fast axis become unstable (see Chapter 1). Non-PM fiber permits nonlinear polarization rotation, tends to have locally linear and small birefringence, and the birefringence axes vary along the length of the fiber (intrinsically) and with time (due to perturbations). There certainly are disadvantages to using ordinary non-polarization-maintaining fiber, but cost and nonuniformity of PM fiber have kept it out of consideration.

Polarization dispersion, which was discussed in the previous section, can lead to excessive dispersive wave shedding. It is important to use low-PMD fiber [154, 29, 155, 157, 156, 153].

4.2.9   Soliton-Soliton Interaction

The phase-dependent soliton-soliton interaction can be described as a force between neighboring solitons, making them attractive or repulsive. The force is mediated by the Kerr effect. An easy way to think about it is that light tries to travel as slowly as possible – it likes to sit in regions of high refractive index. In a medium with positive Kerr effect such as a silica fiber, the presence of light increases the local index of refraction. The center of a soliton (or any bell-shaped pulse) has a high local index, and the index decreases symmetrically away from the center of the pulse. If two solitons are near each other, their wings overlap. If the pulses are in phase, the wings will add constructively, increasing the index in the region between the pulses. Each soliton finds that the index is slightly higher on the side of the neighboring pulse, and the pulses attract. If the solitons are out of phase, the wings tend to cancel. The solitons see net higher index on the side away from the neighboring pulse, and the two repel.

A perturbative formalism for handling pulses with overlapping tails was presented by Karpman and Solov'ev [164]. Gordon treated the special case of two neighboring solitons, showing the exponential interaction clearly [165]. Soliton interaction in a more complicated system, with periodic gain and loss, has also been investigated [166, 167]. Strong multiple-pulse interactions have been investigated numer-

ically by Uzonov et al. [168, 169], using various tricks to suppresss the interaction between the pulses.

Some of these tricks include the following. First, one can in principle adjust the phases between neighboring data pulses so that the interaction is neutralized. This is not likely to be practical in a TDM system with multiple sources. Another alternative is to alternate the intensities (and widths, so the pulses are solitons) of neighboring pulses. The way I like to think about this approach is that the nonlinear wavenumbers ("soliton phase" wavenumbers) of the neighboring pulses are different, so that as the pulses travel down the fiber, the relative phase between the pulses is constantly changing.

Other tricks not considered by Uzonov et al. include the following. Amplitude or phase modulators can keep TDMed pulses from drifting out of their timeslots, but the modulation must be done often enough that the pulses cannot drift far between modulators. Saturable absorption can be used to suppress low-intensity light, including the overlapping pulse tails. With currently known saturable absorbers, this is limited to TDM systems as well. These effects are used in pulse storage rings (see chapters on Stability and on Network Devices).

4.2.10 Asymmetric Collisions (WDM only)

Solitons are truly remarkable in that they are nonlinear entities which emerge unscathed from collisions with others of their kind. A soliton is time-shifted and phase-shifted as the results of a collision, but otherwise returns to its original state.

In a system with periodic amplification and loss, the symmetry of a collision is lost. The cross-phase modulation of one pulse on the other may be different in the first half of the collision than in the second half, resulting in net frequency shifts for the pulses. This is most undesirable in a transmission system because it results in bit-pattern-dependent timing jitter. One way to avoid this problem is to ensure that the shortest soliton collision length is greater than twice the amplifier spacing [122, 170]. This can be done by minimizing the dispersion or the frequency separation of the most widely-spaced WDM channels.

4.2.11 Gain Equalization (WDM only)

In a WDM system, it would be desirable if all of the WDM channels experienced the same path-averaged gain. However, the spectrum of the gain of an EDFA is not flat. Some possible solutions are discussed in the chapter on network devices, in the section on equalizers. My proposal (I am not aware of any prior reference) of the use of inhomogeneously-broadened fiber amplifiers and one possible, albeit complicated implementation, is presented in an earlier chapter and in Ref. [121].

4.3   Raman-Imposed Limitations for Solitons

I have looked at these issues in some detail and some of the results are presented in the chapter on stability and timing maintenance in soliton transmission and memories.

4.4   Third-order dispersion

This is another topic I have considered in some detail and which is addressed in the chapter on stability and timing maintenance of solitons. See also Ref. [171].

4.5   Polarization problems for WDM

There are several scale lengths (times), whose interrelationship determines which set of problems arise for WDMed solitons in non-PM fiber. These scales include the polarization scattering length, the time for the local birefringence axes to change due to thermal and bending effects, the rate of relative polarization scatter for pulses of different frequencies, the pulse collision length, the amplifier spacing, and the soliton period. If the relative polarizations of colliding pulses change rapidly during collision, this could imply that WDM collisions act like ordinary soliton collisions (Manakov [97] limit). At the other extreme, the polarizations of colliding pulses might be frozen but arbitrary and if the slip (number of pulsewidths of relative motion in one soliton period) is too small, dispersive waves and pulse distortion may result. Polarizations which vary slightly during the collision could be even worse, because the collisions could be asymmetrized. Although cotraveling pulses generally scatter around the Poincaré sphere, it is believed that relative polarizations are preserved reasonably well for same-frequency data. The scattering should be frequency-dependent, however.

Time permitting, the author would like to investigate conditions under which the Manakov limit might be achieved. The author is also investigating a novel class of instabilities for WDM solitons, and ways to overcome this problem.

Chapter 5

Stability and Timing Maintenance in Soliton Transmission and Storage Rings

5.1   Introduction

Solitary wave transmission in optical fibers appears very promising for long distance communications, in view of recent experiments [25, 12, 16, 34] using erbium-doped fiber amplifiers. Optical fiber pulse storage rings are also promising [26, 70, 172, 173]. It is therefore important to consider the limitations which such systems face, and how to overcome these limitations. Gordon and Haus [23] have analytically estimated a noise-imparted limitation (see also the more recent references [174, 141]), namely, spontaneous emission noise from the amplifiers can shift the frequency of a soliton, in turn shifting the velocity of the soliton through group velocity dispersion. These random velocity shifts give rise to timing errors. The timing errors limit the achievable bandwidth-transmission distance product.

Here we consider another noise-imparted limitation, due to fluctuations of the Raman self-frequency shift (RSFS). Gordon [175] has provided a simple model for the classical RSFS, and has shown that for a soliton the rate of frequency shift with distance of propagation is inversely proportional to the fourth power of pulse width, in agreement with experiment [176].

In addition to the noise-imparted velocity fluctuations considered by Gordon and Haus, there are photon number fluctuations. Photon number fluctuations are commensurate with pulse width fluctuations as a result of the fixed-area property of solitons. A fluctuation in photon number/pulse width alters the rate of RSFS of a soliton, or equivalently, alters the rate at which the inverse group velocity changes with distance. This is analogous to a changing deceleration.

When integrating over long distances the effect can be important. For comparison, we include the effects of third-order fiber dispersion. The timing jitter from third-order fiber dispersion does not increase as rapidly with distance as the RSFS-imparted jitter. The Raman limitation has been discussed by Wood [113] and studied

numerically by Nakazawa et al. [177]. Finally, we show that filtering can dramatically reduce the growth of the timing variance.

Pulse storage rings are potentially useful devices, e.g. for buffering data in optical communications networks. A variety of such devices have been proposed and built. Perhaps the most successful to date has been the synchronous recirculating loop of Nakazawa et al. [27, 26, 178] (intended as a long-distance transmission simulator, but clearly of use as a storage ring). Filtering and amplitude modulation were used in this loop to preserve the timing of the ONE's (solitons) and to suppress the growth of noise in bit intervals containing ZERO's (absence of solitons). More recently, analyses of the benefits of phase modulation have appeared [179, 172, 180]. Here, we propose the use of intensity-dependent absorption/gain (which we abbreviate FSA for fast saturable absorption, although absorption and gain may both saturate) to provide a thresholding effect which not only guarantees suppression of low intensities (robustness of ZEROs), but also provides a restoring force for intensity, driving the intensity to a fixed value. This is not only beneficial for maintaining the intensity and width (in a near-soliton system, or in a system with feedback to the gain pump) of the pulses, but also for reducing timing jitter, because RSFS and TOD both couple intensity fluctuations into timing jitter. The intensity-dependent absorption may be provided by self-phase modulation followed by an interferometric transformation of phase modulation into amplitude modulation (as in Additive Pulse Mode-Locking [181]).

There are certainly other effects which we have not considered in this work which limit transmission and storage. Pushing to very high bit rates with multi-tens-of-km amplifier spacings, dispersive wave generation should not be overlooked, as it drains energy from the pulses, can be detected as false ONEs, and can induce timing jitter in the ONEs. Deleterious effects of polarization mode dispersion (PMD) are not discussed, as it is assumed that low PMD fibers are used. Also of importance are those effects which couple solitons to their neighbors, such as the phase-dependent soliton-soliton interaction, electrostriction, etc.

5.2 Model

The starting equation includes effects of filters, modulators, and fast saturable absorption, so as to make it applicable to either storage rings or to long distance transmission.

The path-averaged nonlinear Schrödinger equation with (in order of appearance) noise, RSFS, TOD, extra gain required to b⁻ ⁻nce filtering loss, four terms which are a polynomial fit to the intensity-dependent absorption/gain, amplitude modulation, phase modulation, and filtering, can be written

$$
\begin{aligned}
\frac{\partial u}{\partial z} \quad &+ \quad jD\frac{\partial^2 u}{\partial t^2} + jr^2\delta|u|^2 u = S + jc_R r^2\delta\frac{\partial|u|^2}{\partial t}u + \frac{k'''}{6}\frac{\partial^3 u}{\partial t^3} \\
&+ \quad \Delta g u + \left(-L_{FSA} + \gamma_3|u|^2 + \gamma_5|u|^4 + \gamma_7|u|^6\right)u \\
&- \quad \frac{1}{2l_{AM}}M_{AM}\omega_{AM}^2(t + T - T_{AM})^2 u + j\frac{1}{2l_{PM}}M_{PM}\omega_{PM}^2(t + T - T_{PM})^2 u
\end{aligned}
$$

$$+ \frac{1}{l_f}\left\{\left[j\chi - \frac{\chi^2}{2} - j\frac{\chi^3}{3}\right]u + \frac{1}{\Omega_f}\left[-1 - j\chi + \chi^2\right]\frac{\partial u}{\partial t}\right.$$

$$+ \left.\frac{1}{\Omega_f^2}\left[\frac{1}{2} + j\chi\right]\frac{\partial^2 u}{\partial t^2} + \frac{1}{\Omega_f^3}\left[-\frac{1}{3}\right]\frac{\partial^3 u}{\partial t^3}\right\} \tag{5.1}$$

where

$$D = \frac{|k''|}{2} = \frac{1}{2}\left|\frac{\partial^2 k}{\partial \omega^2}\right|, \tag{5.2}$$

$$\delta = \frac{2\pi n_2 \hbar \omega_0}{\lambda_0 A_{\text{eff}}}, \tag{5.3}$$

$$\chi = \frac{p - \omega_{fo}}{\Omega_f}, \tag{5.4}$$

k'' and k''' represent path-averaged values, and c_R is the effective relaxation time associated with RSFS.

A_{eff} is the modal effective area in the fiber, $\hbar(= 1.05 \times 10^{-34}$ J·s) is Planck's constant divided by 2π, ω_0 is the soliton initial carrier (mean) frequency (rad/s), and for silica the nonlinear index $n_2 = 3.2 \times 10^{-20}$ m^2/W. In the case of long-distance transmission, we should also average over the polarization scattering, which gives an extra factor of 8/9 on δ [14]. We have normalized the field such that

$$N = \int_{-\infty}^{\infty} |u|^2 dt \tag{5.5}$$

is the photon number. From path-averaging [174, 182],

$$r^2 = (1 - e^{-2\Gamma l})/(2\Gamma l) \tag{5.6}$$

where Γ is the field loss coefficient which accounts for fiber loss, splice losses, etc. but not filter loss, and l is the distance between successive amplifiers. This factor applies to the self-Raman effect as well as the Kerr effect, which is obvious from the interpretation of the self-Raman effect as a delayed Kerr effect [175, 183]. The coefficient c_R is a measure of the strength of the RSFS term, which is a fraction of the Raman delay time, weighted by the shape of the Raman response curve. Path-averaging is valid if the amplifier spacing l is much less than the soliton phase period (which is eight times larger than z_0, the so-called soliton period) $8z_0 = 2\pi\tau^2/D$.

The filtering terms we have chosen are for illustrative purposes. They are based upon the approximation of the logarithm of a complex Lorentzian for small deviations from the center frequency of the filter. We have truncated the expansion at third order. At the next order, we would have picked up an imaginary third-derivative term which could help to cancel RSFS, but the imaginary first-derivative term already does so in the perturbative treatment.

We define several relevant frequencies and frequency shifts: ω_0 is the initial carrier frequency of the solitons, $(\omega_0 - p)$ is the actual carrier frequency of a soliton, and ω_{fo} is the difference between ω_0 and the filter center frequency. In general, the filter

center frequency may be chosen to be a function of distance, in order to suppress the growth of dispersive waves. Linear shifting has been treated elsewhere [22]. We will consider oscillatory shifting, so that we can use shifting filters in a storage ring, or so that the pulse carrier frequency can be made to be the same at the input and output of the transmission line.

$$\omega_{f0} = \omega_{f00} + F(z) \,, \qquad (5.7)$$

and we shall treat the periodic z-dependent term $F(z)$ as weak and slowly-varying. We define the timing of the initial soliton to be zero, the current timing of the soliton is T, and T_{PM} and T_{AM} are the timing of the phase and amplitude modulation.

Intensity-dependent absorption can be achieved in many ways. Examples include nonlinear Mach-Zender interferometers, asymmetric loop mirrors, and the use of non-linear polarization ellipse rotation with polarizers and waveplates. These examples exhibit absorption which is an oscillatory function of intensity which can be adequately approximated with a polynomial in intensity (simplifying the analysis). In conjunction with gain, this effect can be used to make a storage ring with thresholding. Ideally we would bias the devices so that very low intensities see loss, damping out noise and dispersive waves. At slightly higher intensities, the loss begins to decrease with increasing intensity until it becomes gain. At even higher intensities, the gain decreases with increasing intensity, which provides a restoring force for the peak intensity [112]. For an effective gain vs. intensity curve which has the correct limiting behavior at high intensities, the polynomial coefficients satisfy one of the following two sets of inequalities: (1) $L_{FSA}, \gamma_5 > 0$ and $\gamma_3, \gamma_7 < 0$, or (2) $L_{FSA}, \gamma_3 > 0$, $\gamma_5 < 0$, and $\gamma_7 = 0$. A sample gain vs. intensity curve and the cubic fit are shown in Fig. 5-1.

The analysis in this paper will be based upon soliton perturbation theory, but the utility of this sort of thresholding is not limited to near-solitons. Clearly if the nonlinear absorption/gain is too strong, the pulses will not maintain their hyperbolic secant profiles.

The phase (amplitude) modulation in our model is completely described by a frequency $\omega_{PM}(\omega_{AM})$, timing $T_{PM}(T_{AM})$, and depth of modulation $M_{PM}(M_{AM})$ per length $l_{PM}(l_{AM})$. The modulation frequency is likely to be $2\pi/R$, where R is the bit rate. We use a distributed model for the action of periodic lumped modulators. Suppose the lumped amplitude modulator multiplies the time profile by $(1 - M_{AM} + M_{AM} \cos \omega_{AM} t)$, where M_{AM} is actually half of the full depth of modulation. Then the corresponding distributed oper, or is $(1/l_{AM}) \ln(1 - M_{AM} + M_{AM} \cos \omega_{AM} t)$, which is approximately $-M_{AM} \omega_{AM}^2 t^2/(2 l_{AM})$. If the phase modulator multiplies the time profile by $\exp -j\{\phi_{PM} + M_{PM}(\cos \omega_{PM} t - 1)\}$, then the corresponding distributed operator is $(-j/l_{PM})\{\phi_{PM} + M_{PM}(\cos \omega_{PM} t - 1)\}$, or approximately $-M_{PM} \omega_{PM}^2 t^2/(2 l_{PM})$, where we have ignored the constant phase term which can be trivially scaled out. The obvious implementation is with discrete electro-optic modulators. However, it may be possible to achieve continuous phase modulation using cross-phase modulation. For example, suppose the ring is made with polarization-maintaining fiber and the data remains in one polarization. Broad pulses could be injected in the orthogonal polarization at the appropriate frequency for group-velocity matching. The data are

72
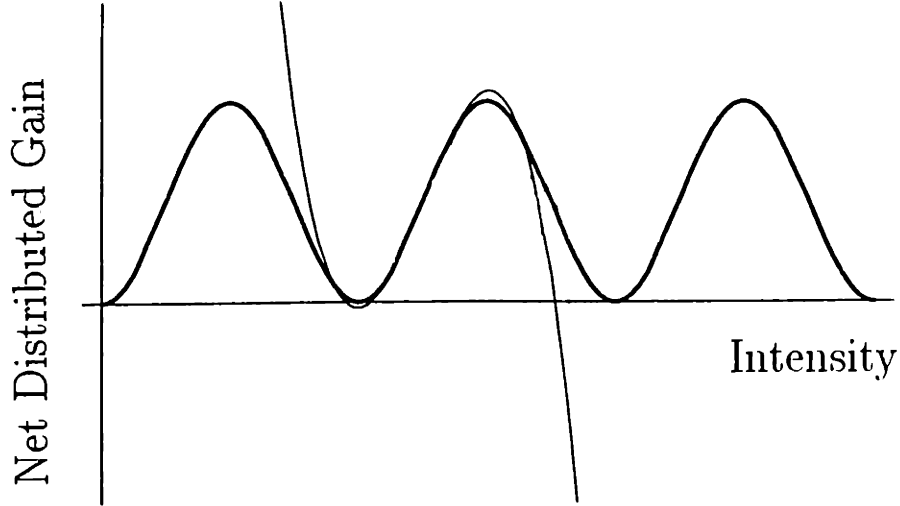
Figure 5-1: Cubic fit to a gain vs. intensity curve with saturating FSA.

matching. The data are likely to distort the phase-modulation pulses, so the latter may need to be removed after a roundtrip and new pulses injected.

The term S represents both the noise introduced by the amplifiers and the noise from zero-point fluctuations due to the loss. It is assumed that the gain balances the loss. Strictly, the noise and the soliton amplitude should be treated as operators. In a quantum analysis, half of the noise is due to the zero-point fluctuations associated with the loss, and half with those associated with the gain (when the gain medium is distributed and perfectly inverted). A semiclassical analysis gives the same result, if the total noise is associated with the compensation by the amplifiers of the loss. In the limit of distributed amplification, with white, delta-function-correlated noise we have [174]

$$\langle S^*(t_1, z_1)S(t_2, z_2)\rangle = \frac{\beta(G-1)}{l}\delta(z_1 - z_2)\delta(t_1 - t_2) , \qquad (5.8)$$

where β is the excess noise parameter [141], G is the power gain of an amplifier, and l is the distance between amplifiers. We have normalized $|u^2|$ to photon flux (photon number per unit time), which accounts for the absence of the factor $\hbar\omega_0$ in (5.8).

If the communication system or memory device is such that the gain is not distributed to cancel the loss at each point, but the gain is lumped into amplifiers, it has been shown [182, 174] that soliton behavior can be maintained on the average under practically realizable conditions. There is a path-averaging noise-penalty

73

factor[174, 141]

$$f = \frac{(G-1)^2}{G\ln^2 G} \tag{5.9}$$

which will arise in our analysis. The gain balances the loss, or $2\Gamma l = \ln G$, where l is the distance between amplifiers. The path-averaging factor r^2 (see Eq. (5.6)) therefore satisfies

$$r^2 = \frac{(G-1)}{G\ln G}. \tag{5.10}$$

Effectively,

$$\langle S^*(t_1, z_1)S(t_2, z_2)\rangle = N_N \delta(z_1 - z_2)\delta(t_1 - t_2) \tag{5.11}$$

where

$$N_N = \frac{2\Gamma\beta f}{r^2}. \tag{5.12}$$

As for actual numbers, with $\Gamma = 0.0242$ km^{-1} (power loss of 0.21 dB/km), we find that for a transmission line with $l = 20$ km, $f = 1.081$ and $r^2 = 0.64$. For a storage ring of length $l = 1$ km, the noise penalty and path-averaging coefficient can be neglected: $f = 1.0002$ and $r^2 = 0.98$.

5.3 Classical Considerations

There are some basic considerations that restrict transmission and storage even in the absence of noise. These include the maximum power the fiber can support without melting, RSFS shifting the pulses beyond the amount deemed tolerable, and shedding of dispersive waves through phase matching when the carrier frequency is near the zero of dispersion. Compensation for some of these effects are discussed here, and noise limitations and further compensation are treated in subsequent sections.

First is the melting threshold. It has been found [113] that the average power should be kept below roughly one Watt. Assuming solitons, the average power is

$$P_{\text{ave}} = 1.135\tau_{FWHM}P_{\text{pk}}R \tag{5.13}$$

$$P_{\text{pk}} = \frac{\lambda A_{\text{eff}}}{4n_2 z_o} \tag{5.14}$$

$$8z_o = \frac{2\pi\tau^2}{D}. \tag{5.15}$$

$$\tag{5.16}$$

As an example, with $n_2 = 3.18 \times 10^{-20}$ m^2/W, $A_{\text{eff}} = 40\mu$m^2, $D' = 1$ ps/nm/km, $\lambda = 1.55\mu$m, and assuming $10R\tau_{FWHM} = 1$, we find $R < 270$ Gb/s.

Raman self-frequency shift is treated by Gordon [175]. For a fundamental soliton, the rate of change of the soliton frequency with distance is

$$\frac{d\omega_0}{dz}(\text{rad/s/m}) = -2.88 \times 10^{-5}\frac{D'\,h(\tau_{FWHM})}{\omega_0^2\tau_{FWHM}^4} \tag{5.17}$$

where all quantities are in SI units (note 1 ps/nm/km = 10^{-6} s/m/m). Gordon introduces a function $h(\tau_{FWHM})$ in his analysis which is based upon actual data for silica. This function is plotted in Ref. [175] and can take on values between zero and unity.

We can estimate the propagation distance or time that it takes for a soliton to frequency-shift by half a pulse bandwidth. The above equation does not take into account the change of dispersion with changing frequency. Let us assume $\lambda = 1.55\mu m$ and $D' = 1$ ps/nm/km. If the pulse width is 1 ps (bandwidth 2.5nm), $h(1ps)= 0.5$, the pulse can propagate for 480 μs, or a distance of 100 km. In an extreme case in which the pulse bandwidth is approximately the same as the erbium gain bandwidth, with a pulse width of 100 fs (bandwidth 25 nm), $h(1ps)= 0.9$, and the pulse can propagate for 270 ns, or a distance of 56 m.

Third-order dispersion is more difficult to handle analytically. It is perhaps best treated by simulation. Nevertheless, we can state a few things. Even weak TOD leads to radiation of dispersive wave tails from the pulse, but this may often be neglected. If TOD is sufficiently strong or the pulse carrier frequency is sufficiently close to the zero-dispersion frequency there is a much more serious problem. The TOD provides automatic phase-matching between a soliton and a certain frequency in the normal dispersion regime. If the soliton has sufficient bandwidth so that it has significant energy at this frequency, then energy will be continuously coupled out of the soliton. We should keep

$$\frac{|k'''|}{6|k''|\tau} < \text{some minimum.} \qquad (5.18)$$

For propagating several soliton periods, without any continuum clean-up mechanism, the minimum should probably be somewhere in the range $0.05 - 0.1$ [149]. For shorter distances, the number may be higher, and for longer distances, lower. Filtering loss, amplitude modulation, and FSA can all help to clean up these dispersive waves, but we do not expect these to suppress the coupling mechanism. Another reason to avoid using sections of fiber in which the dispersion is very low is to reduce the effects of polarization mode dispersion.

However, there is an unexpected benefit of filtering. Compare the filtering term which involves a third-order time derivative with the fiber TOD term. They are of the same form, but fiber TOD is usually positive, while the TOD from filtering is negative. The numbers work out nicely as well. For example, if the spacing between filters is 33 km, and if we choose the filter bandwidth to be ten times the pulse bandwidth, we find that the fiber and filter TODs cancel if the pulse width is 22 ps. If the filter spacing is reduced to 33 m, under the same assumptions, then the TODs cancel at a pulse width of 2 ps. These numbers are rough, of course, but it is clear that filtering can reduce TOD. However, it is equally clear that if the filtering is discrete, it will do little to combat continuum generation in the fiber sections themselves, although it will reduce the noise-imparted fluctuations described below.

Another way to reduce the deleterious effects of TOD is to use only short sections of fiber which violate Eq.(5.18). It may be preferable to use sections of positive dispersion fiber alternating with anomalous instead of either using very low dispersion

fiber or grading the fiber dispersion exactly to preserve solitons in the presence of loss [31, 32]. The average dispersion can be graded to preserve solitons: ordinary grading can be used where the dispersion satisfies Eq.(5.18), and elsewhere alternating positive and anomalous dispersion fibers, which alternate on a distance scale shorter than a soliton period.

There is a classical consideration which does not explicitly appear in our model, but which is very important in determining the conditions under which our perturbation theory is useful. This is the coupling of energy from solitons to dispersive waves through phase-matching via spatial periodicities in the system. A soliton satisfying the nonlinear Schrödinger equation has a positive wavenumber which is a function of its intensity (width). A continuum of low-intensity waves can be supported by, and satisfy the linear dispersion relation of the fiber. These waves have negative semidefinite wavenumbers. Spatial inhomogeneities in the system which have significant spatial frequency components bridging the gap in wavenumbers can allow a soliton to couple its energy into dispersive waves. In a transmission link, amplifier spacings are measured in tens of kilometers. With typical silica fiber loss, this implies gradual loss of several dB between amplifiers and a sudden gain of several dB at an amplifier. This is therefore a dramatic spatial inhomogeneity. To avoid the associated coupling problem, the amplifier spacings are typically chosen to be much less than a path-averaged soliton phase period. Adhering to a minimum amplifier spacing of say 20 km, and demanding that the amplifier spacing be less than say one-fifth of a soliton period, with path-averaged dispersion of 0.4 ps/nm/km, at a carrier wavelength of 1.55 μm, and if we assume that the pulses must be spaced by at least five times the pulse full-width at half-maximum intensity (FWHM), this implies a maximum bit rate of 20 Gb/s, which is less than some of the bit rates considered in this paper. There are other ways to reduce the coupling to the continuum which can relax the constraint that the amplifier spacing be much less than a soliton period. One of these is to use distributed or semi-distributed amplification. Another is to grade the dispersion in the fiber so that a soliton of fixed width is approximately preserved through the fiber, despite the loss. This could be achieved by splicing together sections of fiber with different dispersion, with the strongest dispersion directly following an amplifier [31, 32].

In a storage ring, it is entirely a different matter. The amplifier spacing is likely to be less than or equal to 1 km, making the gain/loss perturbation much weaker. We therefore anticipate that bit rates much higher than 20 Gb/s could be accommodated without the difficult or expensive perturbation-reduction techniques discussed above for transmission.

5.4 The ZEROs

The analysis in this section was performed by William S. Wong.

To analyze the stability of the ZEROs, we ignore the nonlinear and the third-order dispersion terms in Eq. (5.1), and focus on the spectral components of the noise near the passband of the filter where $\chi \approx 0$. We shall determine the conditions under

76

which all eigenmodes of the linear evolution equation are damped.

The equation of motion for low intensity light (well below the intensity of a data pulse) is

$$\frac{\partial u}{\partial z} = S - jD\frac{\partial^2 u}{\partial t^2} + \Delta g u - L_{FSA} u$$
$$- \frac{1}{2l_{AM}} M_{AM}\omega_{AM}^2 t^2 u + j\frac{1}{2l_{PM}} M_{PM}\omega_{PM}^2 t^2 u$$
$$+ \frac{1}{2\Omega_f^2 l_f}\frac{\partial^2 u}{\partial t^2} . \tag{5.19}$$

Following the approach by Haus and Mecozzi [70] we look for an eigenfunction solution to Eq. (5.19) of the form $y_n(z,t) = Z_n(z)T_n(t)$. Substitution of $y_n(z,t)$ yields

$$\left(\frac{1}{2\Omega_f^2 l_f} - jD\right)\frac{d^2 T_n(t)}{dt^2} = \left(\frac{M_{AM}}{2l_{AM}}\omega_{AM}^2 t^2 - j\frac{M_{PM}}{2l_{PM}}\omega_{PM}^2 t^2 + E_n\right)T_n(t) \tag{5.20}$$

and

$$\frac{dZ_n(z)}{dz} = (\Delta g - L_{FSA} + E_n)Z_n(z) + S_n(z) \tag{5.21}$$

If we denote

$$\frac{1}{\tau_0^2} = \left[\frac{\frac{M_{AM}\omega_{AM}^2}{l_{AM}} - j\frac{M_{PM}\omega_{AM}^2}{l_{PM}}}{\frac{1}{\Omega_f^2 l_f} - j2D}\right]^{\frac{1}{2}} , \tag{5.22}$$

the eigenfunctions

$$T_n(t) = \mathcal{H}_n\left(\frac{t}{\tau_0}\right)\exp\left(-\frac{t^2}{2\tau_0^2}\right) \tag{5.23}$$

are Hermite-Gaussian functions where $\mathcal{H}_n(t) = \sum_{m=0}^{n/2}\frac{(-1)^m n!(2t)^{n-2m}}{m!(n-2m)!}$ for $n = 0, 1, 2, \ldots$. The eigenvalues are

$$E_n = -(2n+1)\left[\left(\frac{1}{2l_{AM}}M_{AM}\omega_{AM}^2 - j\frac{1}{2l_{PM}}M_{PM}\omega_{PM}^2\right)\left(\frac{1}{2\Omega_f^2 l_f} - jD\right)\right]^{\frac{1}{2}} . \tag{5.24}$$

There are two criteria to ensure the stability of the ZEROs. Firstly, the evolution of the low-intensity noise is damped provided that all its eigenmodes are damped:

$$\Delta g - L_{FSA} + \text{Re}[E_n] < 0 \tag{5.25}$$

for all n.

The value of Δg is chosen such that there is no systematic change in the photon number. From Eq. (5.39),

$$\Delta g = \frac{1}{6l_f\Omega_f^2\tau^2} + \frac{\pi^2\tau^2}{24l_{AM}}M_{AM}\omega_{AM}^2 + L_{FSA} - \frac{\gamma_3 n_o}{6\tau} - \frac{\gamma_5 n_o^2}{15\tau^2} - \frac{\gamma_7 n_o^3}{35\tau^3} \tag{5.26}$$

Note that if $\text{Re}[E_0] < 0$, $\{\text{Re}[E_0], \text{Re}[E_1], \ldots\}$ forms a monotonically decreasing sequence. Therefore, one only needs to ensure that $\Delta g - L_{FSA} + \text{Re}[E_0] < 0$ for stability. Since one can choose the parameters L_{FSA}, γ_3, γ_5, and γ_7 freely in Eq. (5.26) to satisfy the first criterion, it is immediately clear that fast saturable absorption can suppress the growth of noise.

Secondly, the evolution of the change in the photon number in Eq. (5.40) has to be damped as well. This additional constraint is

$$
-\frac{2}{3l_f\Omega_f^2\tau^2} + \frac{\pi^2\tau^2}{6l_{AM}} M_{AM}\omega_{AM}^2 + \frac{2\gamma_3 n_o}{3\tau} + \frac{8\gamma_5 n_o^2}{15\tau^2} + \frac{12\gamma_7 n_o^3}{35\tau^3} < 0 \qquad (5.27)
$$

Because it is not clear how to implement FSA in a long-haul, non-polarization-preserving transmission system, we shall analyze the stability of ZEROs in a system without FSA. It is useful to define dimensionless variables

$$
F = \frac{\tau^2}{D} \frac{1}{l_f\Omega_f^2\tau^2}
$$

$$
\mu_{AM} = \frac{\tau^2}{D} \frac{M_{AM}\omega_{AM}^2\tau^2}{l_{AM}}
$$

$$
\mu_{PM} = \frac{\tau^2}{D} \frac{M_{PM}\omega_{PM}^2\tau^2}{l_{PM}}
$$

that are proportional to the strength of filtering, amplitude modulation, and phase modulation respectively.

A. Systems with Amplitude Modulation and Filtering

This case was also discussed by Haus and Mecozzi [70]. Without saturable absorption, the gain Δg must be kept below an upper limit set by Eq. (5.25). In terms of dimensionless variables,

$$
\frac{F}{6} + \frac{\pi^2}{24}\mu_{AM} < \left(\frac{\mu_{AM}}{2}\right)^{\frac{1}{2}} \left[\left(\frac{F}{2}\right)^2 + 1\right]^{\frac{1}{4}} \cos\left[\frac{1}{2}\tan^{-1}\left(\frac{2}{F}\right)\right] . \qquad (5.28)
$$

This inequality states that one cannot increase the filtering strength F arbitrarily; otherwise, the limited gain cannot balance the loss caused by filtering.

The use of amplitude modulation tends to shorten the soliton pulse width and broaden its spectrum, which can be counteracted by filtering only if the amount of modulation is not excessive. Specifically, from Eq. (5.27), we require that

$$
\frac{\pi^2}{24}\mu_{AM} < \frac{2}{3}F \qquad (5.29)
$$

The stability region has to satisfy Eq. (5.28) and Eq. (5.29) simultaneously and is given in Fig. 5-2.
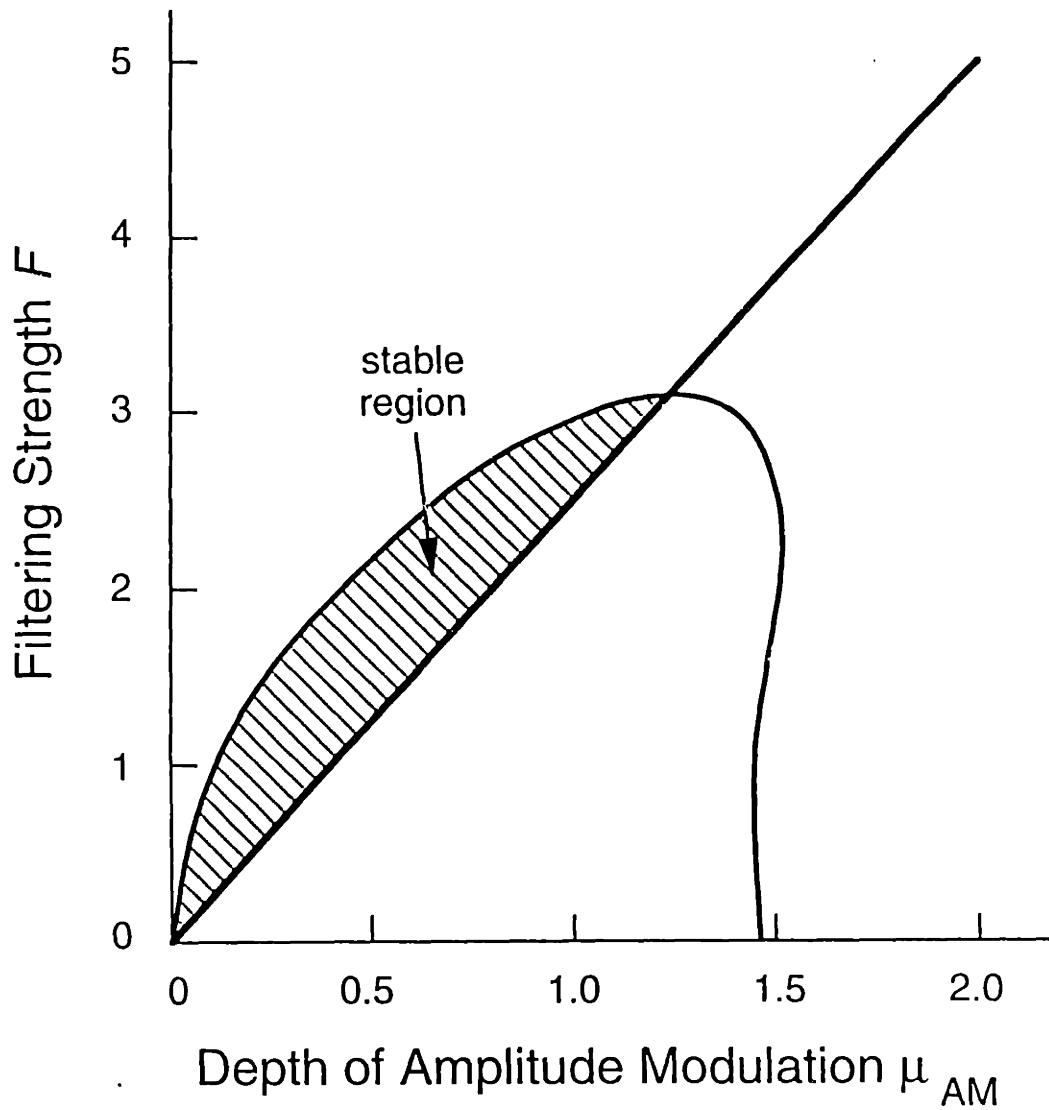
Figure 5-2: Stability diagram for soliton storage ring with amplitude modulation and filtering.

B. Systems with Phase Modulation and Filtering

A phase modulator changes the phase of an input signal while leaving its photon number intact. Therefore, in the absence of amplitude modulation and saturable absorption, the criterion for photon number stability given by Eq. (5.27) is always satisfied provided $F > 0$. The stability region is (see Fig. 5-3):

$$\frac{F}{6} < \left(\frac{\mu_{PM}}{2}\right)^{\frac{1}{2}} \left[\left(\frac{F}{2}\right)^2 + 1\right]^{\frac{1}{4}} \cos\left[\frac{1}{2}\tan^{-1}\left(\frac{F}{2}\right)\right]. \tag{5.30}$$

5.5   The ONEs

We consider classical and noise effects upon near-soliton pulses, using soliton perturbation theory.

A simple fundamental soliton solution of the unperturbed nonlinear Schrödinger equation (Eq. (5.1) without the RHS), is

$$u_0 = A_0 \,\mathrm{sech}\left\{\frac{(t - T - 2Dpz)}{\tau}\right\} \exp j \left\{-\frac{D}{\tau^2}z + Dp^2 z - p(t - T) + \theta\right\}. \tag{5.31}$$

with θ an arbitrary phase, T the temporal displacement, p the change of inverse group velocity, which is equivalent to the shift of frequency as defined above, and which we have labeled 'p' suggestive of quantum mechanical momentum [109]. Note that in this momentum analog, a positive momentum leads to motion in the positive t direction. However, this is a delay, and we are in the anomalous dispersion regime, where lower frequencies are delayed. Thus a positive change in momentum corresponds to a negative change in frequency. The pulsewidth

$$\tau = \left(\frac{4D}{nr^2\delta}\right) = 0.567\tau_{FWHM} \tag{5.32}$$

where τ_{FWHM} is full-width-at-half-maximum-intensity, and

$$2A_0^2\tau = n. \tag{5.33}$$

The perturbation of a soliton may be treated as a perturbation of the photon number Δn, displacement ΔT, momentum Δp, and phase $\Delta\theta$. We can express this as [109]

$$\Delta u(z,t) = f_n(t)\Delta n(z) + f_T(t)\Delta T(z) + f_p(t)\Delta p(z) + f_\theta(t)\Delta\theta(z) + \text{continuum.} \tag{5.34}$$

By 'continuum,' we mean nonsoliton, dispersive wave radiation [2]. One can use the perturbation approach of Haus et al. [109, 21] or equivalently, the approach of Kaup [110] with the pulse amplitude and width coupled.

Our approach will be to expand the driving terms (RHS of Eq.(5.1)) to first order in the soliton parameters, and to solve self-consistently. The continuum plays an important role if, for example, the TOD is sufficiently large, if the soliton period is

80
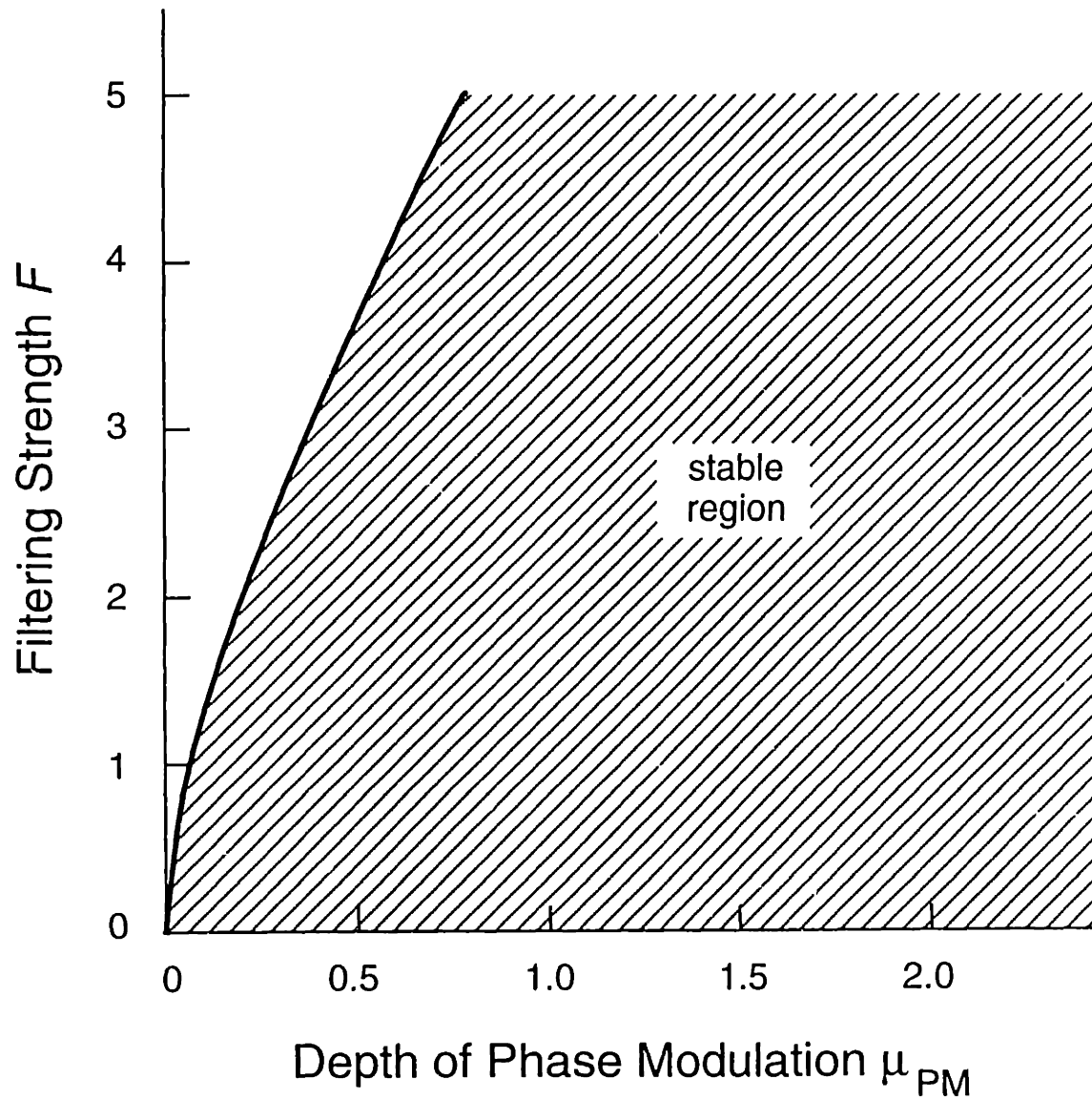
Figure 5-3: Stability diagram for soliton storage ring with phase modulation and filtering. Note that the system is marginally stable with no filtering (along the horizontal axis).

too short, or if narrowband filters with fixed passband are used without saturable gain/absorption. Proper treatment of the continuum could also describe the long-term instability of RSFS and filtering simulated by Blow et al. [184]. The analysis in this section assumes that the influence of the continuum is weak. The parameters of the initial soliton are denoted with '0' subscripts, and without loss of generality, we choose $p=T=\theta=0$ at $z=0$.

The ansatz (5.34) is introduced into (5.1) and the equations for Δn, Δp, ΔT and $\Delta \theta$ are projected out. The projection functions are the adjoints $\underline{f}_i(t)$, obeying the orthogonality relations [109]

$$\text{Re} \int_{-\infty}^{\infty} \underline{f}_i^*(t) f_j(t) dt = \delta_{ij} \quad , i,j \in \{n, T, p, \theta\} \tag{5.35}$$

and equal to

$$\underline{f}_n(t) = 2A_0 \operatorname{sech}\left(\frac{t}{\tau}\right)$$

$$\underline{f}_\theta(t) = \frac{2j}{n}\left\{1 - \left(\frac{t}{\tau}\right)\tanh\left(\frac{t}{\tau}\right)\right\} A_0 \operatorname{sech}\left(\frac{t}{\tau}\right)$$

$$\underline{f}_p(t) = -\frac{2j}{n\tau}\tanh\left(\frac{t}{\tau}\right) A_0 \operatorname{sech}\left(\frac{t}{\tau}\right)$$

$$\underline{f}_T(t) = \frac{2}{n}t A_0 \operatorname{sech}\left(\frac{t}{\tau}\right) .$$

We are not interested in the change of phase θ (it does not couple back to the other parameters). We are interested in change of the soliton position (timing) ΔT due to the fluctuations. The evolution equations of interest have many terms, but all have simple physical interpretation. They are at first presented in full, and then simpler limiting cases will be analyzed, culminating in an analysis of the entire system. The equations are:

$$\begin{aligned}
\frac{d\Delta n}{dz} &= \left[2\Delta g - \frac{1}{3l_f\Omega_f^2\tau^2} - \frac{\omega_{fo}^2}{l_f\Omega_f^2} - \frac{\pi^2\tau^2}{12l_{AM}}M_{AM}\omega_{AM}^2 - \frac{M_{AM}\omega_{AM}^2 T_{AM}^2}{l_{AM}}\right. \\
&\quad + \left.\left(-2L_{FSA} + \frac{\gamma_3 n_o}{3\tau} + \frac{2\gamma_5 n_o^2}{15\tau^2} + \frac{2\gamma_7 n_o^3}{35\tau^3}\right)\right] n_0 \\
&\quad + \left[2\Delta g - \frac{1}{l_f\Omega_f^2\tau^2} - \frac{\omega_{fo}^2}{l_f\Omega_f^2} + \frac{\pi^2\tau^2}{12l_{AM}}M_{AM}\omega_{AM}^2 - \frac{M_{AM}\omega_{AM}^2 T_{AM}^2}{l_{AM}}\right. \\
&\quad + \left.\left(-2L_{FSA} + 3\frac{\gamma_3 n_o}{3\tau} + 5\frac{2\gamma_5 n_o^2}{15\tau^2} + 7\frac{2\gamma_7 n_o^3}{35\tau^3}\right)\right]\Delta n \\
&\quad + \left(\frac{2n_0\omega_{fo}}{l_f\Omega_f^2}\right)\Delta p + \frac{2M_{AM}\omega_{AM}^2 T_{AM}}{l_{AM}}\Delta T + S_n(z)
\end{aligned} \tag{5.36}$$

$$\frac{d\Delta p}{dz} = \left(\frac{16c_R D}{15\tau^4} + \frac{2\omega_{fo}}{3l_f\Omega_f^2\tau^2} + \frac{M_{PM}\omega_{PM}^2 T_{PM}}{l_{PM}}\right)$$

$$+ \left(\frac{64c_R D}{15\tau^4 n_0} + \frac{4\omega_{f0}}{3l_f \Omega_f^2 \tau^2 n_o}\right)\Delta n - \left(\frac{2}{3\tau^2 l_f \Omega_f^2}\right)\Delta p$$

$$- \frac{M_{PM}\omega_{PM}^2}{l_{PM}}\Delta T + S_p(z) \tag{5.37}$$

$$\frac{d\Delta T}{dz} = \left(\frac{k'''}{6\tau^2} + \frac{\pi^2\tau^2 M_{AM}\omega_{AM}^2 T_{AM}}{6l_{AM}} + \frac{1}{l_f\Omega_f} - \frac{\omega_{f0}^2}{l_f\Omega_f^3} - \frac{1}{3l_f\Omega_f^3\tau^2}\right)$$

$$+ \left(\frac{k'''}{3\tau^2 n_0} - \frac{\pi^2\tau^2 M_{AM}\omega_{AM}^2 T_{AM}}{3n_o l_{AM}} - \frac{2}{3l_f\Omega_f^3\tau^2 n_o}\right)\Delta n$$

$$+ \left(2D + \frac{2\omega_{f0}}{l_f\Omega_f^3}\right)\Delta p - \frac{\pi^2\tau^2 M_{AM}\omega_{AM}^2}{6l_{AM}}\Delta T + S_T(z). \tag{5.38}$$

In the equation for Δn, Eq. (5.36), there is excess gain required to offset the loss seen by the pulse from filtering and amplitude modulation. There is filtering loss from the finite bandwidth of the pulse and more loss if the pulse carrier frequency is offset from the center of the filter passband. The amplitude modulator gives loss as a function of timing, so a wider pulse will see more loss. Furthermore, if the pulse is offset from the timing of the modulator, there will be loss. The final four terms multiplying n_o are the FSA terms, which by definition provide loss that is a function of intensity. Next we have a large number of terms multiplying Δn. The interpretation of these is the same as for the terms multiplying n_o, but these terms show the trends as the photon number changes. Most have the same sign, with one exception - the amplitude modulator term which depends on the pulse width. This simply means that there is net loss due to AM, and the loss increases as the pulse gets weaker and wider. The term multiplying Δp shows that as the pulse carrier frequency shifts, the pulse sees more or less loss depending upon whether the carrier frequency is moving away from or towards the center of the filter passband. The ΔT term is similar, showing that as the pulse drifts in time, it sees more or less loss as it moves away from or towards the timing of maximum transmission through the amplitude modulator. The final term is that portion of the noise which affects the photon number of the pulse.

The gain of the fiber amplifiers has to be adjusted so that there is no systematic change of the photon number, i.e.

$$2\Delta g = \frac{1}{3l_f\Omega_f^2\tau^2} + \frac{\omega_{f0}^2}{l_f\Omega_f^2} + \frac{\pi^2\tau^2}{12l_{AM}}M_{AM}\omega_{AM}^2 + \frac{M_{AM}\omega_{AM}^2 T_{AM}^2}{l_{AM}}$$

$$+ 2L_{FSA} - \frac{\gamma_3 n_o}{3\tau} - \frac{2\gamma_5 n_o^2}{15\tau^2} - \frac{2\gamma_7 n_o^3}{35\tau^3}. \tag{5.39}$$

The equation for Δn then simplifies:

$$\frac{d\Delta n}{dz} = \left[-\frac{2}{3l_f\Omega_f^2\tau^2} + \frac{\pi^2\tau^2}{6l_{AM}}M_{AM}\omega_{AM}^2 + \left(\frac{2\gamma_3 n_o}{3\tau} + \frac{8\gamma_5 n_o^2}{15\tau^2} + \frac{12\gamma_7 n_o^3}{35\tau^3}\right)\right]\Delta n$$

$$+ \left(\frac{2n_0\omega_{f0}}{l_f\Omega_f^2} \right) \Delta p + \left(\frac{2M_{AM}\omega_{AM}^2 T_{AM}}{l_{AM}} \right) \Delta T + S_n(z) \qquad (5.40)$$

At least naively, the larger the quantity $(\Delta g - L_{FSA})$, the greater is the opportunity for the growth of noise at the center frequency of the filter and at the maximum transmission of the amplitude modulator. In a memory device, it should be possible to keep $(\Delta g - L_{FSA}) < 0$, suppressing the growth of noise. By simply choosing parameters such that the peak intensity of the pulse sees sufficient loss with increasing intensity from the FSA, the sum of the FSA terms with γ-coefficients in Eq. (5.40) will be negative. Cases with no saturable absorption are treated in Section IV.

In the equation for Δp, Eq. (5.37), the first c_R term is the classical self-frequency shift. The next term is frequency-pulling (from the effective refractive index profile associated with the filter) due to the initial offset of center frequencies. The third term is frequency-pulling from the phase modulator, which chirps mistimed pulses. At the next order, we have the terms multiplying Δn. The first shows that if the photon number fluctuates, then the power and bandwidth of the soliton change, and this alters the rate of RSFS - increased photon number (intensity and bandwidth) implies stronger RSFS. The other term shows that as the pulse bandwidth changes, the frequency pulling due to the filtering changes. The Δp term describes the restoring force which filtering imposes on the pulse center frequency. The ΔT term shows that as the pulse walks off in time, it is chirped by the phase modulator. Finally, there is the noise S_p.

The lowest order terms in Eq. (5.38) are the deterministic timing terms, which, if we are interested in timing jitter only, can be ignored. Briefly, these terms show that larger pulse bandwidths lead to timing shifts via TOD, offset amplitude modulation pulls the timing, the reactive nature of the filtering changes the group spatial velocity directly and also acts like TOD. Next we have three terms by which changes in photon number affect timing. The first says that as the bandwidth changes, TOD changes the group velocity. The second says that if the pulse is offset from the timing of the amplitude modulator, then there is pulling in time, and the strength of the pulling depends on the pulse width. The third is just like the first, except that the filter provides the TOD. The terms multiplying Δp are simply group velocity dispersion terms, one from fiber dispersion, and the other from the dispersive nature of the filtering. The ΔT term shows that amplitude modulation provides a restoring force for timing. The last term is timing noise.

The noise sources $S_i(z)$ are the projections

$$S_i(z) = \mathrm{Re} \int_{-\infty}^{\infty} f_i^*(t) S(t,z) dt . \qquad (5.41)$$

Now that we have obtained the general equations of motion, let us restrict our attention to some specific cases. First we shall consider the uncompensated case, in which RSFS, TOD, and noise-induced jitter go unchecked. We shall find that the growth rate of the soliton timing fluctuations about the deterministic (shifting) position can be greater than the growth rate for Gordon-Haus fluctuations. The

second case of interest is that in which filtering is chosen to preserve the classical (i.e. lowest order, deterministic) photon number, and to cancel the classical RSFS. We assume weak RSFS or closely-spaced filters for RSFS cancellation. At higher bit rates, it may be necessary to downshift the filters with distance, in accordance with the classical RSFS, so that the frequency of a channel as received will be lower than the frequency transmitted.

5.5.1 Long Distance Transmission Without Compensation

Solution of the equations of motion is simplified by unilaterally Laplace transforming in z. We label the transform variable s (to compare with Ref. [21], we can write $s = \text{Re } s - jK$).

We define the autocorrelation with respect to the value at $z = 0$. In the evaluation of noise projections we use

$$\int_{-\infty}^{\infty} dt \, \langle S^*(t,z)S(t',0) \rangle = N_N \delta(z) \,, \tag{5.42}$$

and thus

$$\mathcal{L}\left\{ \int_{-\infty}^{\infty} dt \, \langle S^*(t,z)S(t',0) \rangle \right\} = N_N \tag{5.43}$$

where $\mathcal{L}$ indicates unilateral spatial Laplace transformation. Evaluating the projections, we find

$$\left\langle S_p^*(s)S_p(s) \right\rangle = \left(\frac{4}{3n_0\tau^2} \right) N_N \tag{5.44}$$

$$\left\langle S_n^*(s)S_n(s) \right\rangle = 4n_0 N_N \tag{5.45}$$

$$\left\langle S_T^*(s)S_T(s) \right\rangle = \left(\frac{\pi^2\tau^2}{6n_0} \right) N_N \,. \tag{5.46}$$

Henceforth we adopt the notational simplification $\left\langle S_j^*(s)S_j(s) \right\rangle \rightarrow \left\langle S_j^2 \right\rangle$, $j = n, p, T$.

Without compensation equations of motion are greatly simplified:

$$\frac{d\Delta n}{dz} = S_n(z) \tag{5.47}$$

$$\frac{d\Delta p}{dz} = \left(\frac{16c_R D}{15\tau^4} \right) + \left(\frac{64c_R D}{15\tau^4 n_0} \right) \Delta n + S_p(z) \tag{5.48}$$

$$\frac{d\Delta T}{dz} = \left(\frac{k'''}{6\tau^2} \right) + \left(\frac{k'''}{3\tau^2 n_0} \right) \Delta n + 2D\Delta p + S_T(z) \,. \tag{5.49}$$

Laplace transforming and solving, we find

$$\begin{aligned}
\left\langle \Delta T^2 \right\rangle &= \frac{2^{10}c_R^2 D^2 \delta^2 \tau^4}{225\tau^6} \frac{\left\langle S_n^2 \right\rangle}{s^6} + \frac{2^4 c_R k''' \delta^2 \tau^4}{45\tau^4} \frac{\left\langle S_n^2 \right\rangle}{s^5} \\
&\quad + \frac{k'''^2 \delta^2 \tau^4}{144 D^2 \tau^2} \frac{\left\langle S_n^2 \right\rangle}{s^4} + 4D^2 \frac{\left\langle S_p^2 \right\rangle}{s^4} + \frac{\left\langle S_T^2 \right\rangle}{s^2} \,.
\end{aligned} \tag{5.50}$$

The first term is due to the photon number noise affecting RSFS. The second term is the effect of photon number noise on RSFS and third-order dispersion. The third term is due to photon number noise affecting third-order dispersion alone. The second term can be negative if k''' is negative, but of course the sum of the first three terms is positive semidefinite. The fourth term is noise associated with the Gordon-Haus effect. The fifth term is due to timing noise. Noting the Laplace transform pairs

$$\frac{1}{s^{m+1}} \longleftrightarrow \frac{z^m}{m!} \qquad (5.51)$$

we immediately see the z^3 growth of Gordon-Haus jitter and we see that RSFS can lead to z^5 growth of jitter. Now we can perform the inverse transform to find the limitations.

Let the detector window of acceptance for a signal soliton be $2t_w$. For a specific bit-error rate (BER), we demand

$$\langle \Delta T^2 \rangle \leq (t_w/\sigma)^2 . \qquad (5.52)$$

For $\log_{10} \text{BER} = -9$, $\sigma = 6.1$, while for $\log_{10} \text{BER} = -12$, $\sigma = 7.1$.

First, consider the limitations due to RSFS alone. We find

$$\frac{L^5}{\tau_{FWHM}^7 t_w^2} = \frac{(19.7)c^2}{c_R^2 \lambda_0^4 D'^3 \zeta} \qquad (5.53)$$

where $D' = 4\pi c D/\lambda^2$ is the path-averaged time-of-flight dispersion with units of e.g., ps/nm/km, and

$$\zeta = \frac{2r^2 \delta \lambda_0 N_N \sigma^2}{\omega_0} . \qquad (5.54)$$

Next we determine a reasonable value for c_R. From the analysis of Gordon [175], we find that for a fundamental soliton, the rate of change of the soliton frequency with distance is

$$\frac{d\omega_0}{dz}(\text{rad/s/m}) = -2.88 \times 10^{-5} \frac{D' h(\tau_{FWHM})}{\omega_0^2 \tau_{FWHM}^4} \qquad (5.55)$$

where all quantities are in SI units (note 1 ps/nm/km $= 10^{-6}$ s/m/m). Gordon introduces a function $h(\tau_{FWHM})$ in his analysis which is based upon actual data for silica. This function is plotted in Ref. [175] and can take on values between zero and unity. We have neglected the τ_{FWHM}-dependence of $h(\tau_{FWHM})$. Comparison with our perturbation analysis (see the LHS and substitute n for n_0 in the very first term on the RHS of Eq. (5.37)) yields $c_R = 3h(\tau_{FWHM})$ fs.

If we choose $\tau_{FWHM} R = 1/10$ and $t_w R = 1/2$, where R is the bit rate, $\log_{10} \text{BER} = -9$ ($\sigma = 6.1$), $\Gamma = 0.0242 \text{km}^{-1}$ (corresponding to 0.21 dB/km), $\lambda = 1.65 \mu\text{m}$, $\beta = 1$,

$l \leq 1$ km (storage ring), and $A_{eff} = 40 \mu m^2$, then

$$L_{Mm} = \frac{938}{R_{Gb/s}^{9/5} D'^{3/5}_{ps/nm/km}} .$$ (5.56)

The Gordon-Haus limit alone is

$$\frac{L^3}{\tau_{FWHM} t_w^2} = \frac{10.2}{D'\zeta}$$ (5.57)

which under the same assumptions as above is

$$L_{Mm} = \frac{51.3}{R_{Gb/s} D'^{1/3}_{ps/nm/km}} .$$ (5.58)

The individual Gordon-Haus and RSFS limits are equal for $L = 1.35$ Mm, and the corresponding bit rate is 30 Gb/s with $D' = 2$ ps/nm/km. For the case of transmission with $l = 20$km, the limits are equal for very nearly the same distances and bit rates (replace 938 by 924 in Eq.(5.56) and 51.3 by 50.0 in Eq.(5.58)).

Values for k''' can be estimated with the Sellmeier dispersion equation [144, 145]. We have assumed $k''' = +1.4$ ps^3/km. The limit due to third-order dispersion alone would be:

$$\frac{L^3}{\tau_{FWHM}^3 t_w^2} = \frac{(0.249)\lambda_0^4 D'}{k'''^2 c^2 \zeta} .$$ (5.59)

Under the assumptions above, we have

$$L_{Mm} = \frac{1110 D'^{1/3}_{ps/nm/km}}{R_{Gb/s}^{5/3}} .$$ (5.60)

The mixed RSFS and third-order dispersion term is

$$\frac{L^4}{\tau_{FWHM}^5 t_w^2} = \frac{0.992}{k''' c_R D' \zeta} .$$ (5.61)

For comparison with the other individual limits,

$$L_{Mm} = \frac{819}{R_{Gb/s}^{7/4} D'^{1/4}_{ps/nm/km}} .$$ (5.62)

The individual upper bounds are plotted in Fig. 5-4 for a fixed value of dispersion (1 ps/nm/km). The Gordon-Haus/RSFS crossover distance is independent of dispersion, and both limits become more severe with increasing dispersion. If D were reduced, keeping k''' fixed, the k''' limitation would become more severe than the RSFS limit.

A word about the domain of validity of the perturbation theory is in order. The

UNFILTERED TRANSMISSION LIMITS
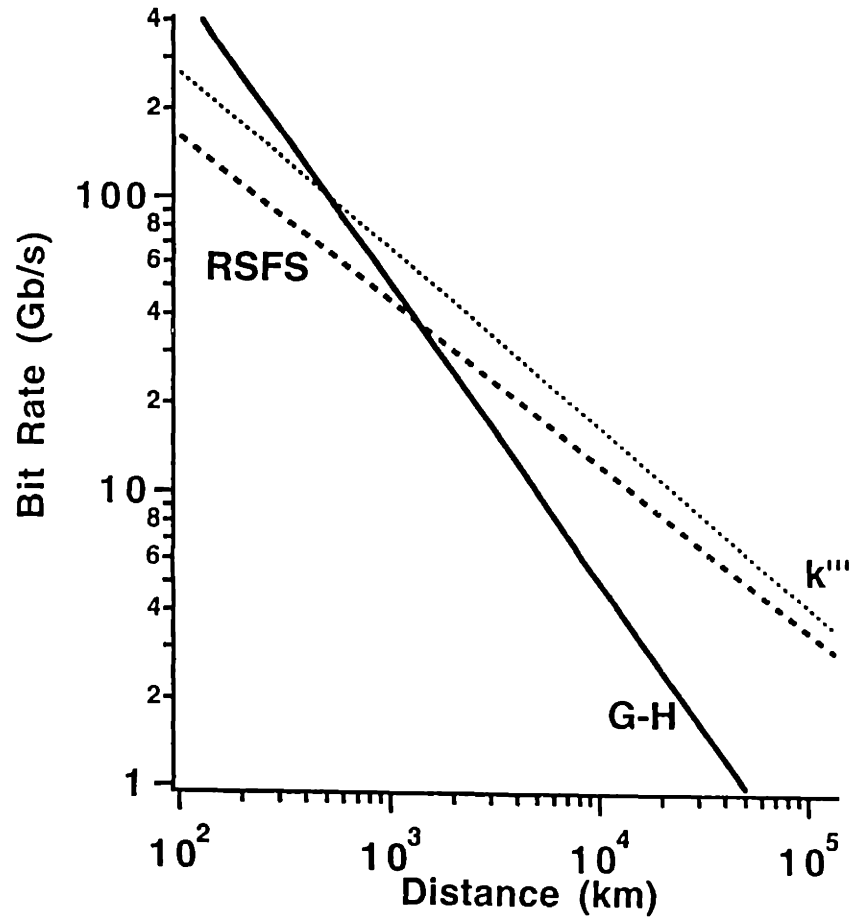
D=1 ps/nm/km
Amplifier Spacing = 250 m
Duty Cycle = 1/10
Log (BER) = -9

Figure 5-4: Unfiltered transmission limits.

path-averaging approach assumes that the soliton period is considerably longer than the amplifier spacing. If we assume that the soliton period must be greater then 5 times the amplifier spacing (so that the soliton phase period is forty times the amplifier spacing), then

$$R \leq \frac{\pi(R\tau)}{\lambda}\sqrt{\frac{c}{5lD'}}. \tag{5.63}$$

With the values selected above, this limit is $R \leq 74$ Gb/s. With such small amplifier spacings, the effects of the gain and loss are small, and it is therefore anticipated that this 74 Gb/s limit may be conservative.

5.5.2 Evolution with Filtering

The benefits of filtering in overcoming the Gordon-Haus limit have been discussed elsewhere [19, 21]. At higher bit rates, the issues become more complex, as we shall address in this section.

Filtering is introduced in order to constrain the spatial growth of the timing variance, and perhaps to inhibit classical RSFS. Inhibiting classical RSFS is equivalent to fixing the momentum p, in the absence of noise, and is likely to be reliable only when the RSFS is small. Filtering introduces loss, which must be balanced by the extra gain Δg, in order to fix the photon number in the absence of noise. To satisfy the latter condition, we must set the constant term in Eq. (5.36) to zero. All variables in this term are positive, which forces the extra gain Δg to be greater than unity, as expected. The coefficient of Δn on the RHS simplifies considerably by imposing the above condition, which is expected since this term is simply the next order in n.

To balance the RSFS downshift "force" with the filter, in the absence of perturbations, we set the constant term in Eq. (5.37) to zero. This determines the frequency separation between the soliton carrier frequency and the filter center frequency:

$$\omega_{f0} = -\frac{8c_R D l_f \Omega_f^2}{5\tau^2}. \tag{5.64}$$

Observe that ω_{f0} is negative. It is clear from the mathematical expression that the center frequency of the filter must be greater than the mean frequency of the pulse: in the frequency domain the RSFS is "pushing" the pulse against the low frequency side of the filter. If we choose Ω_f proportional to the pulse bandwidth, for a fixed l_f, then ω_{f0} is proportional to τ^{-4}.

With these two conditions, the equations of motion simplify to

$$(\frac{d}{dz} + z_n^{-1})\Delta n = A_{np}\Delta p + S_n(z) \tag{5.65}$$

$$(\frac{d}{dz} + z_p^{-1})\Delta p = A_{pn}\Delta n + S_p(z) \tag{5.66}$$

$$\frac{d\Delta T}{dz} = \left(\frac{k'''}{6\tau^2} + \frac{1}{l_f\Omega_f} - \frac{\omega_{f0}^2}{l_f\Omega_f^3} - \frac{1}{3l_f\Omega_f^3\tau^2}\right) + S_T(z)$$

89

$$+ \left(\frac{k'''}{3\tau^2 n_0} - \frac{2}{3 l_f \Omega_f^3 \tau^2 n_0} \right) \Delta n + \left(2D + \frac{2\omega_{f0}}{l_f \Omega_f^3} \right) \Delta p \quad (5.67)$$

where

$$z_n^{-1} = z_p^{-1} = \left(\frac{2}{3\tau^2 l_f \Omega_f^2} \right) , \quad (5.68)$$

and

$$A_{np} = \left(\frac{2 n_0 \omega_{f0}}{l_f \Omega_f^2} \right) , A_{pn} = \left(\frac{8 c_R \delta r^2}{15\tau^3} \right) . \quad (5.69)$$

Henceforth, we replace z_p with z_n.

Inspection of Eqs. (5.65) and (5.66) without the noise and without shifting filters reveals the dynamics of the RSFS/filter balancing. Suppose we begin in a state of equilibrium with $\Delta n = \Delta p = 0$. If we shift the frequency to a lower value (increase Δp), Eq. (5.65) states that Δn decreases, which we expect because the pulse is now further from the center frequency of the filter. Eq. (5.66) then shows that a negative Δn drives Δp negative, which is equivalent to pushing the pulse frequency higher. This is the consequence of the dependence of RSFS on n: as n decreases, the rate of self-frequency shift decreases. Because z_n is positive, we have stable damped oscillations. The natural frequency of oscillation is $k_n = \sqrt{-A_{np}A_{pn}} = 16 c_R D/(5\sqrt{3}\tau^3)$.

Solving Eqs. (5.65) through (5.66) we find

$$\langle \Delta T^2 \rangle = \frac{[A_{Tn}(s + z_n^{-1}) + A_{Tp}A_{pn}]^2 \langle S_n^2 \rangle + [A_{Tp}(s + z_r^{-1}) + A_{Tn}A_{np}]^2 \langle S_p^2 \rangle}{s^2 [(s + z_n^{-1})^2 - A_{np}A_{pn}]^2} + \frac{\langle S_T^2 \rangle}{s^2}$$
$$(5.70)$$

where we have defined

$$A_{Tn} = \left(\frac{k'''}{3\tau^2 n_0} - \frac{2}{3 l_f \Omega_f^3 \tau^2 n_0} \right) , A_{Tp} = \left(2D + \frac{2\omega_{f0}}{l_f \Omega_f^3} \right) \quad (5.71)$$

If we impose $z_n \ll z_0$, then the leading term upon inverse transforming is

$$|\langle \Delta T(z)\Delta T(0) \rangle| = \frac{Q_1}{R^3 Q_2} z + \text{other terms} , \quad (5.72)$$

where Q_1 and Q_2 are quadratics in R^2 and the "other terms" are damped oscillatory terms. This specific R-dependence is the result of choosing the filter bandwidth Ω_f proportional to $(1/\tau)$, while choosing a fixed filter separation l_f. We in fact impose that the filter bandwidth be five times wider than the transform-limited pulse bandwidth, $2\Omega_f = 5.611/\tau$. With the same values as used for Fig. 5-4 we plot the filtered limits in Fig. 5-5.

Including the slowly shifting filters would in general complicate the mathematics considerably, but it need not, and the physics can be simple. The center frequency of the solitons varies slowly, following the sinusoidal (or other) variation of the filter center frequency. The photon number would also see a sinusoidal driving function if it were not for Δg, which can be made a function of distance so as to cancel

FILTERED TRANSMISSION LIMITS
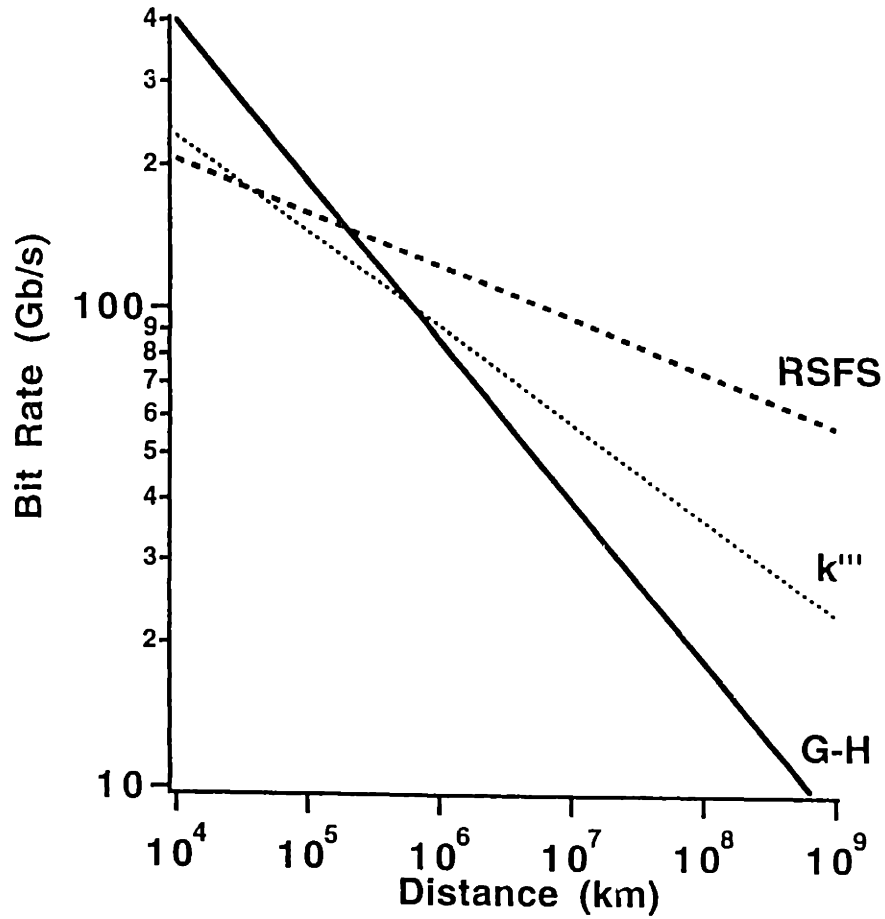
D = 1 ps/nm/km
Amplifier Spacing = 250 m
Duty Cycle = 1/10
Log (BER) = -9

Figure 5-5: Filtered transmission limits.

out this variation. And of course, with sinusoidal frequency variation, there is a deterministic timing variation, but we should define timing jitter to be fluctuations around the deterministic trajectory, so this variation is irrelevant. Modulators could be timed in accord with the deterministic trajectory. Thus, the dynamics of the soliton parameters are the same as in the fixed filter case except that the parameters perform their damped oscillations around the slowly varying frequency trajectory. Of course, if the filter passband were shifted too rapidly (by a significant fraction of a pulse bandwidth over a soliton period) or too discretely (by a significant fraction of a pulse bandwidth between adjacent filters) the dynamics would be considerably more complicated.

For the filter spacings considered in this paper, the limitation on the perturbation theory is the same as for the unfiltered case. For even shorter filter spacings, higher bit rates might be achieved, but one might find that ω_{f0} would have to be greater than Ω_f, making Δg comparable to unity, clearly violating the assumption that the effects are perturbative. However, even for the filter spacings considered here, there is reason to believe that the perturbation theory may not be valid for such high bit rates as in the unfiltered system. Blow et al. [184], in numerical studies of a Stokes solitary wave copropagating with a long stimulated Raman-scattering (SRS) pump pulse, have observed that solitary waves whose carrier frequencies are held fixed through filtering (gain bandwidth limiting in this case) and RSFS are unstable on very long length-scales (even with other than SRS gain). This is not surprising, since the (self-) Raman gain spectrum and the filter transfer function will in general balance only for a single frequency, rather than over the entire pulse bandwidth. If RSFS is too strong, one must either use all-optical regenerators or use (pulse width-dependent) filters which better cancel the Raman gain.

5.5.3 Applications to Memory

Thus far we have studied evolution of ZEROs and ONEs either without compensation or with filtering. The filtering extends the allowed distance of propagation for a fixed error rate, yet does not permit indefinite propagation; eventually, the jitter of the pulses becomes excessive, or the noise in the ZERO-slots builds up to unacceptable levels. If one introduces modulators, propagation can be extended over arbitrary distances. One may show that the signals consisting of ONEs (solitons) and ZEROs (empty time intervals) can be maintained forever. For this purpose one must ascertain the stability of the equations of propagation, i.e. prove that all disturbances die out exponentially. Having demonstrated the stability, one has the essentials for an all-optical memory.

5.5.4 ONEs with General Compensation

The system of equations Eqs. (5.36)-(5.38) may be written

$$\frac{dx}{dz} = \mathbf{A}x + \mathbf{B} + \mathbf{S} \, , \qquad (5.73)$$

where x is the vector of soliton parameters

$$x = [\Delta_{\eta} \ \Delta p \ \Delta T]^{T} \equiv [x_1 \ x_2 \ x_3]^{T} \equiv [x_n \ x_p \ x_T]^{T} \tag{5.74}$$

the superscript T denoting transpose, the system matrix $\mathbf{A}$ being a 3×3 matrix, $\mathbf{B}$ being the vector of constant terms, and $\mathbf{S}$ being the vector of noise terms. The components of $\mathbf{A}$, $\mathbf{B}$, and $\mathbf{S}$ are evident from Eqs. (5.36)-(5.38).

The stability of the system depends upon the location of the poles, which are the zeroes of the characteristic equation

$$
\begin{aligned}
s^3 \ &- \ (A_{nn} + A_{pp} + A_{TT})\, s^2 \\
&+ \ (A_{nn}A_{pp} + A_{nn}A_{TT} + A_{pp}A_{TT} - A_{nT}A_{Tn} - A_{np}A_{pn} - A_{pT}A_{Tp})\, s \\
&- \ A_{nn}A_{pp}A_{TT} - A_{np}A_{pT}A_{Tn} - A_{nT}A_{Tp}A_{pn} \\
&+ \ A_{nn}A_{pT}A_{Tp} + A_{pp}A_{nT}A_{Tn} + A_{TT}A_{np}A_{pn} \\
&\equiv \ s^3 + c_2 s^2 + c_1 s + c_o \ .
\end{aligned}
\tag{5.75}
$$

The Routh-Hurwitz criterion, which checks that all poles are in the left half-s-plane, can be used to determine stability. Direct application gives

$$c_2 \ > \ 0 \tag{5.76}$$

$$c_o \ > \ 0 \tag{5.77}$$

$$c_1 \ > \ \frac{c_o}{c_2} \ . \tag{5.78}$$

In the compensated system, a more realistic design criterion is that the real parts of the poles are all more negative than some minimum negative value, say $-s_{\min}$. In other words, we demand a certain degree of damping over some characteristic distance. For example, we may desire $1/e^m$ damping over the system length, in the case of transmission. Then we would choose $s_{\min} = m/l_{sys}$. By shifting the s-plane, we can use Routh-Hurwitz to obtain a more practical criterion:

$$c_2' \ > \ 0 \tag{5.79}$$

$$c_o' \ > \ 0 \tag{5.80}$$

$$c_1' \ > \ \frac{c_o'}{c_2'} \ , \tag{5.81}$$

where

$$
\begin{aligned}
c_2' \ &= \ c_2 - 3s_{\min} \\
c_1' \ &= \ c_1 - 2s_{\min}c_2 + 3s_{\min}^2 \\
c_o' \ &= \ c_o - s_{\min}c_1 + s_{\min}^2 c_2 - s_{\min}^3
\end{aligned}
\tag{5.82}
$$

The sum of the poles equals the sum of the self-damping coefficients, and Eq.(5.79) says

$$-(A_{nn} + A_{pp} + A_{TT}) > 3s_{\min} \ . \tag{5.83}$$

93

In the case with filtering and no other compensation, we found that A_{nn} and A_{pp} were both negative definite, and A_{TT} was zero (see Eqs.(5.65)- (5.67)). Thus photon number and frequency tended to be self-damping, while timing did not affect itself (in fact, timing was unbounded). Adjusting the ratio of pulse bandwidth to filter bandwidth adjusted the damping rate, but we could not make $s_{\min}$ arbitrarily large with non-shifting filters because of Δg providing gain for noise. Note that the criterion Eq.(5.83) does not actually require that each of the individual parameters be self-damping, just that the negative of the sum of the self-damping coefficients be greater than $3s_{\min}$. Likewise, having all negative self-damping coefficients need not ensure stability, as we shall see in one of the specific cases considered below.

The key element of the novel pulse storage ring is the FSA. The important features are that there is loss for low intensity light ($L_{FSA} > 0$), and the peak intensity of a soliton is such that increasing the peak intensity above the normal value results in greater loss for the pulse. Mathematically, this is expressed in Eq.(5.36) in that the FSA term multiplying n_0 is the net gain for the equilibrium pulse, while the FSA term multiplying Δn is the derivative of the bias term with respect to photon number, evaluated at the equilibrium photon number. Thus, the Δn term is negative because of the bias we have chosen. The actual equation for Δn is Eq.(5.40) and it involves the difference between the slope of the FSA and the net gain of the FSA. In the simplest case of no filtering and no amplitude modulation, the net gain would be zero, so photon number would certainly tend to self-damp. With filtering or amplitude modulation present, it would be preferable to make $\Delta g = 0$ and to compensate the filtering and modulator losses with nonlinear gain from the FSA. With positive net FSA gain, and decreasing gain with increasing photon number, we are absolutely assured that the FSA contribution to Eq.(5.40) is negative, so that it enhances the stability of the system.

Of course, FSA alone cannot eliminate the growth of timing jitter with distance, although it reduces the photon number contribution to timing jitter.

Next we take a less abstract look at the stability (which includes the bounding of timing jitter to a constant) of solitons with some specific combinations of compensation techniques. Four cases are considered, all of which can have timing jitter bounded to a constant. In one case, we discuss a novel mode of instability, and describe how the instability can be avoided.

Case I: FSA and PM

We can determine the signs of the various terms in the **A** matrix from inspection of Eqs.(5.40), (5.37), and (5.38). At lowest order, we choose the FSA to provide no change in photon number, we choose T_{PM} so that the PM can balance the RSFS, and we choose our PM so that it anticipates the velocity shift from TOD. Thus the **B** vector is zero.

It is clear that FSA provides self-damping of photon number, so $A_{nn} < 0$. With no filtering and no amplitude modulation, $A_{pp} = A_{TT} = 0$. So, Eq.(5.76) is satisfied, and we can certainly satisfy Eq.(5.79) as well. As for the cross-terms, the photon number is not affected by either frequency or position, so it is obviously stable. Photon number

94

affects frequency via RSFS, and $A_{pn} > 0$. Phase modulation converts timing shifts to frequency shifts, and $A_{pT} < 0$ if the PM is to counteract anomalous dispersion. Photon number drives timing through third-order dispersion, and in usual fiber $k''' > 0$, so $A_{Tn} > 0$. Finally, dispersion associates frequency with velocity, and $A_{Tp} > 0$. The only nonzero term in c_0 is $A_{nn}A_{pT}A_{Tp}$ which is positive definite, so Eq.(5.77) is satisfied. However, $c_1 = -A_{pT}A_{Tp}$, and we cannot satisfy Eq.(5.78) as an inequality. This is clear because in the absence of any photon number fluctuations, the frequency and timing undergo an undamped oscillation. A damping mechanism is required for true stability. This oscillation does confine the pulse timing to a finite window, which might be acceptable. However, this oscillation is not a natural soliton behavior, and the quadratic nature of the phase from the PM may cause the solitons to shed continuum, although the chirping of the tails may reduce the interaction between neighboring solitons if not too much continuum is shed.

Case II: FSA, PM, and Filtering

At lowest order we can again obtain $\mathbf{B} = 0$, as in the case of FSA and PM, with an extra degree of freedom provided by filtering.

Here FSA and filtering provide photon number self-damping, filtering self-damps frequency, and timing does not self-damp: $A_{nn}, A_{pp} < 0, A_{TT} = 0$, and hence $c_2 > 0$. The offset of the filter, to compensate RSFS, gives $A_{np} < 0$. RSFS and filtering give $A_{pn} > 0$. In cases for which we expect the perturbation theory to apply, we expect dispersion to dominate the dispersion of the offset filter, so $A_{Tp} > 0$. In most fibers, we expect $k''' > 0$, but depending upon the relative strength of filtering and TOD, A_{Tn} could take on either sign. Finally, $A_{nT} = 0$.

We have $c_0 = A_{pT}(A_{nn}A_{Tp} - A_{np}A_{Tn})$. Thus, at the least we require $A_{nn}A_{Tp} < A_{np}A_{Tn}$. The LHS is negative, so if $A_{Tn} < 0$, the inequality is automatically satisfied. Furthermore, if RSFS is very weak, $A_{np} \to 0$. Strengthening any of the compensation methods will improve things with respect to c_0. The third coefficient $c_1 = A_{nn}A_{pp} - A_{np}A_{pn} - A_{pT}A_{Tp}$, and since all three terms are positive, this appears to be a viable stabilization approach.

It is interesting to consider the physics of the instability which occurs if A_{Tn} is large and positive. Suppose there is a positive photon number fluctuation. Then $A_{Tn} > 0$ means that the TOD will cause a positive timing shift. The PM will impart a blueshift to a pulse which has shifted to the right in time ($A_{pT} < 0$). But the filter is offset to a higher frequency than the pulse, in order to compensate the RSFS. Thus this PM-imparted chirp shifts the pulse spectrum towards the center of the passband, the pulse sees gain, and Δn increases ($A_{np} < 0$). Thus there is positive feedback. Note that this failure mode is possible even if there is weak AM, in which case all three parameters, n, p, and T are self-damped. But of course, the instability can be easily avoided.

Case III: FSA, PM, and AM

At lowest order, we can fix the photon number by adjusting the FSA and AM, we can balance RSFS with PM offset, and we can choose a coordinate frame for the modulators such that timing is fixed.

As for the interesting dynamics, the only differences between this case and the case of FSA and PM are that the AM tends to weaken the photon number self-damping (but need not reverse its sign), A_{Tn} can take either sign depending upon the strength of TOD and the offset and strength of the AM, A_{TT} is no longer zero but is negative (self-damped timing), and A_{nT} is proportional to T_{AM} taking either sign.

As usual, it is easy to satisfy $c_2 > 0$, since A_{nn} and A_{TT} are both negative. It is interesting to note that the value of c_2 is the same regardless of the strength (or absence) of the AM, but depends only on the FSA. The coefficient $c_1 = A_{nn}A_{TT} - A_{pT}A_{Tp} - A_{nT}A_{Tn}$. The first two terms are positive definite, and the sign of the third term depends on the TOD and AM. The coefficient $c_0 = A_{Tp}(A_{nn}A_{pT} - A_{nT}A_{pn})$. The first term is positive, and the second term has the opposite sign as T_{AM}. Since there is no obvious reason not to choose $T_{AM} = 0$, let us assume this. Then $c_2, c_0 > 0$, and Eq.(5.78) is equivalent to $A_{nn}{}^2 + A_{nn}A_{TT} + A_{pT}A_{Tp} > 0$. The first two terms are positive and the third is negative, and the inequality can be satisfied. The self-damping of timing provided by the AM provides the stability which was lacking with PM and FSA alone.

Case IV: FSA, AM, and Filtering

At lowest order, the filters, FSA, and AM all contribute to give no net gain. RSFS is balanced by offset filtering, and timing is referenced to the lowest order group velocity.

All soliton parameters can be made self-damping, $A_{np} < 0$ from offset filtering, A_{nT} is proportional to T_{AM} and again there is no reason not to choose $T_{AM} = 0$ at this point, $A_{pn} > 0$ from RSFS, with no PM $A_{pT} = 0$, A_{Tn} can be of either sign, and we expect $A_{Tp} > 0$ in the regime of validity of the perturbation theory.

With the assumption of $T_{AM} = 0$, it is easy to show that all three conditions Eqs.(5.76)-(5.78) are automatically satisfied.

The operation of a memory requires not only the maintenance of the signal packets, but also the loading and unloading of packets. The operation of loading and unloading can be accomplished by fiber-loop switches [185, 100, 103] activated by a train of control pulses of length equal to the packet length. Another possible implementation is by frequency translation via four-wave mixing [46]; the memory stores the signal packets at a carrier wavelength different from the carrier wavelength on the signal bus. Transfer is effected when the pump in the mixing waveguide is turned on and the signal carrier frequency is translated to the memory carrier frequency and coupled to the memory by an appropriate filter [132, 186].

One important effect has to be overcome in loading and unloading, namely the changes in the saturation of the (fiber) amplifiers that have relaxation times long compared with any packet-interval. A means to overcome these saturation transients is to load with each packet the complement of the packet. If the complement is loaded in an orthogonal polarization, another advantage can be gained: one combats

the polarization hole-burning of the erbium amplifiers. Initialization of the memory is effected with a "standard" signal until equilibrium is reached.

Case V: PM, and Filtering

We have numerically simulated this case with a variety of parameters. Ultrafast phase modulation was achieved by coupling in low intensity (roughly an order of magnitude weaker than the data pulses), amplitude-modulated light orthogonally polarized and synchronous with the data at the beginning of the loop, and coupling out at the end of each roundtrip. Because (incoherent) cross-phase modulation is the mechanism, the data and modulator pulses need only be synchronized within a fraction of a pulse width. This pseudo-distributed phase modulation not only reduces jitter, but also can be used to eliminate the classical RSFS.

5.6   Summary and Conclusions

We have considered several designs for soliton storage rings, and have described some of the limitations of these devices and the related limitations on long-distance optical pulse transmission. At high bit rates, we find that the noise-imparted limitation due to RSFS is comparable to, or can exceed that of the Gordon-Haus effect. With very low group velocity dispersion, the noise-imparted limitation due to third-order dispersion can exceed the Gordon-Haus and/or RSFS limiations.

There are several ways to avoid noise-imposed limits. Bandwidth-limiting elements (including finite-bandwidth gain) provide a frequency-pulling effect. This provides a restoring force which tends to keep the pulses near the center of the passband and thereby reduces the growth of the variance of the timing jitter. We have found that the asymptotic growth of timing variance with filtering is linear for all effects considered.

If the rate of self-frequency shift is too great, an alternative to the mean frequency-preserving approach to filtering would be to use filters whose center frequencies (roughly) match those of a classically self-downshifting pulse. In addition to allowing the pulse to shift as it likes, shifting the filters suppresses the growth of dispersive waves. One disadvantage is of course that the channel frequencies are different at the receiver than at the transmitter. Another is that the choice of filter frequencies depends on bit rate. One can also use frequency-shifting filters which do not follow the classical RSFS shift, but rather force the soliton to follow the centers of the passbands of the filters.

Weak amplitude modulation in concert with clock extraction circuitry [26] in the transmission case, could also be used to combat the noise limits. Such a scheme would introduce additional pulse energy variations, however, unless filtering were used as well.

Phase modulators may also be used to suppress frequency shifts. The modulators create potential wells which trap the solitons. If the soliton drifts away from proper timing, it is chirped by the modulator so that group-velocity dispersion brings the

pulse back towards proper timing. As such, this would result in an oscillatory timing, but some damping mechanism, such as filtering (desirable) or loss to continuum (undesirable), will restore the pulse timing. We have proposed a phase modulation scheme for storage rings which can operate at arbitrarily high bit rates, using weak pulses in the orthogonal polarization to impart XPM upon the data. The weak pulses are replaced each roundtrip. With computer simulation, we have achieved stable 100 Gb/s soliton storage for 500km in a storage ring which has a length 30% greater than the soliton period, using this pulsed PM scheme.

Finally, intensity-dependent absorption, or FSA action, can provide intensity thresholding. Dispersive waves away from the pulse are suppressed, while the pulse intensities are driven to a specific value. This has the added advantage that it reduces the timing jitter from mechanisms which couple to intensity, such as RSFS and TOD.

Another way to avoid the usual noise limits is to use a pulse replacement technique. A somewhat exotic proposal is found in [100], employing a high-speed all-optical solitary wave cross-phase modulation switch to perform the replacement, while the timing of the replacement pulses could be established by clock extraction as discussed above. For relatively low bit rates (under 10 Gb/s or so), however, simpler schemes are possible. For example, semiconductor (or other) laser sources could be spaced along the transmission line. Clock extraction would be used to tune the repetition rate of each laser, while the incoming bits could be used to drive a modulator (e.g. $LiNbO_3$) for on-off keying of the laser output. The pulse replacement approach has the obvious advantage that the shape, timing, and spectrum of the pulses are restored. By decreasing L, higher bit rates and therefore shorter pulses are acceptable.

Chapter 6

Devices for Networks

Up to the 1980's, communications networks relied on electrical cables for transmission, and electronic switching and routing elements. Subsequently, optical fibers were used for transmission, again with electronic switching. In long-distance applications (e.g., trans-oceanic), electronic regenerators were used periodically, to restore the degraded optical signals. These regenerators converted the incoming light to electrical signals, "corrected" and amplified the signals, and converted them back to light, to be transmitted through the following section of fiber.

A more recent development in long-distance transmission is the replacement of electronic regenerators by erbium-doped optical fiber amplifiers (EDFAs). No photonic/electronic conversion is required, and these amplifiers are much more compact and less costly than regenerators. Switching is still performed electronically.

An important question is whether or not all-optical switches would have any advantages over electronic switches, particularly in a full-fledged network rather then in a simple single trans-oceanic link.

Another important consideration is that the physics of transmission may suggest that for certain portions of a network, on-off keyed optical solitons may be the ultimate bits, while in other portions NRZ is advantageous.

The objective of this chapter is to present some classes of devices which may be of use in networks, especially networks in which solitons play a role, and to suggest some specific candidate implementations. Clearly this chapter is not complete, and it is be biased towards optical implementations, because electronic implementations are already well-established.

6.1 Sources

Sources for soliton communications must meet several requirements. The following are requirements are not essential, but serve to provide concrete and desirable specifications. The pulses should be nearly hyperbolic secant shaped, nearly chirp-free, of width in the range of 500 fs to 100 ps. The source should have minimal timing jitter, and be able to operate at repetition rates of 5-100+ GHz. It would also be desirable to have tunable sources. Furthermore, sources with adjustable repetition rates would
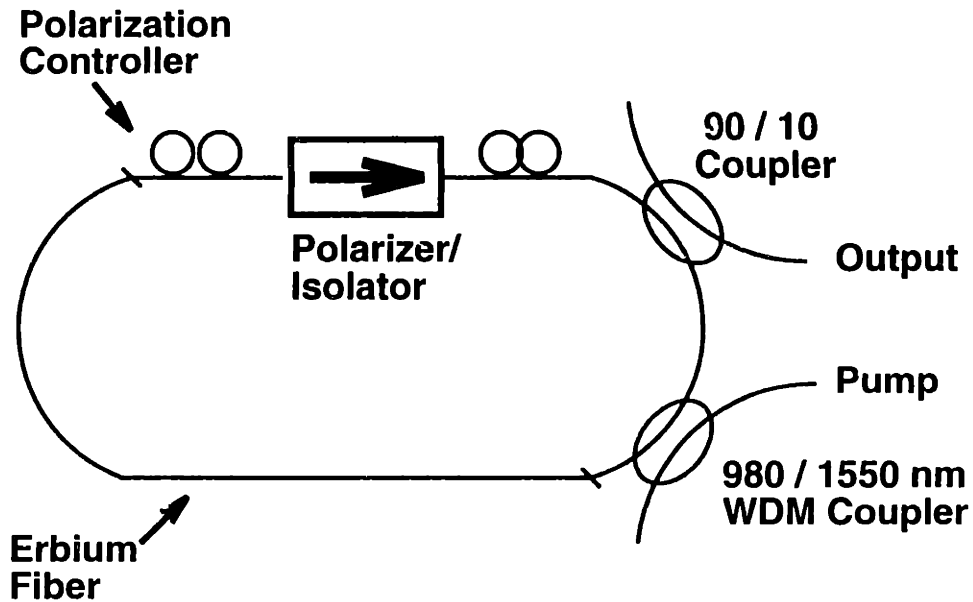
Figure 6-1: MIT erbium fiber soliton laser.

not only be flexible, but could be useful as components in other devices. I shall refer to these criteria in describing different source types below.

Below, four classes of sources are discussed. Although some sources, such as well-designed fiber lasers, are capable of producing transmission quality pulses, it is likely that these sources will either be followed by or contain modulators and/or filters. Therefore, the "Sources" section is not independent of the section on Modulators.

6.1.1 Fiber Lasers

Fiber lasers have been designed to produce very clean soliton-like pulses [64, 63, 187]. An elegant MIT design is shown in Fig. 6-1. Indeed, many fiber lasers are essentially small-scale versions of long distance soliton transmission lines with feedback: they support path-averaged solitons in steady-state [182, 188]. Achieving pulse widths in the desired range is not difficult. Limited tunability has been achieved. At the time of writing, the primary drawback of fiber lasers is that the achievable repetition rates are too low. Recently, however, multi-GHz active mode-lockers have been incorporated into fiber lasers, bringing the repetition rates more in line with the desired rates. Multiplexing of several fiber lasers is always an option. Harmonic mode-locking can be used to achieve bit rates up to the maximum modulator speeds [189, 190, 191,

100

192, 193].

Another drawback is that the periodicity of the laser cavity causes phase-matched generation of sidebands from the pulse[10, 158, 159, 161] which wastes energy in continuum. This is less of a problem in generating pulses for communications which are typically longer than a picosecond than for subpicosecond pulse generation, because the path-averaged soliton period is much greater than the cavity length, so that the coupling between pulse and continuum is very weak.

An idea which has proved valuable for NRZ transmission has also recently proved to be useful in fiber lasers. The idea is to alternate sections of positive and negative dispersion fiber, so that the average dispersion is very low, making the averaged characteristic dispersion length very long, yet the dispersion much more strongly affects the pulse dynamics than SPM. With this "stretched-pulse" approach, much shorter pulses have been achieved than with lasers which maintain near-soliton pulses throughout [194]. Because of the strong stretching and compression of the pulses, they no longer have a unique wavenumber as they traverse the cavity, and this suppresses coupling to the continuum. Therefore there is less loss to continuum. The stretching also inhibits phase-matching of the pulse with itself, or SPM, which raises the threshold for seeing higher-order-soliton-like reshaping. These lasers may be useful even for generating long communications pulses because they can produce higher power pulses.

6.1.2   Integrated Lasers

Semiconductor lasers have properties somewhat complementary to those of fiber lasers. Very high repetition rates can be achieved, covering the desired range. The desired pulse width range can be covered. Also, many of these lasers have significant tuning ranges, and there is great interest in fabricating rapidly-tunable sources. However, gain-switched lasers tend to produce chirped pulses, primarily because under direct modulation of the injection current, the carrier density is time-varying, which results in a time-dependent refractive index. This is a serious drawback, requiring special filtering [195]. The chirp also tends to be sufficiently nonlinear that external dispersive compression, while beneficial, is not adequate for producing transform-limited pulses [196].

Despite continuing improvements such as reduction of parasitic capacitance for better speed, and improved differential gain, it is very possible that external modulation will be the preferred method for producing pulses from semiconductor sources, especially at bit rates of 20 Gb/s and higher [38]. As of early 1993, to my knowledge, the highest reported bandwidth for a modulator is 40 GHz [197, 198, 199]. Modulators which can be used at 1.55 μm include LiNbO$_3$ modulators and InGaAsP/InP and InGaAlAs/InAlAs electroabsorption (Franz-Keldysh or quantum-confined Stark effect) modulators. A rather fortuitous discovery is that by sinusoidally driving an InGaAsP/InP double heterostructure Franz-Keldysh electroabsorption modulator of strip-loaded planar waveguide structure one can produce clean pulses believed to be transform-limited and sech^2-shaped [200]!

Currently, amongst available lasers, strained-layer quantum well laser diodes have

the best performance characteristics. For direct modulation, distributed feedback (DFB) and related designs are preferred because they remain single-mode under direct modulation.

External cavity mode-locked lasers produce better pulses, but are sensitive to temperature and vibration, and the bit rate is fixed by the cavity length. One successful hybrid source (meaning non-monolithic system with external cavity) uses a linearly chirped fiber Bragg reflector for the external cavity [201]. A drawback is the fact that when the operating frequency changes, so does the repetition rate, because of the use of a distributed reflector. This distributed reflector of course also introduces dispersion into the laser, which is a function of the chirp of the Bragg reflector. Monolithic short pulse lasers have also been fabricated, at repetition rates in excess of 100 GHz [202, 203].

There is hope that quantum wire and/or quantum dot laser arrays may have even better performance characteristics [204], but these are still in the laboratory stage. It has been predicted that these lasers could have μA threshold currents. The more localized and narrower density-of-states reduces temperature sensitivity and improves the differential gain which increases the relaxation oscillation frequency and should therefore improve the modulation bandwidth. Increased differential gain further implies reduced carrier fluctuations and therefore reduced index fluctuations, which should result in less chirping under current modulation.

With the hope of spatial parallel optical processing, surface-emitting lasers have been developed. Densely packed, fully monolithic arrays of vertical cavity surface-emitting lasers have been fabricated. Such arrays are perhaps irrelevant for launching solitons onto single transmission fibers, but they may be useful for various processing functions.

6.1.3 Modulational Instability / Two Frequency Beating

From linear thinking, a simple way to generate a train of pulses is to beat two CW beams at two different frequencies [205, 206]. Clearly the resulting pulses are neither sech-shaped nor chirp-free. However, in an anomalously dispersive medium with positive Kerr coefficient, such as an optical fiber at wavelengths longer than 1.3 μ, the process is enhanced by modulational instability (Benjamin-Feir instability). In fact only a small CW seed will cause a larger power CW beam to break up into a train of solitons (and some continuum, of course). This is better than the simple linear scheme, but the residual continuum will make the pulses seem somewhat chirped, not perfectly sech-shaped, and the pulse tails will overlap.

An improvement has been developed by Chernikov and others [207, 208]. The improved scheme uses a fiber whose dispersion decreases along the length of the fiber. From the point of view of the pulses, this is equivalent to an adiabatic gain, and it has been found that cleaner pulses result. If there is a problem with this scheme, it is that the most conveniently generated pulse trains are at bit rates which are higher than the modulation rate of any current modulators. Thus, it would be necessary to DEMUX, modulate, and MUX. In the early experiments, specially-drawn (nonuniform rate drawing) dispersion decreasing fiber was used. Recently, sections of standard fiber of

carefully selected length were spliced between dispersion shifted fiber as an alternative methos of tailoring dispersion, and Chernikov et al. produced trains of 2.2 ps solitons at 59 GHz [209]

Recently, a monolithically integrated DFB laser and electroabsorption modulator has been used in conjunction with a dispersion-decreasing fiber to achieve 2.5 ps pulses at 15 GHz with 0.33 time-bandwidth product [210].

6.1.4 Fourier Phase Filtering

Fourier phase filtering, implemented by Weiner and Leaird [211], converts one high-power broadband pulse into a very high bit rate train of pulses. Gratings and lenses are used to convert a pulse into a spatial pattern corresponding to its temporal Fourier transform. A phase-filter is placed in this plane. The inverse Fourier transform is then performed spatially.

6.2 Modulators

Modulators are of course required in order to encode data which is to be transmitted. They may also prove useful in generating pulses. This is especially true for semiconductor lasers, which when directly modulated produce chirped pulses unsuitable for direct transmission. The frequency chirping is generally significantly less with externally modulated, rather than with directly modulated semiconductor lasers [212]. Soliton transmission experiments have been performed with 10 GHz modulators [26, 34, 30]. KDD has fabricated a Franz-Keldysh-type electroabsorption modulator in InGaAsP which fortuitously imparts a very $sech^2$-like intensity modulation [200]. These have been successfully incorporated into soliton transmission experiments by KDD [213].

All-optical switches can easily operate as modulators at essentially any rate, with one pulse stream switching another. However, the switching stream itself must have been modulated at this high rate, or must consist of several bit streams which were modulated at lower rates and then multiplexed. If constructed with optical fibers, the product of switching energy and device length for all-optical switches is larger than desirable, and one hopes for a medium with larger Kerr coefficient.

Thus far in this section, I have discussed modulators with the assumption that the purpose of the modulator is to output a stream of ONEs and ZEROs which depends upon the signal and control inputs to the modulator. There are other applications of modulators, as in some lasers, memories, and long-distance transmission, where the purpose of the modulator is to impart the same amplitude or phase modulation (usually weak) to every bit interval: i.e., there is no control stream. This may be useful for preserving data which would otherwise degrade. Such modulators are discussed in the chapter on Stability and Timing Maintenance. Up to the present, such modulation has been performed with electrooptic or acoustooptic devices, which are limited to electronics speeds.

I propose that modulation at arbitrary bit-rates can be achieved through the use

of streams of pulses. Phase modulation can be achieved by using (perhaps) small amplitude pulses orthogonaly polarized to, and synchronous with the data. Cross-phase modulation is the modulation mechanism. The modulating pulses can be replaced periodically, ensuring proper behavior. This is a way of artificially ensuring that the data pulses themselves do not alter the properties of the modulator. The synchronization need only be within a fraction of a pulse width because the modulation mechanism is incoherent.

I propose that weak amplitude modulation can be achieved via pulsed Raman pumping. A stream of pulses with a carrier frequency roughly 15 THz higher than the data can be used to pump the data. This obviously provides gain for the data, but if the walk-off is negligible, it also provides amplitude modulation. To avoid walk-off, the pump and data carrier frequencies can be selected to be on opposite sides of the dispersion zero, so that both sets of pulses have the same group velocities. This is very restrictive, however. A more convenient approach would be to use birefringent fiber, with the pump pulses polarized orthogonal to the data. Group velocity match is achieved when

$$\frac{\Delta n(n + \Delta n)}{c^2 D} = \frac{\Delta \nu}{\nu(\nu + \Delta \nu)} \tag{6.1}$$

where n is index of refraction, c is vacuum speed of light, D is time-of-flight dispersion, ν is the data carrier frequency, Δn is the difference in index of refraction between the birefringence axes of the fiber, and $\Delta \nu$ is the frequency difference between pump and data. At a data carrier wavelength of 1.55μm and a pump-signal frequency difference of 13 THz, we require a birefringence of

$$\Delta n = 2.93 \times 10^{-5} \frac{D_{\text{ps/nm/km}}}{n}, \tag{6.2}$$

where $D_{\text{ps/nm/km}}$ is the dispersion in units of ps/nm/km. Thus, with dispersion of 2 or 20 ps/nm/km, we require birefringence of 4×10^{-5} or 4×10^{-4}, respectively. The birefringence of ordinary PM fiber is in this range.

6.3 Amplifiers

Of course the erbium-doped fiber amplifier (EDFA) is recognized as a tremendous breakthrough for optical communications. EDFAs provide gain right in the lowest loss wavelength range for silica fiber, near 1.55 μm. They have gain bandwidths of 25-30 nm. Gain of 30 dB is readily achieved with less than a Watt of electrical power driving a laser diode pump. Their advantages over electronic regenerators include their size and weight which are far less and which make EDFAs much easier to place onto or raise from the ocean floor, and the fact that they simply splice into the transmission fiber. Advantages over semiconductor amplifiers include the "impedance" matching achievable with an EDFA which can be spliced into the transmission line and which has comparable core size and index of refraction, the long upper state lifetime (around 10 ms!) which provides bit-pattern independent gain, absence of (or at

least much, much weaker) problematic nonlinearities such as two-photon absorption, and polarization-independence of the gain.

Semiconductor amplifiers have the advantages of much lower power consumption, size, and the potential for integration. It is very unlikely that they will be used as amplifiers in transmission, but they might be useful at receivers or in intelligent nodes. Their problematic resistive nonlinearities do have potential for some device functions. Their strong reactive nonlinearities, in designs which minimize the resistive nonlinearities, have the potential for fast and compact switches (see the Nondegenerate Four-Wave Mixing subsection of the Packet Switches section).

A variation on the usual EDFA is the EDFA with inhomogeneous broadening. The amount of inhomogeneous broadening depends upon the host glass. These amplifiers may be able to provide equalized gain for several WDM channels [112, 137, 138], unlike ordinary EDFAs which are primarily homogeneously broadened, and could likely provide equal gain for only two channels [16]. This topic is discussed in greater detail in the section on (Resistive) Equalizers, and in Chapter 3.

6.4 Multiplexers

Both time division- and wavelength division multiplexers are needed for a general high-speed network. An essential ingredient for successful MUXing is synchronization, but this topic will be treated in a separate section below.

6.4.1 Time Division Multiplexers

The simplest time-division multiplexers (TDMUXs) might be Y-junctions, with the signals to be multiplexed entering from two different ports, and being merged into a single waveguide/fiber. There will of course be some radiative loss at the merger, but the simplicity of this passive device makes it attractive. It may also be used as a wavelength division multiplexer (WDMUX).

A more complex TDMUX suggested by Molter-Orr et al. [214] has the advantage that it can be operated in reverse as a demultiplexer (TDDEMUX). See Fig. 6-2. The incoming signals on two waveguides enter a 3 dB coupler. The output ports of the coupler become the two arms of a Mach-Zehnder interferometer (MZI), which merge in a Y-junction. One arm of the MZI is electro-optically modulated. A modulation rate of ω achieves multiplexing at (or demultiplexing from) 2ω.

6.4.2 Wavelength Division Multiplexers

At first it might appear that WDMUXing would be easier than TDMUXing. There are some subtleties, however. If one were to send two equal bit-rate streams of solitons at two different carrier frequencies along two different fibers which join in a passive Y-junction, without regard to synchronization of the bit streams, one might find that after several kilometers of propagation the pulses would have undergone bit-pattern-dependent walk-off with respect to each other. The reason is that solitons
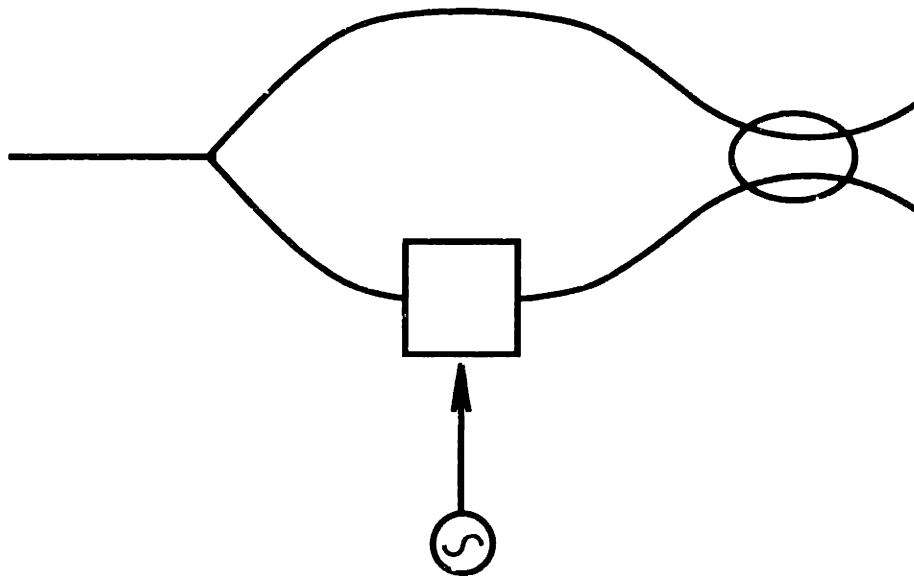
Figure 6-2: TDM (de-)multiplexer.

do not add linearly. In a complete soliton collision, the frequency shift of the first half of the collision is exactly compensated by the frequency shift in the latter half of the collision. If the collision is not complete, however, then there will be a net frequency shift, resulting in a timing offset after propagation through the dispersive medium. If two solitons at different frequencies are overlapped when launched, then by the time they have fully separated they will each have undergone a frequency-shift, because each pulse nonlinearly phase-modulates the other [170, 13]. A pulse which was launched without colliding (i.e., a ONE launched when there was a ZERO in the other WDM channel) will not suffer this walkoff.

There are several ways to avoid this problem. The most obvious but most unappealing approach is to TDMUX the WDM channels at the input. This would severely restrict the number of channels.

The author suggests that a more practical alternative might be to multiplex many pulses nearly simultaneously. If traffic is reliably heavy, with many channels, then each pulse will be launched in a sea of cross-phase modulation and the net frequency shifts should be small. Considering that bursty traffic is likely, extra streams of ONEs could be MUXed with the data. The ONEs could be at frequencies outside the transmission channels, which could be filtered after the MUXes if necessary. If the traffic is quite bursty, the ONEs could be constantly fed into the MUX and recycled in the pulsed source which provided them. If the traffic is only occasionally bursty, the traffic could be monitored upstream of the MUX, and the extra ONE streams could be turned on only when the traffic drops below some threshold.

106

6.5 Demultiplexers

Many proposed DEMUXs are not simply MUXs operated in reverse. Also, the timing constraint for WDMUXs is relaxed for WDDEMUXs.

6.5.1 Time Division Demultiplexers

One possibility is to use the reversible device proposed by MIT, described under Time Division Multiplexers above [214]. This device splits an incoming stream at bit-rate $2R$ into two streams at R. The incoming pulses enter a Mach-Zehnder interferometer (MZI), one arm of which is electro-optically phase-modulated at frequency R. The far end of the MZI is not terminated with the usual passive Y-junction, but rather with a 3 dB coupler.

All-optical cross-phase modulation switches, as discussed in Chapter 2, are suitable for TDDEMUXing [43, 44]. A control stream of pulses, at the DEMUXed bit-rate, is used to switch out the desired bits. As usual, this device can be implemented with orthogonally polarized signal and control pulses, or with signal and control at different frequencies.

The implementation of Andrekson et al. [44] is near the zero-dispersion point of the fiber, to eliminate pulse reshaping in the DEMUX, and the (very small) walkoff is achieved with a small frequency difference between signal and control. It seems that the output pulses must be highly chirped as a result of uncompensated Kerr phase-shifts (the authors discuss neither chirp nor spectra). The design is also limited to one signal frequency, and is 14 km long! The (very long) length is a consequence of their low target switching energy of 1.1 pJ.

Four-wave mixing in fibers can also be used for DEMUXing although with less efficiency [46], and with an attendant carrier frequency shift. Polarization rotation, and XPM-induced frequency shifts have also been proposed for use in DEMUX's [47].

When refined, four-wave mixing in semiconductors may prove to be a very practical means of DEMUXing. Four-wave mixing in semiconductors has been used successfully for wavelength conversion by Tatham et al. [40]. They used a CW pump source, but it should be possible to use pulsed pumps to control the wavelength conversion, for use as a DEMUX or other switch. Coupling losses might be balanced with gain in the semiconductor. The high-power CW pump has the advantage that it can be used to keep the gain of the semiconductor saturated, so that the data are not modulated by their own patterns. In any event, the quality of the output pulses may be a concern (e.g., multi-photon absorption may lead to distortion). The great advantage of semiconductor DEMUXs is the lack of latency and compactness.

There are also resistive DEMUXs. In one implementation, a very short Sagnac loop can be used. It contains an asymmetrically placed semiconductor optical amplifier (SOA). There are several proposed devices employing such loops [84, 41]. The use of a SOA may provide the advantage of shorter devices, but typically this advantage is lost because the device is limited by the gain recovery time. One device, the SLALOM [84], is limited to aggregate data rates of the inverse gain response time. A more recent device, the Terahertz Optical Asymmetric Demultiplexer (TOAD),

which requires a clock input, is limited to TDM channel rates of the inverse gain response time, but the aggregate data rate is limited only by the rise time of the gain response (depletion) and by the propagation delay within the asymmetric nonlinear element. Sub-pJ switching energies may be sufficient. Signal pulses have much lower energy than clock pulses (a factor of thirty in the experiment). The latter are used to saturate the nonlinear element. However, in the experiment, it was supposed that 40 channels were TDMed. The author believes that these devices may exhibit bit-pattern-dependent fluctuations in output, which may require some subsequent pulse standardization device.

6.5.2 Wavelength Division Demultiplexers

Channel-dropping filters (CDFs) seem ideally suited for this purpose [133, 132, 215]. These are resonant devices, with side-coupled quarter-wave ($\lambda/4$) shifted distributed feedback (DFB) resonators adjacent to the waveguide bus which carries the signals. The advantages of these devices are their sharp selectivity, and the fact that they can be used in designs which either extract all information at a preselected frequency, or tap a channel and amplify and reinject it onto the bus. Perhaps the only disadvantage is that it may be difficult to make them tunable. Design and fabrication of CDFs is in progress at MIT [216, 217], Columbia U. [186] and elsewhere.

Fabry-Perots of different free spectral ranges can be cascaded to effect a single-passband filter, but this approach is crude by comparison with CDFs. Design and fabrication of CDFs is in progress at MIT [217], Columbia U. [186] and elsewhere.

Several alternative technologies have been successfully demonstrated. Perhaps the one most closely resembling the CDF is the vertical coupler filter [218]. The device is a grating-assisted coupler which is current-injection- or electro-optically tuned (changes the index of refraction of one of the waveguides), and is narrowband wavelength selective. These devices have been successfully demonstrated.

Very compact and functional monolithic echelle grating - curved waveguide WD-DEMUXers have been fabricated in InGaAsP/InP [219, 220, 221]. These can perform frequency routing functions.

Yet another possibility is to use two star couplers connected by a phased array of waveguides [222].

6.6 Routers

Nodes in general have many input and output fibers. Each fiber may be TDMed or WDMed (or both). The node must decide to which fiber each input signal is to be sent, and send it in the appropriate format, with appropriate synchronization. For simplicity, here we shall consider a router to be a device (or set of devices) which transfer data from one channel to another, but "channels" may be distinct in timing, wavelength, and/or space. Perhaps the simplest routers simply convert timing, wavelength, or spatial distinctions into timing, wavelength, or spatial distinctions.

It is clear that a node might benefit enormously if in addition to these "unin-

telligent" routers there is hardware to handle such issues as channel allocation and contention resolution. Of course, in the case of packet-switched networks, neither the destination information nor the timing nor carrier frequency of the packet are known by the node until the packet itself arrives (see Packet Header Readers). Thus we effectively require that the node have a destination-filter capability, which could be hardwired or dynamic, which converts packets to specific wavelengths, directs them to specific output fibers, and aligns them in time.

6.6.1   Wavelength ↔ Space Routers

These routers can be implemented using any of the devices mentioned in the section entitled Wavelength Division Demultiplexers. The echelle grating and waveguide phased-array DEMUXs were clearly designed with this functionality in mind. A single bus with a series of CDF's, each CDF coupling to a side waveguide, also serves this purpose.

6.6.2   Timing ↔ Space Routers

This seems an unlikely choice for a foreseeable network, because in contrast to wavelength ↔ space routers, there would appear to be a need for an active synchronized switching device which must spatially separate pulses which might be temporally separated by 100 ps. This is beyond anyone's near-term expectations for electronics, but it could be implemented with cross-phase modulation switches.

To implement TDM-to-spatial conversion, one can use a cascade of time division DEMUXs. For example, we can use MIT switches. The data travels along the fiber, through a polarization-selective coupler (cross-state for one polarization, bar-state for the orthogonal polarization) possibly through a nonreciprocal device, and into a Sagnac loop AND gate. The loop is biased so that it is normally reflecting. Locally generated clock pulses are fed into the loop at the TDM repetition rate. Properly timed data pulses (allowing for some timing jitter) will switch control pulses out of the loop (transmission port). The signal pulses which reflect from the loop pass through the nonreciprocal element so that their polarization is orthogonal to what it was as they approached the loop, so that they pass across the polarization-selective coupler and onto the next such stage.

6.6.3   Packet Routers

Here, the packet header must be read so that the desired destination is known. In a relatively "unintelligent" node, this might mean passing the header through a destination filter (a look-up table which maps global addresses to local output fibers). The packet might travel along a section of fiber which contains a series of packet switches, each connecting the bus to a specific output port. The destination filter would send a properly timed pulse to the appropriate packet switch.

There are a great many possible improvements on this simple approach. If packet lengths are not standardized, then a packet length filter is also required so that both

an ON pulse and and OFF pulse can be sent to the packet switch at the proper times.

The above approach cannot handle contention. Each output port might have a set of buffers, one for each input port, with some protocol to fairly order access to the output fiber. If the system is wavelength-multiplexed, we might have wavelength-shifters at the output fiber to convert buffered packets to available wavelength channels. Along with any of these improvements is the need for additional hardware to monitor channel availability and to initiate buffering, wavelength conversion, and transmission.

6.7 Clean-Up Devices

This class of devices is intended to remove continuum between pulses. Two obvious ways to do this are with amplitude modulators or with fast saturable absorbers. Both of these techniques are convenient only for TDM because for WDM it would be necessary to WDDEMUX, go through a bank of modulators or FSAs, and then MUX. Amplitude modulators also require clock recovery.

Artificial FSAs could of course be used, and a simple example is a nonlinear Sagnac loop mirror. Reflections are of some concern with these devices, but perhaps the most serious flaw is the low nonlinearity of silica fiber, which requires that the loops be very long or that amplifiers be used as well. Real FSAs have relaxation times which may be too long to be suitable for pseudorandom high bit-rate data.

Over long distances, periodically spaced filters are quite useful for suppression of continuum. This is a very simple and WDM-compatible solution. To avoid continuum buildup at the filter peak frequencies, the filter peaks can be shifted slightly with distance [22, 15]. The nonlinear pulses can follow gradual frequency shifts, but the continuum cannot.

A device which can serve as both a clean-up device and as a logic level restorer is described under Logic Level Restoration.

6.8 Frequency Converters

The objective of this class of device is to convert data at one frequency to another frequency. Applications include frequency-routing, certain proposed delay lines (see Delay Lines), and certain proposed buffers (see Buffers/Memories). Frequency conversion of pulses, CW, or both might be required. Several of the ideas for frequency translation permit simultaneous switching.

Tunable semiconductor lasers may offer a relatively cheap, compact, and efficient means of achieving these objectives. Tuning can be achieved on a few-nanosecond time scale. The lasers can be designed so that they will operate only at a specific set of discrete frequencies, which is useful for most applications, except perhaps for the delay lines where truly analog frequency control is useful. These lasers typically contain distributed Bragg reflectors (DBRs) which can be index-adjusted by changing the carrier injection to the DBR section.

Fast gain saturation in DBR lasers or in semiconductor optical amplifiers might

be used if the response time were fast enough. The incoming data are fed into the device, modulating the gain seen by a local source (the laser itself, or a source laser for an optical amplifier). Thus the output signal is inverted.

Four-wave mixing (4WM) is another potentially practical possibility. This has been achieved in fibers and in semiconductors. Fiber 4WM requires long lengths of fiber, introducing latency comparable to XPM switches yet with less efficiency. Semiconductor mixers are perhaps more promising because of reduced latency, but some degree of pulse quality must be preserved. Unlike standard semiconductor amplifiers, semiconductor mixers will be quite insensitive to the data patterns because of the strong pump light required (pulse train or CW).

On a more exotic and perhaps less practical note, optical fibers are Raman-active media which are capable of redshifting solitons without distorting them. For solitons, the frequency shift per unit distance is inversely proportional to the fourth power of pulse width. Variable redshifting could be achieved by converting the incoming data to solitons of different widths (see Soliton Pulse Width Converters), propagating the new solitons through a fixed-length section of fiber, and then converting them back to their original widths. One problem with this approach is the inability to blueshift pulses. Sources which can produce solitons of tunable width are certainly possible to design (see Soliton pulse width converters).

6.9 Soliton Pulse Width Converters

Here we can use all-optical AND gates whose input streams are the data stream and a control stream of ONEs with the desired pulse width. The AND gate is configured to replace the data pulses with control pulses. MIT switches would be appropriate, as discussed in Chapter 2.

6.10 Logic Level Restoration

I use the term "restoration" somewhat loosely. The devices discussed here do not in general provide a standard intensity output regardless of input intensity. Rather, they cause the intensity of a pulse to change towards a standard level. By cascading the devices, better standardization might be achieved.

A piece of fiber for polarization rotation, a stable, saturated gain section, waveplates, and a polarizer comprise an intensity restoring stage [61]. Fig. 6-3 shows such a device. There is a relative angle between the polarizations selected by the polarizers. If the stage is biased so that there is net gain at low intensities, the stage might be short, but may encourage noise growth. Instead one should bias so that low intensities see loss and high intensities are driven towards a fixed value. Thus such a stage serves both to suppress continuum and to restore peak intensities. The device as such is not designed to preserve pulse width, but if the pulses are very nearly solitons, this should not be a problem.

A problem with solitons, however, is that in order to get sufficient rotation, the fiber must be a few soliton periods long. We can estimate the minimum length of the
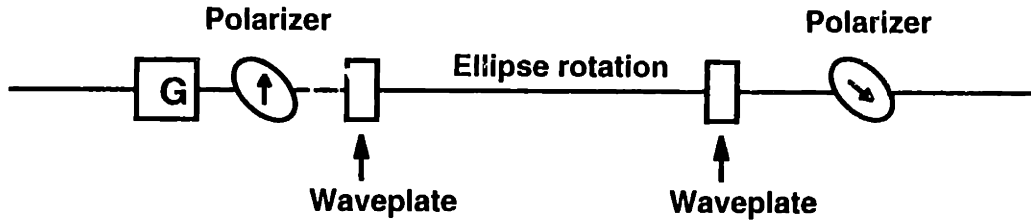
Figure 6-3: An open-loop logic level restorer. G = gain.

device in soliton periods. In the limit of pure Kerr effect, which is an overestimate for solitons by a factor of two, the differential phase between the two circularly polarized components is

$$\Delta phi = \delta_c(|u_c|^2 - |v_c|^2)L \tag{6.3}$$

where δ_c is the SPM coefficient for circular polarization, u_c and v_c are the orthogonally circularly polarized field components, and L is the length of the rotation fiber. The square of the field magnitude of a circularly polarized soliton (this is the worst case - the number changes by up to fifty percent for other polarizations) is

$$- k''/(\delta_c \tau^2) = 2/(\pi \delta_c z_0). \tag{6.4}$$

Thus the maximum differential phase is approximately $2L/(\pi z_0)$. If a differential phase of $\pi/2$ is required, the device must be more than $2.5z_0$ long. Unless the pulse widths are quite short, this could be prohibitive. Of course, pulses of intensity greater than a fundamental soliton might be used to achieve more rapid rotation, and the pulses could be subsequently replaced if necessary.

I propose a simple and obvious way to shorten the device. Excess gain could be introduced at the beginning of the polarization rotation fiber, with balancing loss at the end of the fiber. The device would be shortened by roughly the same factor that the intensity in the rotation fiber was increased. But of course, the pulses would be less solitonlike in the fiber, and the differential phase would likely increase by more than a factor of the intensity gain (Kerr stronger than dispersion, plus soliton compression). The output pulses might be chirped because of the excess Kerr, and if the device is on the order of a dispersion length or more, it is likely that dispersive waves will have been shed which may pass through the polarizer because they were generated within the fiber.

Similar results can be obtained with fixed gain and nonlinear loop mirrors [77, 74, 75, 76], instead of the polarization rotation sections. By including the gain in the loop asymmetrically, a compact device can be made [78, 79, 80, 81, 82, 84]. To make

112

the device even more compact, gain in excess of the desired gain could be placed in one half of the loop, and loss balancing the excess gain could be placed on the other side of the loop. As with the polarization rotator with gain, the output pulses are likely chirped at best, possibly with a pedestal as well.

6.11 Flip-flops, Latches, Multivibrators

In electronics, a flip-flop is a circuit which can store a single bit. There are numerous types of flip-flops, as there are numerous choices such as in what manner the bit is to be stored, the means by which the state of the device is changed, and the response times. As an example, a Type-D flip-flop (a latch), is a device with two inputs: data and clock. The input state is transferred to the output state only when the clock is high. This makes sense in a digital electronic system, where inputs and outputs are voltages which can be in one of two states. While one can imagine NRZ optical signals behaving analogously, it is not possible to make exact analogies with conventional OOK soliton systems, in which the data must consist of discrete pulses. Instead of a high (voltage) constant output, the output of a soliton device might be a train of pulses. This is in a sense similar to digital electronic multivibrator circuits, which produce pulses.

A monostable multivibrator, or one-shot, is named "monostable" because it can remain indefinitely in the low state, but only remains in the high state for a limited and predetermined amount of time. This notion of stability is different from the usual notions of stability for pulsed lasers and other optical short pulse devices. In the sense of the term "stable" as used for electronic multivibrators, a CW laser is stable in its high state and a pulsed laser is not. An optical analogy of a monostable multivibrator is a device which stretches (or narrows) pulses (see Soliton pulse width converters). However, in the electronic device, the amplitude is fixed and the width changes, which would not generally be the case in a soliton system (although it could be, if the dispersion of the output line differed from the dispersion of the input line by the correct amount). NRZ pulse stretching is of course possible.

An astable multivibrator is neither stable in the high nor the low state, and oscillates between the two states at a fixed rate. Thus it is a clock generator.

A bistable multivibrator is a device which can remain low or high indefinitely. RS and JK flip-flops (which I will not define here, but which have two inputs and may or may not have a clock input) are examples. Again to make an analogy with a soliton system, the state "high" must be interpreted to mean a train of solitons. Because, to my knowledge, there are no named digital electronic devices which operate on sets of pulses, I have tried to carefully distinguish devices which are highly analogous (which I term NRZ) from those in which the interpretation of "high" is a train of pulses (which I term "pulsed") synchronous with a clock that is local to the packet.

These sorts of devices are potentially extremely useful, especially in a packet-switched system where one performs switching of a large group of pulses all at the same time.

In principle, all flip-flops can be built from Boolean logic gates with feedback. We

know how to build any all-optical Boolean gate, so in principle, we are able to build any flip-flop. However, when a pulsed flip-flop is high for a long time, the recirculating pulses must be preserved without degradation for a long time. Because a fraction of the pulses must be tapped off as the output, gain is required in the feedback loop. The presence of gain means that we also have to worry about the preservation of ZEROs for long periods of time. Below I offer three possibilities for stable flip-flops. The first and third do not actually store pulses and ZEROs, but replace them regularly. The second approach stores and preserves the ONEs and ZEROs.

6.11.1 Pulsed Haus-Auston Flip-Flops

We can use the same concepts described in the Packet Switches section under "Haus-Auston switches" (please refer to that section for an illustration of basic elements of the device) to build a pulsed flip-flop. Here a pulse (the ON pulse) is used to short the striplines, generating voltage waves on the striplines. The region where the short is created optically is designed so that the source voltage sustains the current between the striplines once the short has been initiated. An OFF pulse might be applied somewhere between the voltage source and the striplines. That is, the OFF pulse shorts the source upstream of the striplines. This short is designed to remain a short only in the presence of the optical pulse - the source cannot sustain it - and this short must last long enough to cause the stripline short to revert to an open. A flip-flop can be made by transmitting an unmodulated stream of pulses (clock) into one of the inputs to the electrooptical coupler imbedded in the substrate. Shorting the striplines routes the clock stream to the other output port. Most electronic flip-flops have two complementary outputs, and this is also a feature of this optical flip-flop.

6.11.2 Pulsed Flip-Flops with Bistable Lasers

The essential ingredients of a flip-flop are a bistable device and a gate which within one bit interval flips the bistable device from one stable state to the other.

The author proposes that such a device can be implemented with an ultrafast logic gate and a pulse storage ring or bistable unidirectional mode-locked laser. In one implementation, the bistable device is an overdriven passively-mode-locked laser which is not self-starting. In this section, I shall call the bistable device a laser, but any bistable pulse storage ring will suffice - and the passive mode-locking (perhaps saturating fast saturable absorption (SFSA), meaning more loss at low intensities and at high intensities and less loss at intermediate intensities) is not an essential ingredient.

If SFSA is used, the laser can be biased so that low intensities, below a threshold, experience net loss. But the laser also supports pulses. Thus the laser is bistable by supporting either mode-locked pulses or nothing, without reconfiguring the laser. A problem with using a soliton-type laser with say polarization rotation as the SFSA mechanism is that the loop must be several soliton periods long in order for the SFSA to work (this was explained in the section on Logic Level Restoration - here dispersive waves would be intolerable, but chirp might not be because of the other elements in

114
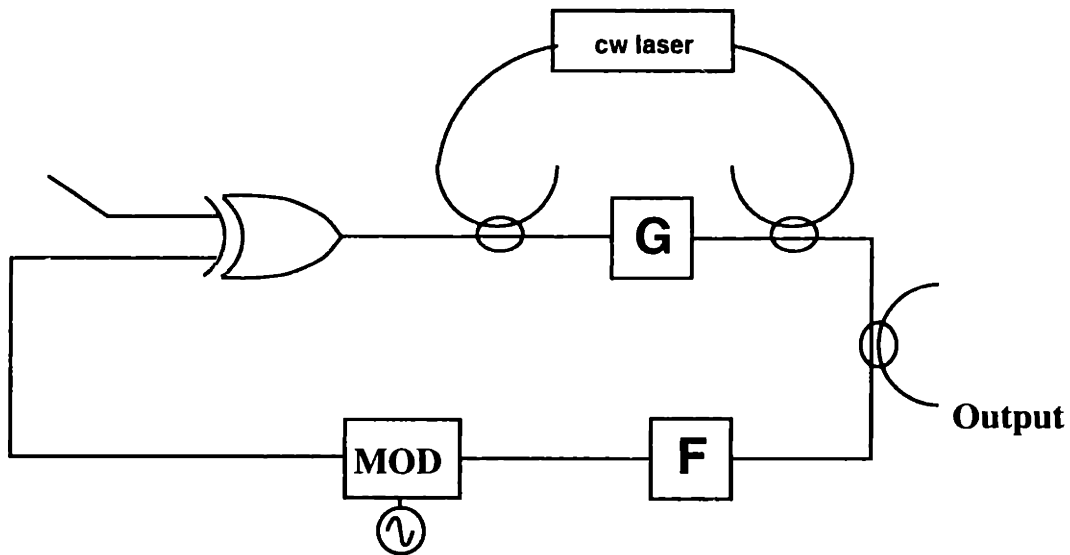
Figure 6-4: A THz flip-flop/multivibrator-like device with all-optical XOR gate incorporated into pulse storage ring.

the cavity). One could harmonically mode-lc ;k, or try to use non-soliton pulses.

The other essential ingredient is the gate which flips the laser from one state (pulsing or empty) to the other. A simple way to achieve this is to include an XOR gate in the laser cavity. One possible implementation is illustrated in Fig. 6-4. One input and the output of the XOR gate form part of the cavity. The extra input port of the gate is for the (in this case, single) flip-flop input. The input pulses are chosen to be very nearly the same as the laser pulses.

If the laser is pulsing, and a flip-flop input pulse is fed into the XOR gate, suddenly the output of the gate will be ZERO, or no pulse. Even if the ZERO of the gate is imperfect, the threshold of the laser will ensure that the laser stops pulsing immediately, and suppresses what any leakage from the gate.

If the laser is not pulsing, it will remain non-pulsing, because it is biased to be non-self-starting. How this is achieved is discussed below. With the laser not pulsing, if a flip-flop input pulse enters the XOR gate, it will pass to the output of the gate and into the laser cavity. Because the pulse closely resembles a steady-state pulse of the laser, the laser will immediately accept and maintain this pulse. If the device is

to be used at an harmonic of the roundtrip frequency, then the XOR gate must itself be a monostable-type device which remains high for one roundtrip time.

Ordinarily, the steady-state gain of such a mode-locked laser would be different depending upon the state of the laser (pulsed or empty). It would be undesirable in a flip-flop to have slow gain transients which would not only impart an undesired intensity modulation on the output of the device, but could also cause the empty state to become unstable. One way to solve this problem is to force the gain to remain within some limited range (ideally fixed), independent of the data, and there are several ways to achieve this. One way is to constantly feed CW, tuned outside the pulse bandwidth but within a homogeneous linewidth of the gain peak, and at a higher power than the data, through the gain medium. If the signal average power is much less than the CW, the change in gain due to data fluctuations (here, ON vs. OFF) will be small. The CW may be filtered out following the gain medium. In fact it might be recycled using a frequency-selective coupler, and fed back into the CW laser. This is the approach illustrated in Fig. 6-4. To make the gain insensitive to the state of the flip-flop, the CW power should be comparable to (probably greater than) the average power internal to the flip-flop when it is high. An advantage is that the gain remains saturated at all times, and a possible disadvantage is that considerable CW power may be required. However, the laser itself could produce rather low-power pulses which are further amplified externally.

An alternative to saturating the gain with power which is distinct from the pulses in frequency, is to use power in a different polarization. By using broadband polarization-selective elements in the cavity, the gain could be saturated using pulses or CW in the orthogonal polarization, again with average power greatly exceeding the data power. Orthogonal pulses can furthermore be used to provide phase modulation, as they cross-phase modulate the pulses (this is discussed in detail in Chapter 5). If nonlinear polarization rotation provides the passive mode-locking, then the orthogonal pulses must most likely not pass through the polarization rotation section.

The complement of the stored data pattern could be stored in the orthogonal polarization, as suggested by C.R.Doerr. This would ensure saturation of the gain at a fixed value, if these orthogonal pulses were fed into the buffer even in the absence of any stored data. The author suggests that a polarization rocking switch [50] without the polarizer could be used to generate the orthogonally polarized data and complement. By using the data as the switching pulse input stream and a sequence of ONEs as the switched pulse input stream, the device would replace the data with new pulses and would output the complement of the data (also new pulses) in the orthogonal polarization.

Yet another way to fix the gain would be to use a feedforward scheme to adjust the pump power supplied to the gain medium. This may be a more difficult approach, but may be more frugal in power. Suppose the integrated tapped output of the flip-flop is the feedback signal. In order to accommodate long periods in the low state, there must be a low level of pumping which ensures that the laser will not lase, yet which provides sufficient gain when the device flips to the high state. The pump must properly cancel the gain saturation transient.

The requirements for the XOR gate are not as stringent in this application as in

other applications. If the XOR gate is an MIT XPM switch (see switching chapter, Chapter 2), designed to output either of its inputs directly unless both are present, then the gate will perform nonideally (small leakage) only in the case of dual inputs. Because the output is ZERO, and the laser suppresses leakage, the nonideality is not crucial. One must evaluate the numbers, but instead of an MIT XPM switch, it might be possible to use a time-domain chirp switch [106] or to use a soliton-dragging switch [107, 108], if an amplitude modulator with deep modulation is used in the laser. The modulator would serve as the "clock" which would eliminate the mistimed pulses which were output from the XOR gate when it received two ONE inputs. Because all-optical fiber switches tend to be lengthier than desired, some sort of semiconductor gate may be preferable. Semiconductor four-wave mixers are natural AND gates because a frequency-shifted output occurs when simultaneous inputs at two different frequencies are present. Polarization rocking switches can be used to make inverters. These two components can be used to make a rather cumbersome XOR gate:

$$A\overline{B} + \overline{A}B = \overline{\overline{(A\overline{B})}\,\overline{(\overline{A}B)}} \ . \tag{6.5}$$

Thus five inversions and three ANDs can simulate XOR. While the MIT XPM XOR is much more straightforward, if it is implemented in fiber, it will introduce a large and undesirable delay.

The flip-flop with the single XOR gate and storage ring is not as fully functional as most flip-flops. I designed it so that it would have a single input which would change the state of the device whenever an input pulse arrived. The idea was really to make something similar to a (pulsed) monostable, for use as a packet switch. To operate it as a monostable, it is necessary to send both a trigger pulse and a clear pulse (to clear the device), and the two should be separated in time by one packet length. This could be done automatically by inserting a coupler and a delay line, so that the trigger pulse is automatically replicated, and the replica is delayed for use as the clear pulse. As described, the device would function improperly if two trigger pulses were sent to the device within one packet interval.

6.11.3 Pulsed Flip-Flops with Regenerative Gates

Instead of requiring the feedback loop to stabilize the ZEROs and ONEs for many roundtrips, one can simply replace the pulses each time. For example, one can use the XOR gate described near the end of the switching chapter, which is symmetric in the two inputs and which has an additional clock input. This approach greatly simplifies the devices, and the only penalty is that the XOR gate is active (must be fed with a stream of pulses at all times).

With this approach, it should be straightforward to map an electronic design into an optical design with little difficulty. In contrast, multiple feedback paths could make the bistable laser approach quite tricky.

An example of a simple NAND gate RS (reset-set) flip-flop is illustrated in Fig. 6-5. The truth table for such a device is presented in Table 6.1.
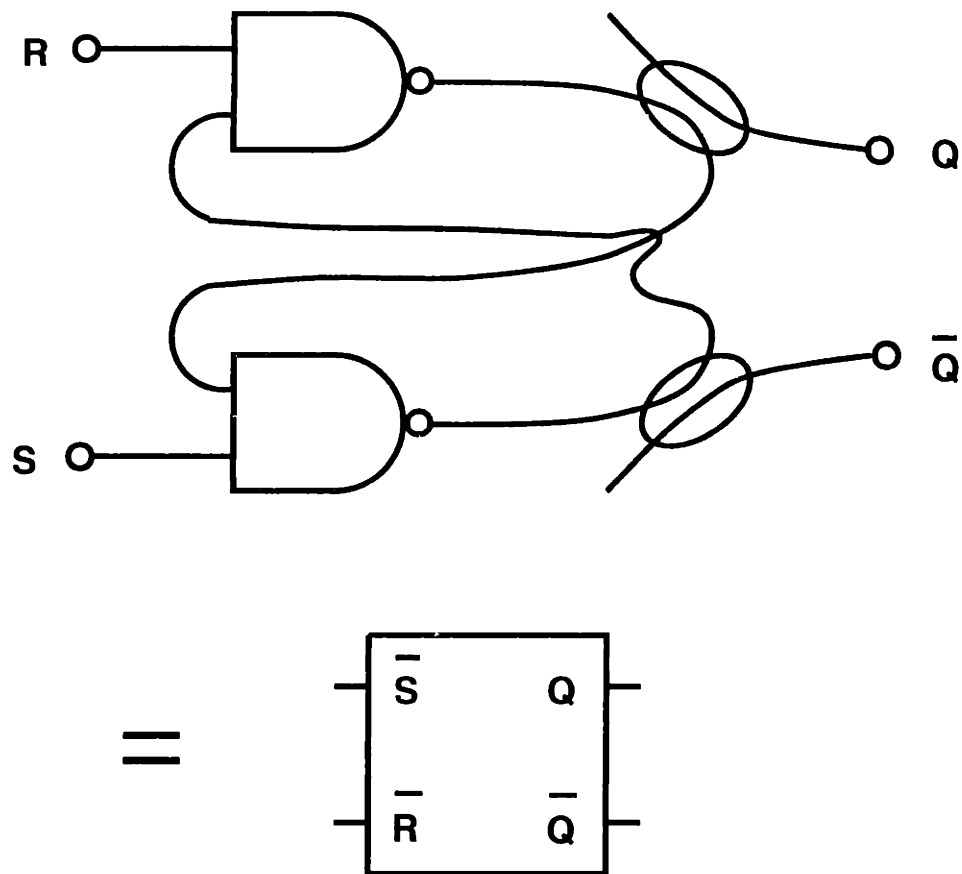
Figure 6-5: Basic all-optical NAND gate RS flip-flop. Electronic symbol for NAND gate is used to represent an all-optical NAND gate.

S	R	Q
0	0	disallowed
0	1	1
1	0	0
1	1	unchanged

Table 6.1: Truth table for NAND gate RS flip-flop.
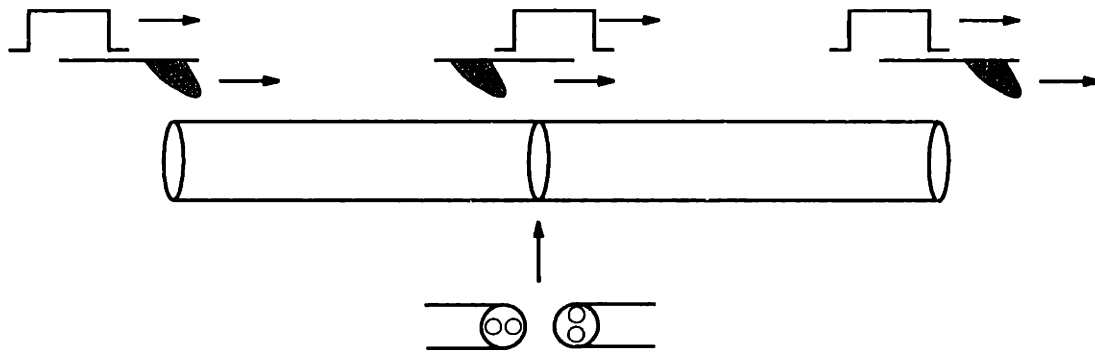
Figure 6-6: Orthogonally polarized NRZ pulse and soliton collide once in each of two sections of cross-spliced high-birefringence fiber.

6.12 Soliton to Non-Soliton Converters

This function can be approximated using XPM switches, with signal and control being of different polarizations or frequencies. One way to achieve this is with an AND gate which is fed a stream of CW, and a switching train of solitons. The solitons should have no timing jitter, and the switch should be such that the relative motion of the solitons and the CW covers precisely one bit interval. The switch replaces the solitons with switched CW. It seems unlikely using this technique that the CW at the edges of a bit interval can be made chirp-free and can be made to mesh cleanly (e.g. two consecutive ONEs without any discontinuity). Thus, this approach is more suitable for conversion to RZ than to NRZ.

Perhaps a simpler solution would be simply to disperse the solitons into broad and relatively flat pulses. Positive GVD with Kerr would serve the purpose. The problems are that the NRZ pulses would again not be true NRZ because we could not expect them to join smoothly at the edges of bit intervals. Furthermore, the nonsoliton entities would likely be highly chirped which would limit the distance over which the pulses could propagate without distortion.

6.13 Non-Soliton to Soliton Converters

This function can be achieved with cross-phase modulation switches. As usual, different polarizations, or different frequencies can be used. A two polarization approach is illustrated in Fig. 6-6. The switches have to be of the pulse-replacement type, and here non-soliton pulses coming in as data are used to switch locally generated solitons out.

Some questions immediately arise, concerning energy ratios and pulse distortion. The energy ratio of solitons to non-soliton pulses is, because of the solitons, a function of the path-averaged dispersion in the soliton channel, and may (depending upon

119

design constraints) be related to the relative amplifier spacings in the non-soliton and soliton channels. The path-averaged dispersion determines the path-averaged power of the solitons, while the amplifier spacings determine how weak the incoming signal will be, and how strong the outgoing pulse must be. Considering the unfavorable energy-length product of current all-optical switches, it is likely that the signals should be amplified prior to switching.

6.14 Bit-Rate Converters

It may be desirable to intentionally change the bit-rate of a given data stream. Large changes, i.e. compression or decompression by factors of 2, 3, ..., can be performed with MUXing and DEMUXing schemes, described elsewhere. In the process, it may be useful to perform pulse width conversion, another topic discussed in this chapter.

6.15 Polarization Standardization

One concern for many all-optical devices, including cross-phase modulation switches, is that the incoming signals are likely to be in arbitrary and time-varying polarization states. It would be helpful to have devices which could standardize polarization. It is likely that the bit-to-bit polarization variation for a data sequence from the same source will be small, even at a distant receiver. In such a situation, an electro-optic device which adjusts to the small bit-to-bit changes is quite suitable. Nevertheless, electro-optic devices are not only limited by the speed of the electronics, but they require electronic feedback as well [223, 14, 224].

The situation may be more complex in a full network. At the receiver, successive packets received may have been sent by different transmitters, and thus their polarization states may be completely different. Thus, there is a need for extremely rapid polarization standardization, or alternatively, for polarization-independent optical circuitry. There have been a few all-optical devices proposed for polarization standardization or insensitivity, some which may work, and some which are likely to be quite poor.

A simple but lossy device for standardizing the signal polarization prior to DE-MUXing shown in Fig. 6-7 is to send the signals through a polarizing coupler (PBC), rotate one of the polarizations, and coherently recombine in a coupler [105]. The figure shows an × but this need not indicate a cross-splice if twisting is permissible. The recombination must be performed within a fraction a wavelength, which is a serious design difficulty, particularly if the device is to operate in an unfavorable environment. However, there is a more serious problem with this approach. If the incoming light can have any polarization, then the two components split by the PBC can have any relative phase. For example, if the delay is such that light linearly polarized at 45 degrees to one of the axes of the PBC adds constructively at the output coupler, then light linearly polarized at -45 degrees to the same axis will completely cancel at the output!

A related but also problematic device is a two-color XPM switch which uses a
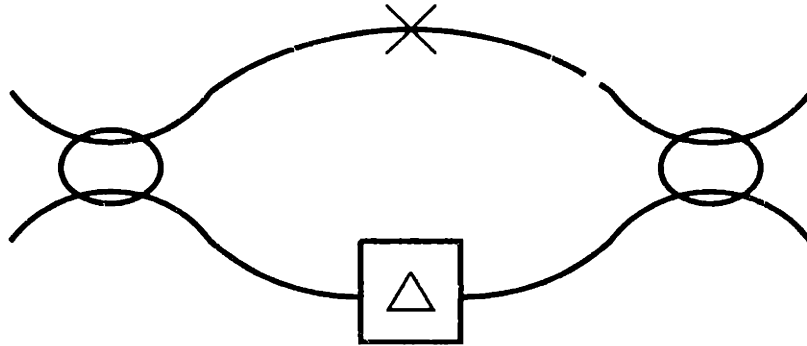
Figure 6-7: Polarization restoration concept device. × = twist by 90 degrees or cross-splice.

control pulse linearly polarized at 45 degrees to the axes of a highly birefringent fiber [96]. The control pulse, which propagates around the loop in one direction, splits evenly between the two polarizations and these two components affect data pulses of any polarization in the same way. Clearly, this cannot be a regenerative switch, and furthermore, the output signal pulse (ideally) has the same polarization it had at the input - polarization is not standardized. Although the values of dispersion for the pulses are not given, I am quite sure that the pulses are way above the soliton power and effectively see a (chromatically) nondispersive Kerr medium in the loop. Thus, the output pulses must be quite chirped, and it is unlikely that many such gates could be cascaded. It would be quite difficult to make this into a soliton device because of the arbitrary power splitting of the signal pulses, and because of the shredding of the control pulses by XPM. Because of the limitations of silica fiber, it is difficult to achieve simultaneously high enough power for switching in a reasonably compact device, and low enough power that high-birefringence fiber can rip a pulse into two orthogonally polarized pulses without chirping and distorting the resulting pulses and generating continuum.

I offer an alternative which is also imperfect. It combines some of the ideas of the previous two, eliminating many of the problems. One can start out with a device such as that shown in Fig. 6-7, but choose the delay in the interferometer to be roughly one pulse width. This way, the output pulses do not overlap except in the wings, but are close to each other. In other words, the one input pulse is converted into two pulses which are as close as possible without introducing excessive randomness in total output power as the input pulse polarization is varied throughout the Poincaré sphere. Now the pair of pulses can be used in a XPM switch in which a locally generated pulse orthogonal to the pair collides with both members of the pair repeatedly. The

121

locally generated pulse replaces the input pulse.

This approach removes the uncertainty from coherent superposition, and avoids the messiness and lack of polarization standardization of the control-splitting approach. However, the pair of copolarized pulses will not generally be solitons, and they will distort and generate dispersive waves. Nevertheless, if they are used in a switch which replaces them with a clean, locally generated pulse, this may not be a problem. Another drawback is that the pair of pulses requires a larger a time interval than the input pulses. This may require large bit-interval-to-pulse-width ratios or may require that incoming data be time-division demultiplexed, polarization-standardized, and re-multiplexed. It may be possible to reduce the pulse pair time interval by designing the interferometer such that the first half of each arm has near-zero dispersion, so that the pulses get chirped proportional to their power via SPM. The second half of the interferometer can be highly anomalously dispersive. This way the pulses will compress proportionally with power.

6.16 Packet Switches

A packet switch is a switch which routes entire packets of bits, rather than individual bits. The data in the data stream does not affect the switching function, except that the lead bit must be located, and if the packets are of variable length then the packet length must be read from the header.

Packet switching is a useful function for sending packets onto buses, for routing packets at nodes, and for tapping packets from buses. Packet buffering is likely a requisite functionality, and reading from and writing to buffers is another application.

6.16.1 XPM Packet Switches

Of course, it is possible to make packet switches using XPM switching concepts, and there are many possible implementations. For example, CW at a slightly different carrier frequency or in the polarization orthogonal to the data (if polarization state is preserved in the system), and with a duration equal to the packet length, could be launched into an XPM switch to route out a packet. In a more complex system, with TDM and packets, a stream of pulses at the DEMUXed rate, and with the duration of the packet, could be used in place of CW.

6.16.2 Haus-Auston Switches

Under the practical assumption that there will be no interleaving of packets (TDM of distinct packets), H.A.Haus has suggested an alternative packet switch which has the advantage of very fast access time and quick rise time, but which may be difficult to implement. This device is based upon the "Auston switch" concept, named for Dave Auston [225, 226]. A simple Auston switch consists of two parallel striplines separated by a relatively small gap (say 5-10 μm), and grown on a semiconductor substrate. A DC voltage is applied across the two lines. If a laser beam with photon
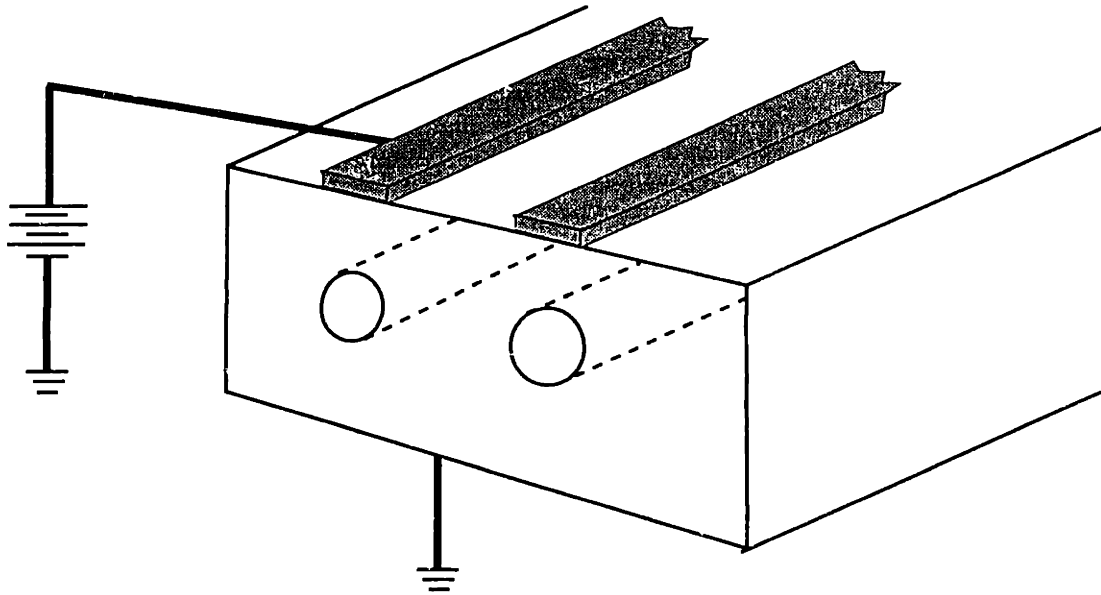
Figure 6-8: Basic components for Haus-Auston switch. Metal striplines on semiconductor substrate with embedded optical coupler.

energy above the bandgap of the semiconductor substrate is focused between the two striplines, free carriers will be excited in the substrate, shorting the striplines. Traveling voltage waves will be excited on the striplines. H.A.Haus has proposed embedding a coupler in the substrate, with one arm below each stripline. A portion of such a device is shown in Fig. 6-8. The substrate and one of the striplines is grounded, while the second stripline is at some voltage V, and is electrically isolated from the substrate. However, the electric field does penetrate the substrate, and if the waveguides of the coupler have a significant electrooptic coefficient, this field will cause a difference between the indices of refraction of the two arms of the coupler, Shorting the striplines with a laser beam causes voltage transients on the striplines which alter the electric field in the substrate, changing the index of refraction in the waveguides, and therefore changing the coupling length. In this steady condition, optical signals entering the coupler in one port exit the coupler from one output port, which we label port A (either same fiber or opposite fiber depending upon the design). If the numbers are right, then in regions under the voltage transients, the coupler will route optical signals to port B, rather than to the usual port A. As a packet switch, the carrier-exciting laser could be turned on for the duration of one packet.

There are a number of design challenges to be overcome, in order for the Haus-

123

Auston switches as described to become practical. First, it is important that the electric field at the coupler integrate to the right amount for each bit as the data traverses the coupler, to ensure uniform coupling for all bits. Second, it makes sense that the stripline voltage waves should be group velocity matched to the optical data, which may be challenging. Third, the risetime and carrier recombination times should be as rapid as possible, in order not to require "guard intervals" between packets for the transients. Fourth, these devices are resistive and likely to be inefficient.

6.16.3 Nondegenerate Four-Wave Mixing

An alternative might be to use nondegenerate four-wave mixing (4WM) in semiconductor traveling wave amplifiers [40]. The data and a frequency-shifted pump (e.g., a train of pulses or a block of strong CW of length equal to that of a packet) would mix in the TWA and generate new pulses at a new frequency which could then be filtered out. One problem is that the new pulses are likely not transform-limited – two photon absorption and self- and cross-phase modulation degrading the pulses.

The approach works well for switching data into a buffer. If this approach were used for switching out of a soliton storage ring, the residual pulses would be a problem. As a possibility, successful tapping could trigger the suppression of a packet's worth of clock pulses in a regenerative AND gate buffer (see Buffers/memories). Or, in a laser-style buffer, the 4WM pump could be fed into the loop to saturate the gain to kill the residual data. The pump could be filtered out of the loop after one roundtrip. This approach might render the ring inoperable for an unacceptably long time, however.

6.16.4 Polarization Rocking Switches

Polarization rocking switches are described in the chapter on switching, Chapter 2. By removing the polarizer from the original design of Krautschik et al. [59], the device outputs the data in one of two orthogonal polarizations, depending upon the presence or absence of control light. A polarization selective coupler or beamsplitter can then be used for routing.

6.17 Packet Header Identifiers

It seems extremely likely that a standard convention for packet construction will be established for a given network. For example, if the packets are truly asynchronous in their timing as entire packets, every packet might be preceded by a unique pattern of N_b bits which is otherwise forbidden (preferably impossible, by choice of coding). Even in a system in which the packets are synchronous as packets, headers of a standard format are likely. The packets might have a fixed number of header bits for information such as destination address, source address, length of packet, error checking, intermediate routing information, etc. Other schemes for embedding control information in a packet are of course possible, such as modulating the packet at a slow rate for electronic header processing, etc., but these will not be considered here.

In the above scenario in which a unique string precedes each packet, header identification is a fairly simple operation. All that is required is a device which performs pattern matching to a single pattern. This could be performed with a cascade of XPM Boolean logic gates which tests every set of N_b consecutive bits for the proper sequence. The only tricky part is that we must test all possible sets of N_b bits, and these sets overlap with each other.

An obvious, albeit inefficient, way to implement such a function would be to replicate the data stream N_b times, delay the jth stream from the 1st stream by $j - 1$ bit intervals, perform parallel $\overline{\text{XOR}}$ operations of the data with the pattern to be recognized (the jth stream AND the jth bit of the header identifier), and then perform ANDs on the outputs of these gates until only a single bit remains, which will be a ONE for pattern match or a ZERO otherwise. Replication and delay can be implemented with couplers and delay lines, and an amplifier will likely be necessary. This approach requires that N_b copies of the data be made and amplified, requires N_b $\overline{\text{XOR}}$ gates to compare with the pattern, and $\lceil \log_2 N_b \rceil$ two-input AND gates (or a special N_b-input AND gate) to test for pattern-match.

An alternative approach, which is considerably more efficient, is to perform comparisons of the data with itself, with the header identifier pattern hardwired into the logic. Since one can make all-optical AND gates, and one can make all-optical inverters, either or both of the inputs to an AND gate can be inverted, so that a gate can be made which outputs a ONE only for a specific pair of inputs (e.g., a gate which outputs a ONE for a 10 input but ZERO for 00, 01, or 11). Of course, more efficient designs of these gates may be possible. If the gates are chosen to output a ONE for pairwise pattern-matching, then a set of AND gates can be used to obtain a single bit identifying a header. In this approach, N_b copies are made and delayed as before, $\lceil N_b/2 \rceil$ pairwise pattern-matching gates, and $\lceil \log_2(N_b/2) \rceil$ two-input AND gates. Again, multi-input gates could be used to reduce the total number of gates. However, a single multi-input gate would likely contain nearly as much hardware as a set of two-input gates in parallel and would almost certainly impose significantly more latency.

6.18   Packet Header Readers

See also the section entitled Packet Header Identifiers.

First, of course, if packets have been WDMed into subpackets, WDDEMUXing must occur before headers are read. As for the reading of the individual headers, there are only a few options with currently available devices. If the header is transmitted at a lower bit rate than the data, then the header can be read with conventional electronic processing. Or, the header can be at the same bit rate as the data, and then the header must be TDDEMUXed to be fed to electronic processing. To date, and to my knowledge, a high bit rate all-optical header reader has yet to be built.

It is possible to implement the header reader with optical logic gates... The header ID reader could be particularly simple, because only a single pattern needs to be matched. Other information, such as destination ID, can also be handled with

all-optical logic, but with more complexity and greater power requirements. The set of all possible destination IDs must be partitioned into M subsets, where M is the total number of input/output fibers at the node. That is, a predetermined mapping of destination IDs with optimal output fibers is hardwired into the logic. The header could be split into $M - 1$ copies and sent through $M - 1$ sequences of logic gates, only one of which will give an output, thus spatially identifying the output fiber. Each logic output could be directly connected to an Auston switch (Auston switches are described under "Packet Switches") which is used to send the packet off. Of course, other logic will read the length of the packet from the header, which will determine for how long the Auston switch is to remain ON. Furthermore, the switches to the output channels must be tapped, and the information that the switch is ON must be transmitted back, so that a logic stage can test for contention at that switch. If the switch is found to be ON, the subsequent command to turn the switch ON, the ON duration information, and the packet must all be buffered until the switch becomes available again. Several packets may be attempting to use the same switch, so pointers must be associated with each buffered packet, and some contention algorithm hardwired into logic. With limited buffering capacity, excessive contention may require that packets be thrown away, or rerouted to the second-best output fiber.

More features could be built in, of course, but the reality of the large energy-length product of current all-optical switches will quickly squelch ideas of highly complex all-optical nodes. A materials breakthrough, permitting energy-length products at least two orders of magnitude smaller, would make a tremendous difference in node capabilities.

6.19   Equalizers

I have divided this section into active and passive equalization categories. However, the real distinction is that there may be a need to correct spectral deformation of the pulses themselves and/or the resulting timing jitter ("reactive" equalization), and there is a need to tailor the net gain in a WDM transmission line so that each channel sees the same amount of net gain ("resistive" equalization).

6.19.1   Resistive Equalization

For WDM soliton transmission, it will be necessary to equalize the net gain for each channel. The amplifier gain and fiber loss vary with wavelength. If the path-averaged soliton approach is to be used, the net gain must be the same for each channel. Mollenauer et al. have performed two-channel experiments in which the two channels are on opposite sides of the erbium gain peak and experience equal gain [16]. Some fancy filtering might permit more than two-channel operation, but with passive filtering, the equalization cannot adapt to changing environments and data statistics.

A simple fix is to adjust the input powers so that the channel with the least gain starts out with the most power. This will be difficult in long-haul transmission, and even more difficult in a full network where signal paths are allocated en route.

An alternative is to use inhomogeneously-broadened fiber amplifiers [121]. One candidate is the germanosilicate-core erbium-doped fiber amplifier, which exhibits considerable inhomogeneous broadening [129, 227]. Even some aluminosilicate-core erbium-doped fibers may be sufficiently inhomogeneously broadened [138]. One way of achieving equal gain for all WDM channels would be to use filters to perform approximate equalization, and then to use several low power cw lasers, separated in wavelength by roughly a homogeneous linewidth (which itself is usually a function of wavelength) of the inhomogeneous gain, and of course tuned to wavelengths which will not interfere with the WDM channels (allowing for wavelength wobble due to interchannel collisions). A small fraction of the transmitted data power would be tapped off for feedback adjustment of the power to the cw lasers. The cw lasers would thus provide adaptive equalization. One would not want the cw laser power to be transmitted along the data fiber, so CDFs could be used to remove this power. A potential problem with this approach is that if we demand minimal crosstalk between channels, the minimum WDM channel spacing would be established by the homogeneous linewidths of the gain. These linewidths tend to be large compared with the maximum channel spacing established by the requirement that the collision lengths be at least twice the amplifier spacing so that the power-asymmetry frequency shifts at the amplifiers approximately cancel [122]. As amplifiers become cheaper, it will be desirable to move them closer to each other for many reasons, such as noise penalty, asymmetric collisions, etc.

It is also possible in the long-term that distributed fiber amplifiers will become cost-effective. A transmission line with alternating homogeneously-broadened distributed amplifiers, and inhomogeneously-broadened lumped amplifiers could be used to overcome the asymmetric collision problem (and of course the noise penalty), therefore allowing wider WDM channel spacings.

Another implementation of the inhomogeneously-broadened amplifier idea is the use of a twincore erbium fiber acting as a coupler whose coupling length is different for each WDM channel, and therefore each channel samples a different set of ions [139]. This is a spatial hole burning type of inhomogeneous broadening.

A group at Bellcore has succeeded in equalizing the gain of an inhomogeneously-broadened amplifier by incorporating the amplifier into a ring laser, so that ASE in the ring fixes the gain to the ring loss [137]. Later, the same group demonstrated considerably worse performance but in a greatly simplified system: they simply cascaded the inhomogeneous amplifiers with no feedback control [138].

An alternative to inhomogeneously broadened amplifiers, suggested by Haus [126], would be to use no equalization for the gain itself, but rather to scramble the channels every so often. That is, the data-wavelength matching is permuted every so often, in such a manner that path-averaged solitons obtain. This averaging is now performed over a distance approximately equal to the product of the number of channels and the distance separating permutation stages.

6.19.2   Reactive Equalization

For nonsoliton transmission, it is not only important to equalize the gain, it is also very important that the dispersion and nonlinearity be compensated. In other words, solitons require "resistive equalization" and little "reactive equalization," but nonsoliton communication demands both "resistive" and "reactive equalization." Achieving very low path-averaged dispersion for solitons may nevertheless be facilitated by the use of these techniques, rather than the use of sections of fiber with very specific dispersion.

As discussed elsewhere in this thesis, a transmission fiber consisting of sections of fiber with alternating zero-dispersion wavelengths can be used to achieve very low path-averaged dispersion.

I thought of a simple way to perform dispersive equalization of data, which likely has been proposed earlier, though I am not aware of a reference. One can simply perform nondegenerate four-wave mixing of the data to a frequency in the opposite dispersion regime. For example, data launched at 1.57μm into dispersion-shifted fiber with zero dispersion at 1.55μm, could be frequency-translated to 1.53μm halfway across some transmission link. The first half of the propagation would be in the anomalous dispersion regime, and the second half would be in positive dispersion. If necessary, frequency hops could be performed periodically along the transmission link. The technique is limited by the bandwidth of the frequency translation device. This approach may be more cost-effective than splicing together sections of fiber with shifting zero-dispersion wavelengths. And it would certainly be easier to install a SLA into a link buried in the ground than to introduce en route dispersion-compensation fibers. Another alternative for equalization might be to use chirped fiber gratings

Nonsoliton systems can be designed so that the equalization is performed only at the ends of the transmission links. This is especially desirable for use of terrestrial fiber which is already in place (e.g., buried in the ground). Dispersive compensation, as discussed below should be useful in many cases. For longer links or higher bit rates, some sort of pre- and/or post-processor scheme might be useful. For example, an effective transfer function can be found for a particular type of signal transmitted over a particular link. A filter with the inverse of this transfer function can (in principle) be designed and placed at the end of the link [228]. We can of course preprocess the data with some sort of filter before transmitting on the link, and this preprocesser/postprocessor combination can be optimized for each particular link, for each bit rate.

Solitons can benefit from some reactive equalization as well, for reducing timing jitter. A section of positive dispersion fiber can be used following the transmission fiber [229]. From the various sources of timing jitter in transmission, each bit may be displaced in time from the center of its allotted bit interval, and each bit will in general have a slightly different carrier frequency than it did when launched. Using a post transmission positive dispersion fiber assumes that at the end of the transmission, a typical bit will be traveling away from the center of its bit interval, rather than towards the center. While it is certainly possible that some individual bits will in fact be traveling towards the center of their bit slots, a simple calculation reveals that the

probability is very low for a typically large number of amplifiers in a link of thousands of km. Thus the predicted timing variance at the end of the compensation fiber is lower than without the compensation fiber.

Another reactive equalization approach which may be applicable to both nonsoliton and soliton transmission is "spectral inversion." This means phase-conjugation of the data during transmission. Because of the spectral inversion, the (nearly same) dispersion which spread the pulses is used, following inversion, to recompress the pulses. This can be performed with nondegenerate four-wave mixing in a dispersion-shifted fiber [230, 231, 232]. In experiments, the DSF was 20km long, and it was necessary to operate very close to the zero dispersion wavelength of the DSF. It may be much more convenient to achieve spectral inversion using nondegenerate four-wave mixing in semiconductor laser amplifiers [40]. The gain bandwidth of a SLA is on the order of 50nm [40]. Note that this approach does not cancel third-order dispersion, which could be a problem. A pair of spectral inversions could be used to frequency translate the data from one dispersion regime to the other, for the frequency-hopping scheme discussed above.

6.20 Clock Recovery

In most systems today, clock recovery simply means extraction of timing information from a data stream of a known bit rate. This is often simply done with an open loop structure such as high-Q resonant "tank" circuit. The tank has a fixed resonance frequency. The signal stream is sampled, and any Fourier components at the resonance frequency are resonantly enhanced, and the output of the tank is then a sinusoid at the clock frequency which, with proper length calibrations, is synchronized with the incoming data. Of course, this also implies that some fraction of the signal data stream has been converted from optical to electronic format. A tank circuit with rapidly adjustable Q has been fabricated, so that the Q can be reduced for quickly acquiring the clock of a short data sequence (as short as four bits!) such as a packet header and increased for the packet data [233], but the device operated at a mere 600 Mb/s. A 10.368 Gb/s clock recovery circuit has been built using a dielectric resonator and an electronic bandpass amplifier [234].

Some current electronic systems use closed loop clock recovery, such as phase-locked loops (PLLs). The adaptive nature of such devices is laudable, but at this time, there is no reliable all-optical version, and the electronics technology is currently limited to around 10 Gb/s. A hybrid optical-electronic DEMUX was implemented using 8 GHz electronic PLL clock recovery [235, 48].

A closed loop, electronically tuned YIG filter has been fabricated which can be tuned to extract clocks in the range of 2-18 GHz [236]. The device operates in a similar fashion to a PLL, but with the VCO replaced by a tunable filter, and lock can be attained over a much wider frequency range.

An all-optical approach is to feed the data stream into a fiber laser. One way this might work is that the data effectively provides a periodic phase perturbation within the cavity and achieves FM mode-locking via cross-phase modulation [190,

129

191]. Another approach is to feed the data to a self-pulsating semiconductor laser diode [237, 238, 49].

6.21 Clock Restoration

This section is distinct from the previous one, in order to clarify a semantic issue. It is not a major issue, but should be considered in the design process. Clock recovery usually is taken to refer to the generation of a periodic wave whose period is the *fixed* clock interval for the system. Synchronization is the only consideration in this view.

Pushing the limits of optical transmission may require new classes of devices for clocking. The reason is that the bit rate of a data stream may shift from the transmitted bit rate, either locally within a packet, or for the entire packet. Timing jitter alone is not the serious consideration in this case, for several reasons: (1) because a microwave tank circuit would still extract the correct clock, (2) a timing-jitter insensitive switch such as those described in the switching chapter (Chapter 2) would restore the proper clock, or equivalently, since the switch is actually operating on a stream of ONEs which is just the output of a local mode-locked laser, one can say that it is possible to modulate a mode-locked laser at the correct bit-rate, and (3) it should also be possible to drive a more conventional modulator at a DEMUXed rate, again for modulating mode-locked lasers.

It would be more serious if the local bit rate compressed or decompressed over a sufficiently large distance. With a fixed bit rate, once the header is accurately timed, one can think of the data as traveling in fixed bit slots, equally spaced following the beginning of the header. Presumably there are no intrachannel collisions, and the discussion of timing jitter above appears applicable. If however the local bit rate were to increase from R to $R + \Delta R$, and if the new rate were to persist for $N + 1$ bits, where

$$\frac{N}{R} \geq \frac{N+1}{R + \Delta R}$$

then the $(N + 1)$st bit would necessarily be (and other bits might be) completely out of their expected (based on the rate R) bit slots.

This unfortunate circumstance might arise from thermal expansion/contraction and fluctuations in tension of the transmission fibers. As long as these changes are small or average to zero on a timescale typical of a packet, then one of the clock-recovery schemes (see Clock Recovery) should be able to handle the deviations. Note that while heating or cooling the fiber, as L.F.Mollenauer's group has done, by metal-coating a fiber and applying current to heat or applying a cold finger to cool, is a useful technique for adjusting cavity lengths of fiber lasers to adjust their periods, here we would actually need to expand or contract the fiber while the data was passing through it. We would need not to adjust the length, but rather the rate of change of length of the fiber.

Another source of compression is the Raman self-frequency shift, which I have investigated, but never seen in any publication. This weak effect is discussed in the chapter on high bit-rate limitations, Chapter 4, in the section on Raman Bit-Rate

Compression. In any event, it seems unlikely that the data would undergo enough compression within a node to cause problems, unless the travel distance within the node were very great.

A theoretical discussion of clock restoration is found in Ref. [239].

6.22   Circulators

A fairly low-loss (<2dB), relatively polarization-independent all-optical circulator has been proposed and built by Fujii with very good isolation over the wavelength range 1.2-1.4μ [240]. Other circulators can be imagined, using nonreciprocal elements, but which may require keeping track of polarizations.

6.23   Receivers

In general, when speaking of receivers, people are referring to optical-to-electronic converters, and that is what we discuss in this section. For more network-oriented concepts of receivers, see the discussions of simple networks in the next chapter. Only direct detectors will be considered here, because it seems unlikely, at least in the long-haul arena, that coherent detection of solitons will be used.

6.23.1   Avalanche Photodiodes

Avalanche photodiodes (APDs) remain an excellent choice for converting light to electrons when phase is irrelevant, as in a pulse code modulation (PCM) system. They are diodes biased near the breakdown voltage, so that photoelectrons (or holes) will be avalanche multiplied, overcoming receiver thermal noise. For 1.3-1.55 μm, InGaAs APD's are good low noise receivers. Currently, APD's are limited by the avalanche build-up time to around 10 GHz [38, 241].

6.23.2   PIN Photodiodes

PIN photodiodes under more conventional bias have no gain but can operate at higher speeds than APDs. Improved sensitivity can be achieved by inserting an optical preamplifier and narrowband filter before the PIN photodiode. The sensitivity can in fact be much better than with an APD alone, but rejection of amplified spontaneous emission (ASE) from the preamp is critical [38, 241].

6.24   Delay Lines

Variable delay lines are useful for synchronization at any level: bit, word, or packet. It may be necessary to have different types of devices performing the delaying at the different time scales. Thus this section has three subsections in which three important time scales are considered.

One of the most conceptually simple ideas for a delay line for pulses is the use of frequency translation and a dispersive medium such as a fiber (see the section on Frequency Converters). Incoming pulses are first frequency-translated (and adjusted in power if solitons are to be maintained). The shifted pulses propagate through the dispersive fiber at a frequency-dependent group velocity. Finally, the pulses are translated back to their original carrier frequencies (and power-adjusted).

6.24.1 Delay Lines - Nanosecond+

Optical buffers could be suitable for this application (see the section on Buffers/Memories). The delay is in multiples of the buffer roundtrip time. Or if switches are placed equidistant around the buffer, then the delay is in multiples of the switch-to-switch travel time. There may be additional overhead delay if switches with nonnegligible latency are employed for switching into or out of the buffer. Note that unlike some of the other delay lines discussed in this section, the delay time is real - it is not a delay in the moving frame of the pulses.

6.24.2 Delay Lines - Picosecond-Nanosecond

This is perhaps the most suitable time scale for the delay lines discussed in the introduction to this section, which utilize tunable sources and dispersive delay lines. Either the time scale in the moving frame of the pulses (relative delay) or real delay could be in the ps-ns range.

6.24.3 Delay Lines - Subpicosecond-Picosecond

This is a natural application for XPM switches, As discussed elsewhere, XPM switches can be designed with intrinsic insensitivity to timing jitter in the incoming data, up to a good fraction of a bit interval. Rather than to correct timing jitter, this feature can be used to impart a fixed timing shift to data which is already well-aligned in time. The design is then the same as for a packet switch, as discussed in the section on Packet Switches.

The only problem with this is that this subpicosecond delay is a *relative* delay seen in the coordinate frame of the moving pulses: the actual laboratory-frame delay from entering to leaving the gate will (with current fiber switches) be much longer than subpicosecond. But as long as the devices which use the subpicosecond delay are compensated for the gate delay, this will not be a problem, but merely an undesired latency.

6.25   Buffers/Memories

Buffers are crucial elements in any practical network. For example, if several packets arrive at the same transmitter within one packet interval, and packets can only be processed serially, then it will be necessary to buffer all but the first packet, and

process them one-by-one. The same thing can happen at nodes, when multiple packets which would all be preferably routed to the same channel arrive within a packet interval. There are further obvious applications.

Electronic buffers are easy to build. However, photonic wavepackets do not lend themselves easily to many tasks for which electronics is well-suited. A class of these tasks, critical in memory applications, is the ability to store information statically and locally. It is rather difficult to convince a photonic wavepacket to sit in a little box until you are ready to access it.

In electronic devices, one generally has a bias voltage across the chip. Thus there is constantly power available, so that devices can appear to statically maintain states, despite the fact that electrons may be flowing all over the place dynamically. Of course there exist devices such as charge-coupled devices (CCD's) which actually keep electrons in fixed locations (briefly), but localizing electrons is certainly not essential to designing a very good electronic memory.

Early optical memories typically employed a high-finesse ring to store pulses for some finite amount of time. Gain could be introduced into the cavity to prolong the lifetime, but it was necessary that the cavity loss exceed the gain in order to avoid lasing [67]. Another idea was to include a gating function in the loop, i.e. an active mode-locker [69], but the number of roundtrips was very limited, because this technique could not preserve ZEROs. Such short-term memory, whose stored pulses have time-varying energy, are quite limited.

A more successful approach involves regeneration. The "stored" pulses are being used each roundtrip to gate out new replacement pulses from a source stream. This approach can have the advantage of great stability (provided by the local source), as long as the switching operation corrects for errors, so that ZEROs and ONEs remain distinct. A disadvantage is that much energy must be expended if the pulses are to be replaced every roundtrip.

Yet another alternative, which is an improvement on the standard ring, is to include filtering in addition to modulation. This has been proposed and demonstrated with amplitude modulation [70, 26], and is expected to work with phase modulation as well (analyzed in this document).

In the next subsection, soliton ring buffers, utilizing modulation and filtering, will be described. These are buffers which preserve the traveling wavepacket nature of the data. The remaining subsection is devoted to some new ideas of the author for all-optical buffering which avoids many of the problems associated with soliton rings.

6.25.1 Soliton Ring Buffers

When transmitting optical pulses as data, it is natural to try to design storage rings which can preserve the pulses for very many roundtrips. It would be especially convenient if the pulses did not have to be altered when entering or exiting such a ring. This idea has been around for a long time, appearing in references in the early 1980's. A recent implementation in a ring with an erbium-doped fiber amplifier achieved thousands of recirculations, but did not preserve pulse intensity [67]. The device was essentially a high-finesse (150000) ring with enough gain to cancel much of the ring
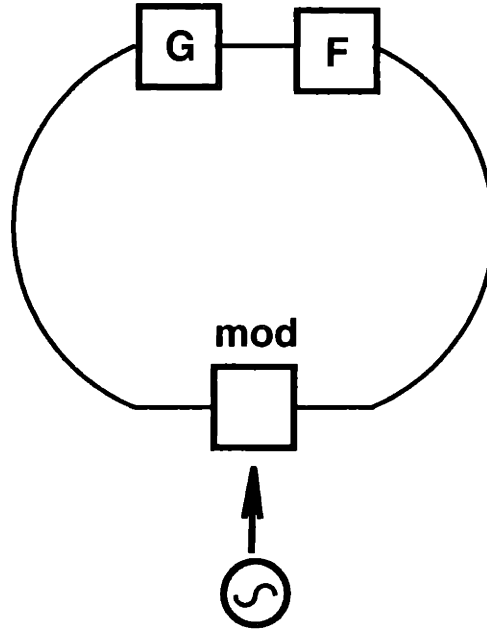
Figure 6-9: Block diagram of ring buffer. F=filter, G=gain, mod=modulator.

loss, but not enough gain to initiate lasing.

A ring can also be made using concepts very similar to those used in mode-locked lasers and for transmitting soliton data over long distances [70, 26, 193]. A block diagram of a ring with filtering, gain, and modulation (amplitude and/or phase) is shown in Fig. 6-9. Filtering preserves the spectrum, while amplitude modulation (active or passive mode-locking) preserves the pulse shape. Gain balances the losses from couplers, filtering, modulators, the fiber itself, etc. This ring, like the previous design, preserves the original input pulses. This filtered ring has the advantage of preserving the pulses (and ZEROs) for much longer periods of time.

The presence of gain raises the question of stability against the growth of continuum, because narrowband continuum near the peak of the filter transmission sees more net gain than a broadband pulse which samples a larger portion of the filter bandwidth. The primary concern is that continuum might grow in bit intervals in which there are ZEROs, i.e. no pulses. Rings with filters and active mode-lockers have been discussed by Haus and Mecozzi [70], where they claim that it should be possible for data to be preserved for many roundtrips. Nakazawa et al. at NTT have proposed essentially the same scheme, in linear rather than ring topology, for long distance data transmission, claiming that "unlimited distance" propagation is possible [27]. An alternative to amplitude modulation might be phase modulation [172, 179, 180], and again filtering would be required to stabilize the ZEROs. Naively, one might expect continuum suppression to be less successful with phase modulation and filtering than with amplitude modulation and filtering, but this should be investigated.

The experiments to date have used modulators which are limited in speed by their electronics. I have proposed modulators which can operate at any data bit rate. These are discussed in the section on Modulators in this chapter, and in the chapter discussing Stability and Timing Maintenance, Chapter 5.

Switching pulses into and out of the ring at extremely high data rates is also a problem. At low rates, acousto-optic switches have worked well in experiments by Mollenauer et al. at AT&T and by Nakazawa et al. at NTT. At higher rates, all-optical switches are possibilities, but not very good choices with ordinary fiber because of the latencies which can be comparable to the circulation time. Some alternatives are suggested in the section on Packet Switches.

Once a ring is designed which has the right stability properties, other difficulties remain. For example, it will be desirable to access the buffered data as quickly as possible. Suppose the ring is to hold a 1000 bit packet at a 50 GHz rate. Then the ring must be at least

$$\frac{(1000\text{bits})c}{(50\text{GHz})n} = 4\text{m}$$

long, with a circulation time of 20 ns. This length of time may be greater than the desired access time, so it may be necessary to have several access ports around the ring.

Then there is the question of how to remove a packet from a ring.

Soliton ring buffers in general have certain intrinsic access problems. While Auston switches might have the advantage of negligible latency, the soliton ring buffer by its very nature tends to introduce some latency. The operation of switching data out of the buffer must begin precisely when the first bit of the packet enters the switch. Thus, before packet switching can occur, a packet header location operation must occur. This might be done with a packet header identification switch, which if implemented in fiber could introduce considerable delay of its own.

Alternatively, the header location could be identified when the packet enters the buffer. The buffer would have an associated clock which would feed a switch a clock bit only when a packet lead bit was about to enter the switch. Header timing would then be reduced to a single AND operation, at the expense of introducing pre-buffer header identification and a clock.

Clocking in a polarization-preserving buffer could be a very simple matter. Prior to launching into the buffer, the packet can be preceded by an orthogonally polarized pulse at the correct carrier frequency for group velocity match within the buffer. Thus this clock pulse copropagates with the data, and can be easily read by the packet switch, so that the switching can be properly timed. While this approach to packet timing is very simple, it might not be sufficiently accurate for some applications. Clocking in a non-polarization preserving buffer might be more difficult, and the solution might be more complex than using a packet header identification switch.

Using these current ideas for soliton storage ring design, it seems unlikely that a WDM ring could be built which would adequately preserve the data, for many reasons. First, fiber is a dispersive medium, and the data in the different channels will collide regularly, rendering useless active or passive mode-lockers for pulse shape

preservation. Suppose we can design a ring without a mode-locker, then there are still problems both because of timing errors introduced by interchannel soliton collisions, cross-Raman, etc. and because one could not easily design a ring so that a packet could be removed when none of its bits were in collision with bits from another channel. Although colliding bits can be separated by filtering if the carrier frequencies are sufficiently widely spaced, solitons in collision are chirped via cross-phase modulation. Thus, pulses extracted while colliding will have slightly different carrier frequencies and therefore slightly different group velocities from other bits in the same channel. Unless this can be quickly compensated, timing errors will result.

6.26   Regenerative Soliton Ring Buffers

In this approach proposed by the author, the pulses being stored in the ring are periodically replaced with fresh new pulses. Such buffers are extremely simple in principle because no fancy schemes for preserving ONEs and ZEROs for long periods of time are necessary. The ring simply consists of a ring of fiber containing an AND gate, a source of clock pulses for the AND gate, and input/output ports for the ring. The data traveling around the ring is ANDed with the clock, in an AND gate which uses the clock pulses as the output pulses.

In practice, an all-optical fiber AND gate might require so much fiber that the gate itself is of length comparable to the entire ring. This need not be a problem, however. Recalling the design of the simple two-input AND gate discussed in the switching chapter, it is the clock which is split by the Sagnac, not the data. Thus, the data can be tapped directly from within the AND gate, or from anywhere else in the ring.

6.27   "Stationary" Nonsoliton All-Optical Buffers

The primary motivation for the ideas in this section is to avoid the primary drawback of soliton rings, namely that the information is not static but travels around the ring and the location of the leading bit must be constantly monitored. The proposed alternative does not use solitons, but the data remains optical throughout. The idea is to convert the temporal information in a packet to another form.

6.27.1   WDM CW Ring

One possibility is to define a map between a bit sequence in a packet and a set of discrete frequencies. The presence or absence of CW power at one of these discrete frequencies represents part of the temporal sequence of bits in the packet. To reduce the number of discrete frequencies required, it might be possible to quantize the power at each frequency. The advantage of this is that this CW power at all of the discrete frequencies can be launched into an extremely short ring so that the ring is filled. Then the information can be instantly accessed, without the overhead of monitoring the location of a lead bit.

When accessed, the CW power can be passed through a filter/modulator bank which performs the inverse map of frequency to temporal information, by appropriately modulating a very fast source or a bank of sources whose output can be MUXed. At a transmitter, the data to be transmitted could very well be arriving in nonsoliton format anyway, so in this scheme we delay the conversion to solitons until after the buffering stage, whereas in the soliton ring paradigm, we convert the data to solitons prior to buffering.

Likewise, at a receiver, in the above scenario, one converts the solitons to CW, buffers, and then sends to the final destination. In the soliton ring paradigm, the solitons are buffered and then converted and sent to the final destination.

The problem with this approach is how to design a ring which can support a set of N_w frequencies, but in operation must sustain only a certain subset of these CW lines and must prevent the growth of noise in the complementary subset. If the storage time is not too long, then a simple ring might suffice, but without some sort of low-power, "inhomogeneously broadened" (independent for each discrete frequency) saturable absorber plus flat net linear gain, it is not clear that the frequencies which are on will remain on, and those that are off will remain off.

Designing a FSA which acts independently for each frequency may not be impossible. As long as the FSA action need not be too strong as in this application, it might be possible to cascade multiple quantum well samples, and which have slightly shifted $n=1$ heavy-hole exciton absorption lines. The exciton shift could be strain-induced, or electric-field (Stark-) induced. In the 1.5 μm regime, InGaAsP/InP would be an appropriate family of materials. Typical linewidths are 3-5meV, and the room temperature homogeneous linewidth, dictated by phonon-induced ionization, is around 2.5 meV at room temperature [242]. At 1.55 μm, this is a linewidth of around 5 nm, which is very reasonable for this application. To sharpen the hh exciton lines, low temperature operation is possible, but the improvement is probably not sufficient to justify the added complexity.

The MQWs will be quite lossy, so amplification will likely be necessary between MQWs, and semiconductor amplifiers might be suitable. Because the FSA is intended for use in a CW ring, concerns about the response time of exciton absorption lines or of semiconductor amplifiers are far less important than they would be for pulsed data.

6.27.2 Many CW Rings

If an adequately stable multiple frequency CW storage ring cannot be constructed, there are some less desirable alternatives. One could use many rings rather than one ring. This could mean 500 separate rings for buffering one 500 bit packet, however, and this is unlikely to be a popular implementation. An advantage is that the same CW frequency could be used in each ring. An variant on this principle, which would require far fewer storage rings, but which would also require strong nonlinearity and may pose difficulties of coupling in and out, is proposed below.

6.27.3 Quantized CW Rings

A novel possibility is the use of an artificial fast saturable absorber (FSA) whose transmissivity is a periodic function of intensity. This is the case for an interferometric artificial FSA, as in additive pulse mode-locking. Here, rather than using the periodic transmissivity to generate and sustain pulses, we use it to obtain quantized CW power at one discrete frequency. The implementation could be in a two-cavity configuration or in a single-cavity configuration, and to be practical would require much stronger nonlinearities than ordinary fiber could provide. Active semiconductors might be more suitable for this application than fibers. Some of the problems of using semiconductors for the switching of pulses, such as pulse distortion due to two photon absorption, may be far less of a problem in this CW application.

The theory is extremely simple. Whether it is a two-cavity or single-cavity configuration, we can model the effect on the main cavity CW to be an oscillatory gain/loss which is a function of CW intensity. Thus the equation might look like

$$\frac{\partial I}{\partial z} = [C + A\sin(\kappa I + \phi)]\, I \qquad (6.6)$$

where z is distance along the main cavity, I is the intensity of the CW, κ is the rate of accumulation of phase shift with intensity, ϕ is a bias phase which is the linear phase difference (difference in optical path length) between the two cavites (or is a polarization state bias in a single-cavity polarization rotation system, etc.), $2A$ is the peak-to-peak swing of the reflectivity/transmissivity curve, and C is the net intensity gain averaged over all intensities. Because C implicitly contains the saturable gain, C may be a function of intensity, but presumably a much weaker function than the reflectivity. Likewise two-photon absorption would introduce a correction to the right-hand side to order I^2 which we ignore for now. As a storage ring, we would insist upon having

$$C + A\sin(\phi) < 0$$

so that the ring will not begin to lase from noise. And of course the actual reflectivity is not a true sinusoid, but the arguments here can be easily modified to accommodate the actual reflectivity function. Filtering and dispersion have been ignored because only CW excitations are being considered, but in practice a narrowband filter might be necessary to force operation at the desired frequency.

The steady-state solutions to Eq. (6.6) are simply the solutions to the transcendental equation which results from setting the left-hand side to zero. Thus there are infinitely many discrete solutions. However, only half of these are stable. This is easy to see from the full equation by seeing what happens when we perturb I slightly. What we would like is that increasing (decreasing) I slightly on the right-hand side will make $\frac{\partial I}{\partial z}$ negative (positive). Thus any fluctuations in intensity will be damped out. It is easy to see that a solution I_k will be stable if and only if it is on a portion of the reflectivity curve which has negative slope, i.e. where

$$\frac{\partial}{\partial I}[A\sin(\kappa I + \phi)]\,|_{I=I_k} < 0 \ .$$

Half of the solutions are on the positive slope and are unstable, and half are on the negative slope and are stable.

Coupling light into a high "energy level" could prove challenging because of rise-times. It remains to be shown which cavity operators (dispersion, filtering, gain saturation, etc.) would provide the necessary forces to make the device self-correcting. That is, as an example, if the device were 80 percent filled with light at intensity I_1, we might like the device to "fill in" the remaining 20 percent by itself, and without jumping to another level. The higher-order complex Ginzburg-Landau equations support traveling kink solutions which would likely achieve this goal [243, 244, 112].

The bottom line is that if the numbers are reasonable, this approach would allow for the design of a multi-stable CW storage ring, which is useful here for storing information via quantized intensity. A material with a large Kerr coefficient would be required, but many of the problems which make some materials impractical for the switching of pulses are irrelevant in the simpler CW ring. Semiconductors may be appropriate.

Bibliography

[1] A.Hasegawa and F.Tappert, "Transmission of stationary nonlinear optical pulses in dispersive dielectric fibers. I. anomalous dispersion," *Appl. Phys. Lett.*, vol. 23, pp. 142–144, 1973.

[2] V.E.Zakharov and A.B.Shabat, "Exact theory of two-dimensional self focusing and one-dimensional self modulation of waves in nonlinear media," *Sov.Phys.JETP*, vol. 34, pp. 62–69, 1972.

[3] L. Mollenauer, "Color center lasers," in *Laser Handbook*, pp. 143–228, Elsevier Science Publishers B.V., 1985.

[4] L. Mollenauer, R. Stolen, and J. Gordon, "Experimental observation of picosecond pulse narrowing and solitons in optical fibers," *Physical Review Letters*, vol. 45, pp. 1095–1098, September 1980.

[5] L. Mollenauer and R. Stolen, "The soliton laser," *Optics Letters*, vol. 9, pp. 13–15, January 1984.

[6] F. Mitschke and L. Mollenauer, "Stabilizing the soliton laser," *Journal of Quantum Electronics*, pp. 2242–2250, December 1986.

[7] F. Mitschke and L. Mollenauer, "Ultrashort pulses from the soliton laser," *Optics Letters*, pp. 407–409, June 1987.

[8] A.Hasegawa and Y.Kodama, "Signal transmission by optical solitons in monomode fiber," *Proc. IEEE*, vol. 69, no. 9, pp. 1145–1150, 1981.

[9] A.Hasegawa and Y.Kodama, "Amplification and reshaping of optical solitons in a glass fiber - I," *Optics Letters*, vol. 7, no. 6, pp. 285–287, 1982.

[10] L.F.Mollenauer, J.P.Gordon, and M.N.Islam, "Soliton propagation in long fibers with periodically compensated loss," *IEEE J.Quantum Electronics*, vol. QE-22, no. 1, pp. 157–173, 1986.

[11] M.Nakazawa, Y.Kimura, K.Suzuki, and H.Kubota, "Wavelength multiple soliton amplification and transmission with an Er^{3+}-doped optical fiber," *J.Appl.Phys.*, vol. 66, no. 7, pp. 2803–2812, 1989.

[12] N.A.Olsson, P.A.Andrekson, J.R.Simpson, T.Tanbun-Ek, R.A.Logan, and K.W.Wecht, "Bit-error-rate investigation of two-channel soliton propagation over more than 10000km," *Electronics Letters*, vol. 27, no. 9, pp. 695–697, 1991.

[13] Y.Kodama and A.Hasegawa, "Effects of initial overlap on the propagation of optical solitons at different wavelengths," *Optics Letters*, vol. 16, no. 4, pp. 222–299, 1991.

[14] S.G.Evangelides, L.F.Mollenauer, J.P.Gordon, and N.S.Bergano, "Polarization multiplexing with solitons," *J. Lightwave Tech.*, vol. 10, no. 1, pp. 28–35, 1992.

[15] L.F.Mollenauer, E.Lichtman, M.J.Neubelt, and G.T.Harvey *Electronics Letters*, vol. 29, p. 910, 1993.

[16] L.F.Mollenauer, E.Lichtman, G.T.Harvey, M.J.Neubelt, and B.M.Nyman, "Demonstration of error-free soliton transmission over more than 15000km at 5 Gbit/s, single-channel, and over more than 11000km at 10 Gbit/s in two-channel WDM," *Electronics Letters*, vol. 28, no. 8, pp. 792–794, 1992.

[17] A.Hasegawa and T.Nyu, "Eigenvalue communicaton," *J. Lightwave Tech.*, vol. 11, no. 3, pp. 395–399, 1993.

[18] N.N.Akhmediev, G.Town, and S.Wabnitz, "Soliton coding based on shape invariant interacting packets: the three-soliton case," *Opt. Comm.*, vol. 104, no. 4,5,6, pp. 385–390, 1994.

[19] A.Mecozzi, J.D.Moores, H.A.Haus, and Y.Lai, "Soliton transmission control," *Optics Letters*, vol. 16, no. 23, pp. 1841–1843, 1991.

[20] Y.Kodama and A.Hasegawa, "Generation of asymptotically stable optical solitons and suppression of the Gordon-Haus effect," *Optics Letters*, vol. 17, no. 1, pp. 31–33, 1992.

[21] A.Mecozzi, J.D.Moores, H.A.Haus, and Y.Lai, "Modulation and filtering control of soliton transmission," *J.Opt.Soc.Am.*, vol. B9, pp. 1350–1357, Aug. 1992.

[22] L.F.Mollenauer, J.P.Gordon, and S.G.Evangelides *Optics Letters*, vol. 17, pp. 1575–1577, 1992.

[23] J.P.Gordon and H.A.Haus, "Random walk of coherently amplified solitons in optical fiber transmission," *Optics Letters*, vol. 11, p. 665, 1986.

[24] J.D.Moores and H.A.Haus, "Intrapulse-Raman-scattering soliton timing jitter in ultralong distance transmission," San Jose, CA, paper TuA4, Nov. 3-8, 1991.

[25] L.F.Mollenauer, M.J.Neubelt, M.Haner, E.Lichtman, S.G.Evangelides, and B.M.Nyman, "Demonstration of error-free soliton transmission at 2.5 Gbit/s over more than 14000km," *Electronics Letters*, vol. 27, no. 22, pp. 2055–2056, 1991.

[26] M.Nakazawa, E.Yamada, H.Kubota, and K.Suzuki, "10 GBit/s soliton transmission over one million kilometres," *Electronics Letters*, 1991.

[27] M.Nakazawa, K.Suzuki, E.Yamada, H.Kubota, Y.Kimura, and M.Takaya, "Experimental demonstration of soliton data transmission over unlimited distances with soliton control in time and frequency domains," *Electronics Letters*, vol. 29, no. 9, pp. 729–730, 1993.

[28] E.P.Ippen *private communication.*

[29] C.D.Poole and C.R.Giles, "Fading in lightwave systems due to polarization-mode dispersion," *Optics Letters*, vol. 13, pp. 155–157, 1988.

[30] K.Iwatsuki, K.Suzuki, S.Nishi, and M.Saruwatari, "80 Gb/s optical soliton transmission over 80 km with time/polarization division multiplexing," *IEEE Photonics Tech. Letters*, vol. 5, no. 2, pp. 245–248, 1993.

[31] K.Tajima, "Compensation of soliton broadening in nonlinear optical fibers with loss," *Opt. Lett.*, vol. 24, pp. 54–56, 1987.

[32] S.Chi and M.-C. Lin, "Concatenated soliton fibre link," *Electronics Lett.*, vol. 27, no. 3, pp. 237–238, 1991.

[33] A.Hasegawa and Y.Kodama, "Guiding-center soliton in fibers with periodically varying dispersion," *Optics Letters*, vol. 16, no. 18, pp. 1385–1387, 1991.

[34] M.Nakazawa, K.Suzuki, E.Yamada, H.Kubota, and Y.Kimura, "10 Gbit/s, 1200km error-free soliton data transmission using erbium-doped fibre amplifiers," *Electronics Letters*, vol. 28, no. 9, pp. 817–818, 1992.

[35] M.Nakazawa, K.Suzuki, E.Yamada, and H.Kubota, "Observation of nonlinear interactions in 20 Gbit/s soliton transmission using erbium-doped fibre amplifiers," *Electronics Letters*, vol. 27, no. 18, pp. 1662–1663, 1991.

[36] A.D.Ellis, J.D.Cox, D.Bird, J.Regnault, J.V.Wright, and W.A.Stallard, "5 gbit/s soliton propagation over 350km with large periodic dispersion coefficient perturbations using erbium doped fibre amplifier repeaters," *Electronics Letters*, vol. 27, no. 10, pp. 878–880, 1991.

[37] M.Asobe, H.Itoh, T.Miyazawa, and T.Kanamori, "Efficient and ultrafast all-optical switching using high δn, small core chalcogenide glass fibre," *Electronics Letters*, vol. 29, no. 22, pp. 1966–1968, 28 Oct., 1993.

[38] T.Ikegami, "Survey of telecommunications applications of quantum electronics - progress with optical fiber communications," *Proc. IEEE*, vol. 80, no. 3, pp. 411–419, 1992.

[39] G.I.Stegeman, "Nonlinear guided wave optics," in *Contemporary Nonlinear Optics* (G.P.Agrawal and R.W.Boyd, eds.), pp. 1–40, Academic, 1992.

[40] M.C.Tatham, G.Sherlock, and L.D.Westbrook, "20-nm optical wavelength conversion using nondegenerate four-wave mixing," *IEEE Photonics Tech. Letters*, vol. 5, no. 11, pp. 1303–1306, 1993.

[41] J.P.Sokoloff, P.R.Prucnal, I.Glesk, and M.Kane, "A Terahertz optical asymmetric demultiplexer (TOAD)," *IEEE Photonics Tech. Letters*, vol. 5, no. 7, pp. 787–790, 1993.

[42] H.A.Haus, "Matching of distributed-feedback structures," *Optics Letters*, vol. 17, no. 16, pp. 1134–1136, Aug.15, 1992.

[43] N.A.WhitakerJr., H.Avramopoulos, P.M.W.French, M.C.Gabriel, R.E.LaMarche, D.J.DiGiovanni, and H.M.Presby, "All-optical arbitrary demultiplexing at 2.5 Gbit/s with tolerance to timing jitter," *Optics Letters*, vol. 16, no. 23, pp. 1838–1840, 1991.

[44] P.A.Andrekson, N.A.Olsson, J.R.Simpson, D.J.DiGiovanni, P.A.Morton, T.Tanbun-Ek, R.A.Logan, and K.W.Wecht, "Ultra-high speed demultiplexing with the nonlinear optical loop mirror," Optical Fiber Communications Conference, vol. 4 of 1991 OSA Technical Digest Series, Paper PD8.

[45] P.A.Andrekson, N.A.Olsson, and J.R.Simpson, "Ultra-high speed demultiplexing with the nonlinear optical loop mirror," *Photonics Tech. Letters*.

[46] P.A.Andrekson, N.A.Olsson, J.R.Simpson, T.Tanbun-Ek, R.A.Logan, and M.Haner, "16 Gbit/s all-optical demultiplexing using four-wave mixing," *Electronics Letters*, vol. 27, no. 11, pp. 922–924, 23 May 1991.

[47] D.M.Patrick and A.D.Ellis, "Demultiplexing using crossphase modulation-induced spectral shifts and Kerr polarisation rotation in optical fibre," *Electronics Letters*, vol. 29, no. 2, pp. 227–229, 21 Jan. 1993.

[48] S.Kawanishi, H.Takara, K.Uchiyama, and M.Saruwatari, "64 to 8 Gbit/s all-optical demultiplexing experiment with clock recovery using new phase lock loop technique," *Electronics Letters*, vol. 29, no. 2, pp. 231–233, 21 Jan. 1993.

[49] D.J.As, R.Eggemann, U.Feiste, M.Mohrle, E.Patzak, and K.Weich, "64 to 8 Gbit/s all-optical demultiplexing experiment with clock recovery using new phase lock loop technique," *Electronics Letters*, vol. 29, no. 2, pp. 141–142, 21 Jan. 1993.

[50] C.G.Krautschik, P.Wigley, G.I.Stegeman, and R.H.Stolen, "Demonstration of demultiplexing with a rocking filter fiber," *Appl. Phys. Letters*, vol. 63, no. 7, pp. 860–862, 16 Aug. 1993.

[51] H.A.Haus, *Waves and Fields in Optoelectronics*. Prentice-Hall, 1984.

[52] C.R.Menyuk, "Pulse propagation in an elliptically birefringent Kerr medium," *IEEE J.Quantum Electronics*, vol. QE-25, no. 12, pp. 2674–2682, 1989.

[53] P.D.Maker and R.W.Terhune, "Study of optical effects due to an induced polarization third order in the electric field strength," *Phys. Rev. A*, vol. 137, no. 3A, pp. A801–A818, 1 Feb. 1965.

[54] H.G.Winful, "Self-induced polarization changes in birefringent optical fibers," *Appl.Phys.Lett.*, vol. 47, no. 3, pp. 213–215, 1985.

[55] H.G.Winful, "Polarization instabilities in birefringent nonlinear media: application to fiber-optic devices," *Optics Letters*, vol. 11, no. 1, pp. 33–35, 1986.

[56] F.Matera and S.Wabnitz, "Nonlinear polarization evolution and instability in a twisted birefringent fiber," *Optics Letters*, vol. 11, no. 7, pp. 467–469, 1986.

[57] K.J.Blow, N.J.Doran, and D.Wood, "Polarization instabilities for solitons in birefringent fibers," *Optics Letters*, vol. 12, no. 3, pp. 202–204, 1987.

[58] S.Wabnitz, G.R.Boyer, and X.F.Carlotti, "Modulation polarization instability of light in a nonlinear birefringent dispersive medium," *Phys.Rev.A*, vol. 38, no. 4, pp. 2018–2021, 1988.

[59] A.D.Boardman and G.S.Cooper, "Power-dependent polarization of optical pulses," *J.Opt.Soc.Am.*, vol. B5, no. 2, pp. 403–418, Feb., 1988.

[60] R.Kashyap and N.Finlayson, "Nonlinear polarization coupling and instabilities in single-mode liquid-cored fibers," *Optics Letters*, vol. 17, no. 6, pp. 405–407, 1992.

[61] R.H.Stolen, J.Botineau, and A.Ashkin, "Intensity discrimination of optical pulses with birefringent fibers," *Optics Letters*, vol. 7, no. 10, pp. 512–5140, 1982.

[62] B. Nikolaus, D. Grischkowsky, and A. Balant, "Optical pulse reshaping based on the nonlinear birefringence of single-mode fibers," *Optics Letters*, vol. 8, pp. 189–191, March 1983.

[63] V.J.Matsas, T.P.Newson, D.J.Richardson, and D.N.Payne, "Selfstarting passively mode-locked fibre ring soliton laser exploiting nonlinear polarisation rotation," *Electronics Letters*, vol. 28, no. 15, pp. 1391–1393, 16 July 1992.

[64] K.Tamura, H.A.Haus, and E.P.Ippen, "Self-starting additive pulse mode-locked erbium fibre ring laser," *Electronics Letters*, vol. 28, no. 24, pp. 2226–2227, 19 Nov. 1992.

[65] L.F.Stokes, M.Chodorow, and H.J.Shaw, "All-single-mode fiber resonator," *Optics Letters*, vol. 7, no. 6, pp. 288–290, June 1982.

[66] T.Aida and P.Davis, "Storage of optical pulse data sequences in loop memory using multistable oscillations," *Electronics Letters*, vol. 27, no. 17, pp. 1544–1546, 15 Aug. 1991.

[67] J.T.Kringlebotn, P.R.Morkel, C.N.Pannell, D.N.Payne, and R.I.Laming, "Amplified fibre delay line with 27000 recirculations," *Electronics Letters*, vol. 28, no. 2, pp. 201–202, 16 Jan. 1992.

[68] V.I.Belotitskii, E.A.Kuzin, M.P.Petrov, and V.V.Spirin, "Demonstration of over 100 million round trips in recirculating fibre loop with all-optical regeneration," *Electronics Letters*, vol. 29, no. 1, pp. 49–50, 7 Jan. 1993.

[69] E.Dietrich, G.Grosskopf, *et al.*, "Ber measurements in random access fibre loop optical memory," *Electronics Letters*, vol. 27, no. 17, pp. 1585–1586, 15 Aug. 1991.

[70] H.A.Haus and A.Mecozzi, "Long-term storage of a bit stream of solitons," *Optics Letters*, vol. 17, no. 21, pp. 1500–1502, 1992.

[71] R.B.Dyott, V.A.Handrek, and J.Bello *Proc. Soc. Photo-Opt. Instrum. Eng.*, vol. 479, p. 23, 1984.

[72] N.Finlayson, B.K.Nayar, and N.J.Doran, "Switch inversion and polarization sensitivity of the nonlinear-optical loop mirror," *Optics Letters*, vol. 17, no. 2, pp. 112–114, Jan. 15, 1992.

[73] K.Otsuka, "Nonlinear antiresonant ring interferometer," *Optics Letters*, vol. 8, p. 471, 1983.

[74] N.J.Doran, K.J.Blow, and D.Wood *Proc.SPIE*, vol. 836, p. 238, 1987.

[75] N.J.Doran and D. Wood, "Nonlinear-optical loop mirror," *Optics Letters*, vol. 13, no. 1, pp. 56–58, 1988.

[76] N.J.Doran, D.S.Forrester, and B.K.Nayar *Electronics Letters*, vol. 25, p. 267, 1989.

[77] K.Smith, N.J.Doran, and P.G.J.Wigley, "Pulse shaping, compression, and pedestal suppression employing a nonlinear-optical loop mirror," *Optics Letters*, vol. 15, no. 22, pp. 1294–1296, 1990.

[78] A.J.Schmidt *et al.* in *QELS Technical Digest - Poster*, 1990.

[79] M.E.Fermann, F.Haberl, M.Hofer, and H.Hochreiter *Optics Letters*, vol. 15, pp. 752–754, 1990.

[80] A.W.O'Neill and R.P.Webb, "All-optical loop mirror switch employing an asymmetric amplifier/attenuator combination," *Electronics Letters*, vol. 26, no. 24, pp. 2008–2009, 1990.

[81] D.J.Richardson, R.I.Laming, and D.N.Payne *Electronics Letters*, vol. 26, p. 1779, 1990.

[82] K.Smith, E.J.Greer, N.J.Doran, D.M.Bird, and K.H.Cameron, "Pulse amplification and shaping using a nonlinear loop mirror that incorporates a saturable gain," *Optics Letters*, vol. 17, no. 6, pp. 408–410, March 15, 1992.

[83] M.Eiselt, W.Pieper, and H.G.Weber, "Decision gate for all-optical data retiming using a semiconductor laser amplifier in a loop mirror configuration," *Electronics Letters*, vol. 29, no. 1, pp. 107–109, 7 Jan. 1993.

[84] M.Eiselt, "Optical loop mirror with semiconductor laser amplifier," *Electronics Letters*, vol. 28, p. 1505, 1992.

[85] A.Ehrhardt, M.Eiselt, *et al.*, "Semiconductor laser amplifier as optical switching gate," *IEEE J. Lightwave Tech.*, vol. 11, no. 8, pp. 1287–1295, Aug. 1993.

[86] S.M.Jensen, "The nonlinear coherent coupler," *IEEE J. Quantum Electronics*, vol. QE-18, no. 10, pp. 1580–1583, Oct. 1982.

[87] A.W.Snyder, D.J.Mitchell, L.Poladian, D.R.Rowland, and Y.Chen, "Physics of nonlinear fiber couplers," *J.Opt.Soc.Am.*, vol. B8, no. 10, pp. 2102–2118, Oct. 1991.

[88] S.Trillo and S.Wabnitz, "Weak-pulse-activated coherent soliton switching in nonlinear couplers," *Optics Letters*, vol. 16, no. 1, pp. 1–3, 1991.

[89] M.C.Farries and D.N.Payne, "Optical fiber switch employing a Sagnac interferometer," *Appl.Phys.Letters*, vol. 55, no. 1, pp. 25–26, 1989.

[90] K.J.Blow, N.J.Doran, B.K.Nayar, and B.P.Nelson, "Two-wavelength operation of the nonlinear fiber loop mirror," *Optics Letters*, vol. 15, no. 4, pp. 248–250, 1990.

[91] M.Jinno and T.Matsumoto, "Ultrafast all-optical logic operations in a nonlinear Sagnac interferometer with two control beams," *Optics Letters*, vol. 16, no. 4, pp. 220–222, Feb. 15, 1991.

[92] A.D.Ellis and D.A.Cleland, "Ultrafast all optical switching in two wavelength amplifying nonlinear optical loop mirror," *Electronics Letters*, vol. 28, no. 4, pp. 405–406, 13 Feb. 1992.

[93] M.Jinno and M.Abe, "All optical regenerator based on nonlinear fibre Sagnac interferometer," *Electronics Letters*, vol. 28, no. 14, pp. 1350–1352, 2 July 1992.

[94] J.-M. Jeong and M.E.Marhic, "All-optical logic gates based on cross-phase modulation in a nonlinear fiber interferometer," *Optics Communications*, vol. 85, pp. 430–436, 1991.

[95] B.P.Nelson, K.J.Blow, *et al.*, "All-optical Gbit/s switching using nonlinear optical loop mirror," *Electronics Letters*, vol. 27, no. 9, pp. 704–705, 25 Apr. 1991.

[96] K.Uchiyama *et al.*, "Ultrafast polarisation-independent all-optical switching using a polarisation diversity scheme in the nonlinear optical loop mirror," *Electronics Letters*, vol. 28, no. 20, pp. 1864–1866, 24 Sep. 1992.

[97] S.V.Manakov, "On the theory of two-dimensional stationary self-focusing of electromagnetic waves," *Sov.Phys.JETP*, vol. 38, no. 2, pp. 248–253, 1974.

[98] V.E.Zakharov and E.I.Schulman *Physica D*, vol. 4, p. 270, 1982.

[99] J.D.Moores, K.Bergman, H.A.Haus, and E.P.Ippen, "Demonstration of optical switching by means of solitary wave collisions in a fiber ring reflector," *Optics Letters*, vol. 16, no. 3, pp. 138–140, 1991.

[100] J.D.Moores, K.Bergman, H.A.Haus, and E.P.Ippen, "Optical switching using fiber ring reflectors," *J.Opt.Soc.Am.*, vol. B8, no. 3, pp. 594–601, 1991.

[101] M.Shirasaki, H.A.Haus, and D. Wong, "Nonlinear fiber interferometer and logic gate," paper THO1, Apr. 30, 1987.

[102] C.-J. Chen, P.K.A.Wai, and C.R.Menyuk, "Soliton switch using birefringent optical fibers," *Optics Letters*, vol. 15, no. 9, pp. 477–479, May 1, 1990.

[103] H.Avramopoulos, P.M.W.French, M.C.Gabriel, H.H.Houh, N.A.WhitakerJr., and T.Morse, "Complete switching in a three-terminal Sagnac switch," *Photonics Tech. Letters*, vol. 3, no. 3, pp. 235–237, 1991.

[104] N.A.WhitakerJr., M.C.Gabriel, H.Avramopoulos, and A.Huang, "All-optical, all-fiber circulating shift register with an inverter," *Optics Letters*, vol. 16, no. 24, pp. 1999–2001, 1991.

[105] N.A.WhitakerJr., P.M.W.French, and M. H.Avramopoulos, "Polarization-independent all-optical switching," *Photonics Tech. Letters*, vol. 4, no. 3, pp. 260–263, 1992.

[106] M.N.Islam, C.-J.Chen, and C.E.Soccolich, "All-optical time-domain chirp switches," *Optics Letters*, vol. 16, no. 7, pp. 484–486, Apr.1, 1991.

[107] M.N.Islam, "All-optical cascadable nor gate with gain," *Optics Letters*, vol. 15, no. 8, pp. 417–419, Apr.15, 1990.

[108] M.N.Islam, C.D.Poole, and J.P.Gordon, "Soliton trapping in birefringent optical fibers," *Optics Letters*, vol. 14, no. 18, pp. 1011–1013, Sept.15, 1989.

[109] H.A.Haus and Y.Lai, "Quantum theory of soliton squeezing: a linearized approach," *J. Opt. Soc. Am.*, vol. B7, no. 3, pp. 386–392, 1990.

[110] D.J.Kaup, "Perturbation theory for solitons in optical fibers," *Phys.Rev.A*, vol. 42, no. 9, pp. 5689–5694, 1990.

[111] J.D.Moores, *Collisions of orthogonally polarized solitary waves.* S.M. thesis MIT, 1989.

[112] J.D.Moores, "On the Ginzburg-Landau laser mode-locking model with fifth-order saturable absorber term," *Optics Communications*, vol. 96, pp. 65–70, 1993.

[113] D.Wood, "Constraints on the bit rates in direct detection optical communication systems using linear or soliton pulses," *J. Lightwave Tech.*, vol. 8, no. 7, pp. 1097–1106, 1990.

[114] M.N.Islam, C.R.Menyuk, C.-J.Chen, and C.E.Soccolich, "Chirp mechanisms in soliton-dragging logic gates," *Optics Letters*, vol. 16, no. 4, pp. 214–216, Feb.15, 1991.

[115] M.N.Islam and et.al., "Prechirper to relax the timing restrictions for soliton-dragging logic gates," *Optics Letters*, vol. 16, no. 8, pp. 593–595, Apr.15, 1991.

[116] M.N.Islam and et.al., "All-optical timing restoration using a hybrid time-domain chirp switch," *Optics Letters*, vol. 16, no. 14, pp. 1116–1118, July 15, 1991.

[117] C.R.Menyuk, "Stability of solitons in birefringent optical fibers. I: Equal propagation amplitudes," *Optics Letters*, vol. 12, no. 8, pp. 614–616, 1987.

[118] C.R.Menyuk, "Stability of solitons in birefringent optical fibers. II: Arbitrary amplitudes," *J.Opt.Soc.Am.*, vol. B5, no. 2, p. 392, 1988.

[119] M.V.Tratnick, "Twisted solitons in birefringent optical fibers," *Optics Letters*, vol. 17, no. 13, pp. 917–919, July 1, 1992.

[120] R.H.Stolen, A.Ashkin, W.Pleibel, and J.M.Dziedzic, "In-line fiber-polarization-rocking rotator and filter," *Optics Letters*, vol. 9, no. 7, pp. 300–302, 1984.

[121] J.D.Moores, "Ultra-long distance soliton transmission using inhomogeneously-broadened fiber amplifiers," *J. Lightwave Tech.*, vol. 10, no. 4, pp. 482–487, 1992.

[122] L.F.Mollenauer, S.G.Evangelides, and J.P.Gordon, "Wavelength division multiplexing with solitons in ultra-long distance transmission using lumped amplifiers," *J. Lightwave Tech.*, vol. 9, no. 3, pp. 362–367, 1991.

[123] D.Marcuse, A.R.Chraplyvy, and R.W.Tkach, "Effect of fiber nonlinearity on long-distance transmission," *J. Lightwave Tech.*, vol. 9, no. 1, pp. 121–128, 1991.

[124] D.Marcuse, "Single-channel operation in very long nonlinear fibers with optical amplifiers at zero dispersion," *J. Lightwave Tech.*, vol. 9, no. 1, pp. 121–128, 1991.

[125] R.Ramaswami and P.Humblet, "Amplifier induced crosstalk in multichannel optical networks," *J. Lightwave Tech.*, vol. 8, no. 12, pp. 1882–1896, 1991.

[126] H.A.Haus *private communication*.

[127] R.I.Laming, L.Reekie, P.R.Morkel, and D.N.Payne, "Multichannel crosstalk and pump noise characterization of Er^{3+}-doped fibre amplifier pumped at 980 nm," *Electronics Letters*, vol. 25, no. 7, p. 455, 1989.

[128] K.Inoue, H.Toba, N.Shibata, K.Iwatsuki, and A.Tahada, "Mutual signal gain saturation in Er^{3+}-doped fibre amplifier around 1.54 μm wavelength," *Electronics Letters*, vol. 25, no. 9, p. 594, 1989.

[129] J.L.Zyskind, E.Desurvire, J.W.Sulhoff, and D.J.DiGiovanni, "Spectral gain hole-burning in an erbium-doped fiber amplifier with $GeO_2:SiO_2$ core," in *Optical Amplifiers and their Applications, Technical Digest Series Volume 13*, p. MD4, 1990.

[130] J.L.Zyskind, E.Desurvire, J.W.Sulhoff, and D.J.DiGiovanni, "Determination of homogeneous linewidth by spectral gain hole-burning in an erbium-doped fiber amplifier with $GeO_2:SiO_2$ core," *Photonics Tech. Letters*, vol. 2, no. 12, pp. 869–871, 1990.

[131] E.Desurvire, M.Zirngibl, H.M.Presby, and D.DiGiovanni, "Dynamic gain compensation in saturated erbium-doped fiber amplifiers," *Photonics Tech. Letters*, vol. 3, no. 5, p. 453, 1991.

[132] H.A.Haus and Y.Lai, "Narrow-band optical channel-dropping filter," *J. Lightwave Tech.*, vol. 10, no. 1, pp. 57–62, Jan., 1992.

[133] H.A.Haus and Y.Lai, "Narrow-band distributed feedback reflector design," *J. Lightwave Tech.*, vol. 9, no. 6, pp. 754–760, 1991.

[134] C.R.Giles and E.Desurvire, "Modeling erbium-doped fiber amplifiers," *J. Lightwave Tech.*, vol. 9, no. 2, pp. 271–283, 1991.

[135] A.Yariv, *Optical Electronics, 3rd Edition*. CBS College Publishing, 1985.

[136] W.Koechner, *Solid-State Laser Engineering, 2nd Ed.* Springer-Verlag, 1988.

[137] V.L.daSilva *et al.* in *Proc. Conf. Optical Fiber Commun.*, p. ThD2, 1993.

[138] E.L.Goldstein, V.daSilva, L.Eskildsen, M.Andrejco, and Y.Silberberg, "Spectral gain hole-burning at 1.53μm in erbium-doped fiber amplifiers," *IEEE Photonics Tech. Letters*, vol. 5, no. 5, pp. 543–545, 1993.

[139] R.I.Laming, J.D.Minelly, L.Dong, and M.N.Zervas, "Twincore erbium-doped fibre amplifier with passive spectral gain equalisation," *Electronics Letters*, vol. 29, no. 6, pp. 509–510, 18 March 1993.

[140] A.Yariv, "Signal-to-noise considerations in fiber links with periodic or distributed optical amplification," *Optics Letters*, vol. 15, no. 19, pp. 1064–1066, 1990.

[141] J.P.Gordon and L.F.Mollenauer, "Effects of fiber nonlinearities and amplifier spacing on ultra-long distance transmission," *J. Lightwave Tech.*, vol. 9, no. 2, pp. 170–173, 1991.

[142] X.Tang and P.Ye, "Calculation of the bit error rate for optical soliton communication systems with lumped amplifiers," *Optics Letters*, vol. 17, pp. 1156–1158, 1993.

[143] B.Wedding, "New method for optical transmission beyond dispersion limit," *Electronics Letters*, vol. 28, pp. 1298–1300, 1992.

[144] S.Kobayashi, N.Shibata, S.Shibata, and T.Izawa, "Characteristics of optical fibers in infrared wavelength region," *Review of the Electrical Communication Laboratories*, vol. 26, no. 3-4, pp. 453–467, 1978.

[145] M.Miyagi and S.Nishida, "Pulse spreading in a single-mode fiber due to third-order dispersion," *Applied Optics*, vol. 18, no. 5, pp. 678–682, 1979.

[146] D.Marcuse, "Effect of fiber nonlinearity on long-distance transmission," *Appl. Optics*, vol. 19, p. 1653, 1980.

[147] P.K.A.Wai, C.R.Menyuk, Y.C.Lee, and H.H.Chen, "Nonlinear pulse propagation in the neighborhood of the zero-dispersion wavelength of monomode optical fibers," *Optics Letters*, vol. 11, no. 7, pp. 464–466, 1986.

[148] P.K.A.Wai, C.R.Menyuk, H.H.Chen, and Y.C.Lee, "Soliton at the zero-group-dispersion wavelength of a single-mode fiber," *Optics Letters*, vol. 12, no. 8, pp. 628–630, 1987.

[149] S.Wen and S.Chi, "Approximate solution of optical soliton in lossless fibres with third-order dispersion," *Optical and Quantum Electronics*, vol. 21, pp. 335–341, 1989.

[150] N.Gisin, Y.Salama, and M.O.Hongler, "Polarization mode dispersion for single-mode fibers with polarization dependent loss," *Optics Communications*, vol. 101, no. 5,6, pp. 333–336, 1 Sept. 1993.

[151] B.M.Nyman and G.Wolter, "High-resolution measurement of polarization dependent loss," *IEEE Photonics Tech. Letters*, vol. 5, no. 7, pp. 817–818, July 1993.

[152] B.L.Heffner, "Accurate, automated measurement of differential group delay dispersion and principal state variation using Jones matrix eigenanalysis," *IEEE Photonics Tech. Letters*, vol. 5, no. 7, pp. 814–817, July 1993.

[153] N.Gisin, R.Passy, J.C.Bishoff, and B.Perny, "Experimental investigations of the statistical properties of polarization mode dispersion in single mode fibers," *IEEE Photonics Tech. Letters*, vol. 5, no. 7, pp. 819–821, July 1993.

[154] C.D.Poole and C.R.Giles, "Polarization-dependent pulse compression and broadening due to polarization dispersion in dispersion-shifted fiber," *Optics Letters*, vol. 13, pp. 155–157, 1988.

[155] L.F.Mollenauer, K.Smith, J.P.Gordon, and C.R.Menyuk, "Resistance of solitons to the effects of polarization dispersion in optical fibers," *Optics Letters*, vol. 14, no. 21, pp. 1219–1221, 1989.

[156] P.K.A.Wai, C.R.Menyuk, and H.H.Chen, "Effects of randomly varying birefringence on soliton interactions in optical fibers," *Optics Letters*, vol. 16, no. 22, pp. 1735–1737, Nov. 15, 1991.

[157] S.Betti, F.Curti, B.Daino, G. Marchis, E.Iannone, and F.Matera, "Evolution of the bandwidth of the principal states of polarization in single-mode fibers," *Optics Letters*, vol. 16, no. 7, pp. 467–469, 1991.

[158] N. Pandit, D. Noske, S. Kelly, and J. Taylor, "Characteristic instability of fibre loop soliton lasers," *Electronics Letters*, vol. 28, pp. 455–6, 27th February 1992.

[159] S. Kelly, "Characteristic sideband instability of periodically amplified average soliton," *Electronics Letters*, vol. 28, pp. 806–7, 9th April 1992.

[160] N.J.Smith, K.J.Blow, and I.Andonovic, "Sideband formation in soliton lasers and transmission," seminar given at MIT, May 1992.

[161] D.U.Noske, N.Pandit, and J.R.Taylor, "Source of spectral and temporal instability in soliton fiber lasers," *Optics Letters*, vol. 17, no. 21, pp. 1515–1517, 1992.

[162] K.Smith and L.F.Mollenauer, "Experimental observation of soliton interaction over long fiber paths: discovery of a long-range interaction," *Optics Letters*, vol. 14, no. 22, pp. 1284–1286, 1989.

[163] E.M.Dianov, A.V.Luchnikov, A.N.Pilepetskii, and A.N.Staromudov, "Long-range interaction of soliton pulse trains in a single-mode fibre," *Sov.Lightwave Communications*, vol. 1, no. 1, pp. 37–44, Feb. 1991.

[164] V.I.Karpman and V.V.Solov'ev *Physica*, vol. 3D, p. 487, 1981.

[165] J.P.Gordon, "Interaction forces among solitons in optical fibers," *Optics Letters*, vol. 8, no. 11, pp. 596–598, Nov. 1983.

[166] D.Anderson and M.Lisak, "Bandwidth limits due to mutual pulse interaction in optical soliton communication systems," *Optics Letters*, vol. 11, no. 3, pp. 174–176, Iar. 1986.

[167] C.Desem and P.L.Chu, "Soliton interaction in the presence of loss and periodic amplification in optical fibers," *Optics Letters*, vol. 12, no. 5, pp. 349–351, May 1987.

[168] I.M.Uzunov, V.D.Stoev, and T.I.Tzoleva, "N-soliton interaction in trains of unequal soliton pulses in optical fibers," *Optics Letters*, vol. 17, no. 20, pp. 1417–1419, 15 Oct. 1992.

[169] I.M.Uzunov, V.D.Stoev, and T.I.Tzoleva, "Influence of the initial phase difference between pulses on the N-soliton interaction in trains of unequal solitons in optical fibers," *Optics Communications*, vol. 97, no. 5,6, pp. 307–311, 1 Apr. 1993.

[170] P.Andrekson, N.A.Olsson, J.R.Simpson, T.Tanbuk-Ek, R.A.Logan, and K.W.Wecht, "Observation of collision induced temporary soliton carrier frequency shifts in ultra-long fiber transmission systems," *J. Lightwave Tech.*, vol. 9, no. 9, pp. 1132–1135, 1991.

[171] H.A.Haus, J.D.Moores. and L.E.Nelson, "The effect of third-order dispersion on passive mode-locking," *Optics Letters*, vol. 18, no. 1, pp. 51–53, 1993.

[172] S.Wabnitz, "Suppression of interactions in a phase-locked soliton optical memory," *Optics Letters*, vol. 18, no. 8, pp. 601–603, Apr. 15, 1993.

[173] S.Wabnitz, "Phase modulator memory," *Optics Letters*, vol. 18, no. large, p. ???, Late, 1993.

[174] H.A.Haus, "Quantum noise in a solitonlike repeater system," *J.Opt.Soc.Am.*, vol. 8, no. 5, pp. 1122–1126, 1991.

[175] J.P.Gordon, "Theory of the soliton self-frequency shift," *Optics Letters*, vol. 11, no. 10, pp. 662–664, 1986.

[176] F.M.Mitschke and L.F.Mollenauer, "Discovery of the soliton self-frequency shift," *Optics Letters*, vol. 11, no. 10, pp. 659–661, 1986.

[177] M.Nakazawa, H.Kubota, K.Kurokawa, and E.Yamada, "Femtosecond optical soliton propagation over long distances using adiabatic trapping and soliton standardization," *J. Opt. Soc. Am.*, vol. B8, no. 9, pp. 1811–1817, 1991.

[178] H.Kubota and M.Nakazawa, "Soliton transmission with long amplifier spacing under soliton control," *Electronics Letters*, vol. 29, no. 20, pp. 1780–1781, 30 Sept. 1993.

[179] S.Wabnitz, "Suppression of soliton interactions by phase modulation," *Electronics Letters*, vol. 29, no. 19, pp. 1711–1713, 16 Sept. 1993.

[180] N.J.Smith, K.J.Blow, W.J.Firth, and K.Smith, "Soliton dynamics in the presence of phase modulators," *Optics Communications*, vol. 102, no. 3,4, pp. 324–328, 1 Oct. 1993.

[181] H.A.Haus, J.G.Fujimoto, and E.P.Ippen, "Structures for additive pulse mode locking," *J.Opt.Soc.Am.*, vol. B8, no. 10, pp. 2068-2076, 1991.

[182] L.F.Mollenauer, S.G.Evangelides, and H.A.Haus, "Long-distance soliton propagation using lumped amplifiers and dispersion shifted fiber," *J. Lightwave Tech.*, vol. 9, no. 2, pp. 194-197, 1991.

[183] C.R.Menyuk, M.N.Islam, and J.P.Gordon, "Raman effect in birefringent optical fibers," *Optics Letters*, vol. 16, no. 8, pp. 566-568, 1991.

[184] K.J.Blow, N.J.Doran, and D. Wood, "Suppression of the soliton self-frequency shift by bandwidth-limited amplification," *J. Opt. Soc. Am.*, vol. B5, no. 6, pp. 1301-1304, 1988.

[185] K.J.Blow, N.J.Doran, and B.K.Nayar, "Experimental demonstration of optical soliton switching in an all-fiber nonlinear Sagnac interferometer," *Optics Letters*, vol. 14, no. 14, pp. 754-756, 1989.

[186] M.Levy, L.Eldada, R.Scarmozzino, J. R.M.Osgood, P.S.D.Lin, and F.Tong, "Fabrication of narrow-band channel-dropping filters," *IEEE Photonics Tech. Letters*, vol. 4, no. 12, p. 1378, Dec. 1992.

[187] I.N.DulingIII, "All-fiber ring soliton laser mode locked with a nonlinear mirror," *Optics Letters*, vol. 16, no. 8, pp. 539-541, 1991.

[188] A.Hasegawa and Y.Kodama, "Guiding-center soliton," *Phys.Rev.Letters*, vol. 66, no. 2, pp. 161-164, 1991.

[189] J.D.Kafka and T.Baer *Optics Letters*, vol. 14, pp. 1269-1271, 1989.

[190] E.J.Greer and K.Smith, "All-optical fm mode-locking of fibre laser," *Electronics Letters*, vol. 28, no. 18, pp. 1741-1743, 27 Aug. 1992.

[191] K.Smith and J.K.Lucek, "All-optical clock recovery using a mode-locked laser," *Electronics Letters*, vol. 28, no. 19, pp. 1814-1816, 10 Sept. 1992.

[192] G.T.Harvey and L.F.Mollenauer *Optics Letters*, vol. 18, pp. 107-109, 1993.

[193] C.R.Doerr, H.A.Haus, E.P.Ippen, M.Shirasaki, and K.Tamura, "Additive pulse limiting," *Optics Letters*, vol. 19, no. 1, pp. 31-33, 1 January 1994.

[194] K.Tamura, E.P.Ippen, and H.A.Haus, "77-fs pulse generation from a stretched-pulse mode-locked all-fiber ring laser," *Optics Letters*, vol. 18, no. 13, pp. 1080-1082, 1 July 1993.

[195] M.Nakazawa, K.Suzuki, and Y.Kimura, "Transform-limited pulse generation in gigahertz region from gain-switched distributed-feedback laser diode using spectral windowing," *Optics Letters*, vol. 15, pp. 715-717, 1990.

[196] K.A.Ahmed, H.F.Liu, N.Onodera, P.Lee, R.S.Tucker, and Y.Ogawa, "Nearly transform-limited pulse (3.6 ps) generation from gain-switched 1.55 μm distributed feedback laser by using fibre compression technique," *Electronics Letters*, vol. 29, no. 1, pp. 54–56, 7 Jan. 1993.

[197] K.Wakita, I.Kotaka, O.Mitomi, and M.Naganuma, "High-speed InGaAlAs/InAlAs multiple quantum well optical modulators," *J. Lightwave Tech.*, vol. 8, pp. 1027–1032, July 1990.

[198] S.K.Korotky *et al.*, "Optical intensity modulation to 40 GHz using a waveguide electrooptic switch," in *Picosecond Electronics and Optoelectronics II* (F.J.Leonberger *et al.*, eds.), pp. 272–275, Springer-Verlag Berlin Heidelberg, 1987.

[199] K.Rauschenbach *private communication.*

[200] M.Suzuki, H.Tanaka, K.Utaka, N.Edagawa, and Y.Matsushima, "Transform-limited 14ps optical pulse generation with 15ghz repetition rate by InGaAsP electroabsorption modulator," *Electronics Letters*, vol. 28, no. 11, pp. 1007–1008, 1992.

[201] P.A.Morton *et al.*, "Mode-locked hybrid soliton pulse source with extremely wide operating frequency range," *IEEE Photonics Tech. Letters*, vol. 5, no. 1, pp. 28–31, 1993.

[202] Y.K.Chen, M.C.Wu, T.Tanbun-Ek, R.A.Logan, and M.A.Chin *Appl. Phys. Letters*, vol. 58, p. 1253, 1991.

[203] C.F.Lin and C.L.Tang, "Colliding pulse mode locking of a semiconductor laser in an external ring cavity," *Appl. Phys. Letters*, vol. 62, no. 10, pp. 1053–1055, 1993.

[204] E.Kapon, "Quantum wire lasers," *Proc. IEEE*, vol. 80, no. 3, pp. 398–410, 1992.

[205] A.Hasegawa *Optics Letters*, vol. 9, pp. 288–290, 1984.

[206] K.Tai, A.Tomita, J.L.Jewell, and A.Hasegawa, "Generation of subpicosecond solitonlike optical pulses at 0.3THz repetition rate by induced modulational instability," *Appl. Physics Letters*, vol. 49, no. 5, pp. 236–238, 1986.

[207] E.M.Dianov, P.V.Mamyshev, A.M.Prokhorov, and S.V.Chernikov, "Generation of a train of fundamental solitons at a high repetition rate in optical fibers," *Optics Letters*, vol. 14, no. 18, pp. 1008–1010, 1989.

[208] S.V.Chernikov, D.J.Richardson, R.I.Laming, E.M.Dianov, and D.N.Payne, "70 Gbit/s fibre based source of fundamental solitons at 1550 nm," *Electronics Letters*, vol. 28, no. 13, pp. 1210–1212, 18 June 1992.

[209] S.V.Chernikov, J.R.Taylor, and R.Kashyap, "Integrated all optical fibre source of multigigahertz soliton pulse train," *Electronics Letters*, vol. 29, no. 20, pp. 1788-1789, 30 Sept. 1993.

[210] K.Suzuki, K.Iwatsuki, S.Nishi, M.Saruwatari, K.Sato, and K.Wakita, "2.5 ps soliton pulse generation at 15ghz with monolithically integrated MQW-DFB-LD/MQW-EA modulator and dispersion decreasing fibre," *Electronics Letters*, vol. 29, no. 19, pp. 1713-1714, 16 Sept. 1993.

[211] A.M.Weiner and D.E.Leaird, "Generation of terahertz-rate trains of femtosecond pulses by phase-only filtering," *Optics Letters*, vol. 15, no. 1, pp. 51-53, 1990.

[212] Y.Suematsu, K.Iga, and S.Arai, "Advanced semiconductor lasers," *Proc. IEEE*, vol. 80, no. 3, pp. 383-397, 1992.

[213] K.Tamura *private communication*.

[214] L.A.Molter-Orr, H.A.Haus, and F.J.Leonberger, "20 GHz optical waveguide sampler," *IEEE J.Quantum Electronics*, vol. QE-19, no. 12, pp. 1877-1883, 1983.

[215] H.A.Haus and Y.Lai, "Theory of cascaded quarter wave shifted distributed feedback resonators," *IEEE J.Quantum Electronics*, vol. 28, no. 1, pp. 205-213, Jan., 1992.

[216] J.N.Damask, *A new photonic device: the integrated resonant channel-dropping filter*. S.M. thesis MIT, May, 1993.

[217] J.Ferrera *et al.*, "Spatial-phase-locked electron-beam lithography: initial test results," *J.Vac.Sci.Technol. B*, Nov./Dec. 1993.

[218] R.C.Alferness *et al.*, "Broadly tunable InGaAsP/InP buried rib waveguide vertical coupler filter," *Appl. Phys. Letters*, vol. 60, no. 8, pp. 980-982, 24 Feb. 1992.

[219] J.B.D.Soole, A.Scherer, *et al.*, "Monolithic InP-based grating spectrometer for wavelength division multiplexed system at 1.5 μm," *Electronics Letters*, vol. 27, no. 2, pp. 132-134, 1991.

[220] J.B.D.Soole, A.Scherer, *et al.*, "Monolithic InP/InGaAsP/InP grating spectrometer for the 1.48-1.56 μm wavelength range," *Appl. Physics Letters*, vol. 58, no. 18, pp. 1949-1951, 1991.

[221] M.Fallahi, K.A.McGreer, *et al.*, "Grating demultiplexer integrated with msm detector array in InGaAs/Al GaAs/ GaAs for wdm," *IEEE Photonics Tech. Letters*, vol. 5, no. 7, p. 794, July 1993.

[222] C.Dragone, "An N×N optical multiplexer using a planar arrangement of two star couplers," *IEEE Photonics Tech. Letters*, vol. 3, pp. 812-814, 1991.

[223] F.Heismann and M.S.Whalen, "Broadband, reset-free, automatic polarization controller," *Electronics Letters*, vol. 27, pp. 377–379, Feb. 1991.

[224] F.Heismann, P.B.Hansen, S.K.Korotky, G.Raybon, J.J.Veselka, and M.S.Whalen, "Automatic polarisation demultiplexer for polarisation-multiplexed transmission systems," *Electronics Letters*, vol. 29, pp. 1965–1966, 28 Oct. 1993.

[225] D.H.Auston in *Picosecond Optoelectronic Devices* (C.H.Lee, ed.), pp. 73–116, Academic, London, 1984.

[226] D.Grischkowsky *et al.*, "Photoconductive generation of subpicosecond electrical pulses and their measurement applications," in *Picosecond Electronics and Optoelectronics II* (F.J.Leonberger *et al.*, eds.), pp. 11–17, Springer-Verlag Berlin Heidelberg, 1987.

[227] E.Desurvire, J.L.Zyskind, and J.R.Simpson, "Spectral gain hole-burning at 1.53μm in erbium-doped fiber amplifiers," *IEEE Photonics Tech. Letters*, vol. 2, p. 246, 1990.

[228] T.Ozeki, "Optical equalizers," *Optics Letters*, vol. 17, no. 5, pp. 375–377, Mar.1, 1992.

[229] W.Forysiak, K.J.Blow, and N.J.Doran, "Reduction of Gordon-Haus jitter by post transmission dispersion compensation," *Electronics Letters*, vol. 29, pp. 1225–1226, 1993.

[230] A.Yariv, D.Fekete, and D.M.Pepper *Optics Letters*, vol. 4, pp. 52–54, 1979.

[231] S.Watanabe, T.Naito, and T.Chikama *IEEE Photonics Tech. Letters*, vol. 5, p. 92, 1993.

[232] R.M.Jopson, A.H.Gnauck, and R.M.Derosier *Electronics Letters*, vol. 29, p. 576, 1993.

[233] Y.Nagasako and T.Nakashima, "Fast timing extraction method for an optical passive bus," *Electronics Letters*, vol. 26, no. 15, pp. 1168–1169, 19 July 1990.

[234] P.Monteiro, J.N.Matos, A.Gameiro, and J. Rocha, "10 Gbit/s timing recovery circuit using dielectric resonator and active bandpass filters," *Electronics Letters*, vol. 28, no. 9, pp. 819–820, 23 Apr. 1992.

[235] S.Kawanishi and M.Saruwatari, "10 GHz timing extraction from randomly modulated optical pulses using phase-locked loop etc.," *Electronics Letters*, vol. 28, no. 5, pp. 510–511, 27 Feb. 1992.

[236] C.D.O'Shea, "Novel wideband 2-18 GHz clock extraction circuit for optical transmission systems," *Electronics Letters*, vol. 27, no. 25, pp. 2324–2326, 5 Dec. 1991.

[237] M.Jinno and T.Matsumoto, "All optical timing extraction using a 1.5 μm self-pulsating multielectrode dfb ld," *Electronics Letters*, vol. 24, pp. 1426–1427, 1988.

[238] P.Phelan, G.Farrell, and J.Hegarty, "All-optical synchronization and multiplication of the frequency of mode-locked signals," *IEEE Photonics Tech. Letters*, vol. 4, no. 12, pp. 1332–1335, Dec. 1992.

[239] B.S.Koh and H.S.Lee, "Detection of symbol rate of unknown digital communication signals," *Electronics Letters*, vol. 29, no. 3, pp. 278–279, 4 Feb. 1993.

[240] Y.Fujii, "Compact, high-isolation, polarization-independent optical circulator," *Optics Letters*, vol. 18, pp. 250–252, 1993.

[241] N.A.Olsson, "Semiconductor optical amplifiers," *Proc. IEEE*, vol. 80, no. 3, pp. 375–382, 1992.

[242] S.Kaushik *private communication.*

[243] P.Winternitz, A.M.Grundland, and J.A.Tuszyński, "Exact solutions of the multidimensional classical ϕ^6-field equations obtained by symmetry reduction," *J.Math.Phys.*, vol. 28, no. 9, pp. 2194–2212, 1989.

[244] L.Gagnon and P.Winternitz, "Lie symmetries of a generalised non-linear Schrodinger equation: II. Exact solutions," *J.Phys.A*, vol. 22, pp. 469–497, 1989.